UNIVERSIDAD CARLOS III DE MADRID
Departamento de Ciencia e Ingeniería de Materiales

PROYECTO FIN DE CARRERA

Improving the Fracture Toughness of Dual-phase Austempered Ductile Iron

Autor: *Javier Hidalgo García*
Directores: *Dr. Henrik Borgström*
Dr. Kenneth Hamberg
Tutor: *Dr J.M Torralba Castelló*

Proyecto realizado en conjunción con la Chalmermers University of Technology

PREFACIO

RESUMEN DEL PROYECTO EN CASTELLANO

El presente proyecto fue realizado durante una estancia con beca Erasmus en la Chalmers University of Technology en Göteborg, Suecia, durante el transcurso del curso 2007-2008. El proyecto fue redactado y defendido en lengua inglesa ante un tubunal y ante la evaluación del examinador y catedrático Lärs Nyborg de la Chalmers University of Technology en Goteborg, competente de dictaminar la calificación final del mismo, obteniéndose la calificación máxima de A equivalente a diez, matricula de honor. Este dictamen fue revisado y ratificado por el catedrático José Manuel Torralba de la Universidad Carlos III de Madrid, tutor del proyecto en España. Los directores del proyecto fueron el Dr. Kenneth Hamberg y el Dr. Henrik Borgström.

Las siguientes líneas representan un breve resumen del proyecto de diez páginas aproximadamente de extensión en lengua castellana según lo estipulado por la normativa de la Universidad Carlos III de Madrid

Introducción

Las fundiciones dulces con tratamiento de *austempering* o también conocidas por su acrónimo anglosajón ADI (*Austempered Ductile Iron*) comprenden una familia de aleaciones Fe-C con una microestructura característica que les confiere propiedades adecuadas para su utilización en diversas y muy variadas aplicaciones industriales. Entre estas propiedades destacan una buena resistencia a tracción, elevada ductilidad, elevada tenacidad, baja densidad, buena resistencia al desgaste y buena mecanibilidad, todo ello a un precio más reducido en comparación con los aceros convencionales y aluminios. Estas propiedades son consecuencia de su microestructura característica que consiste en grafito esferoidal en una matriz de ferrita bainítica y austenita sobresaturada de carbono (o austenita retenida), a lo que comúnmente se refiere como microestructura ausferrítica. Para conseguir esa microestructura particular, las fundiciones dulces son llevadas a un tratamiento isotérmico a temperaturas comprendidas entre el rango del comienzo de la precipitación de bainita y el comienzo de la formación de martensita; el tratamiento térmico de *austempering*.

Como ejemplo de sus excelentes propiedades, se pueden comparar sus características de módulo elástico con las del aluminio. Éste es del orden de tres veces superior al mejor de los aluminios forjados y, aunque un ADI tenga una densidad 2,4 veces superior, un ADI es 2,3 veces más resistente y más barato, lo cual hace que si se comparan las propiedades específicas y con respecto a costes de estos materiales, un ADI está en clara ventaja. Ocurre algo similar con los aceros. Comparado con la mayoría de estos, un ADI suele tener mayor resistencia específica debido a que su densidad es un 10% menor. Si además se incluye el parámetro precio, los ADI se muestran más competitivos que sus materiales ingenieriles homólogos en muchas aplicaciones, como por ejemplo, en cigüeñales para automoción.

Además, las propiedades de fractura y fatiga de los ADI son iguales o mejores que la de los aceros forjados. Valores típicos que se obtienes para los ADI se encuentran en el rango de 55-102 $MPa \cdot m^{1/2}$ a temperatura ambiente, aunque se cree que se podrían obtener valores superiores a los 100 $MPa \cdot m^{1/2}$ si se mejoran ciertos parámetros de las fundiciones y los

tratamientos térmicos. Sus destacables propiedades de tenacidad a un reducido coste frente a los aceros, convierte a esta propiedad, en su característica más sobresaliente.

Los ADI han sido reconocidos como un material potencialmente ingenieril desde su descubrimiento haya por los años sesenta, pero debido a su complejidad en diversos aspectos, como lo pueden ser la difícil comprensión de la relación entre microestructura y propiedades o la difícil reproducibilidad de estas para una misma aleación, aún se cree que este material todavía no ha sido explotado hasta su máximo potencial. Por tanto, está ampliamente justificada y muy motivada la continuidad en las investigaciones dentro del campo de estas aleaciones peculiares. Un ejemplo de innovaciones dentro del mundo de los ADI ha sido el descubrimiento de los llamados DPADI o ADI de de fase dual, lo que ha supuesto el descubrimiento de una aleación con una mejora sustancial de las ya de por si buenas ductilidad y tenacidad que presentaban las aleaciones ADI. La microestructura de un DPADI se compone de las ya mencionados micro-constituyentes, ausferrita y grafito esferoidal, común en todos los ADI, a la que ha de añadirse una nueva fase, la ferrita alotrópica o pro-eutectoide, que precipita preferiblemente los dominios de grano de esta aleaciones. Esta distribución de fases en muy similar a la que se aprecia en los aceros TRIP que han demostrado tener propiedades excepcionales de tenacidad, a lo que habría que añadir en los ADI las ventajas de reducción de costes e incremento de las propiedades especificas sobre todo en tenacidad. Este último aspecto posicionaría a los DPADI como candidatos de primera categoría para aplicaciones que requieran una elevada tenacidad a fractura como lo pueden ser componentes de suspensión en la industria del motor.

Para procesar una aleación DPADI se sigue el proceso térmico convencional común para el desarrollo de la familia de las ADI pero con algunos pasos añadidos existiendo varias variantes del proceso. Para el desarrollo de las microestructuras DPADI, en este proyecto se siguió el ciclo térmico que se detalla a continuación:

1) Una austenización en dos etapas: la primera etapa, conocida como austenización completa, consiste en llevar el material por encima de su temperatura crítica superior (en torno a los 1000º C según composición y para el intervalo hipereutéctico de composiciones para aleaciones Fe-C-Si) y mantenerla durante un tiempo determinado para disolver adecuadamente y homogeneizar los elementos aleantes. En especial, se pretende disolver el carbono, aportado como principal fuente por el grafito, saturando así la austenita de este elemento. Además se pretende promover que la austenita recristalice en dominios mas pequeños a los formados durante el enfriamiento de la aleación base de DI, lo cual, según se argumentará en el texto del proyecto, será un factor beneficioso para la microestructura. Después se realiza un temple hasta una temperatura inferior situada en el intervalo "intercrítico" de temperaturas donde coexisten las fases austenita, ferrita y grafito. Esta pequeña ventana de fases tiene un intervalo de temperaturas de aproximadamente 750º C para la temperatura inferior y 860º C para la temperatura superior (según composiciones este rango suele ser más o menos estrecho o puede estar más o menos desplazado) y el objetivo es precipitar ferrita en los bordes de grano austeníticos saturando aún más en carbono la austenita

2) Temple: Tras mantenerse un determinado tiempo en la región anteriormente mencionada, el material se enfría súbitamente hasta el intervalo de temperaturas de *austempering* que corresponde a las temperaturas superiores a la temperatura de formación de martensita e inferiores a las de precipitación de bainita. El enfriamiento se realiza a grandes velocidades en sales fundidas para intentar eludir la nariz perlítica y evitar así la precipitación de esta fase tan

frágil que estropearía las buenas propiedades a tenacidad del material conferidas por la ausferrita que precipitará en la posterior etapa.

3) ***Austempering:*** El material se mantiene en el rango de temperaturas descrito en 2) durante el tiempo mínimo suficiente para propiciar una reducción de tensiones derivadas del brusco descenso de temperaturas y la formación de la ausferrita, y el máximo necesario para evitar la descomposición de austenita retenida en perlita. A este periodo de tiempo se le conoce como "ventana de proceso". Se ha de recalcar que la austenita saturada es una fase metaestable que tiende a descomponer por "envejecimiento" tras la aplicación de temperatura y/o por acciones mecánicas. Ésta se cree que es una de las claves de las buenas propiedades de tenacidad de los ADI ya que en esta transformación de fases se absorbe parte de la energía mecánica suministrada al material.

4) Enfriamiento: tras la etapa de austemperizado se enfría el material a temperatura ambiente a una velocidad lo suficientemente lenta para evitar la precipitación de martensita que fragilizaría de forma inapropiada el material

Los parámetros temperatura y tiempo son parámetros de regulación del proceso y han demostrado ser de suma importancia para obtener las propiedades mecánicas optimas de los materiales formados tras el ciclo térmico. Entre otras cosas, estos parámetros pueden afectar a la fracción en volumen de austenita retenida, al contenido en carbono en las diferentes regiones de la microestructura, así como de la difusión de los elementos microaleantes en ésta, el tamaño de los dominios cristalinos y entre fases, así como su morfología, precipitación de fases indeseadas y formación de carburos. Todas estas propiedades microestructurales están relacionadas de forma biunívoca con características mecánicas. El proceso puede llegar a ser muy sensible a pequeños cambios de estos factores, los cuales han de ser por tanto controlados de forma precisa para conseguir homogenización en los resultados de producción. Ya se han mencionado algunos ejemplos de cómo afectan estos parámetros en la microestructura. En el texto del proyecto ésta asunto se aborda de forma más detallada.

Aunque muchos estudios han sido ya realizados con el objetivo de controlar la fracción en volumen de austenita retenida y el contenido en carbono en las diferentes regiones de la microestructura durante el proceso de formación de un ADI, sólo se han encontrado en la bibliografía unos cuantos intentos de controlar las fracciones en volumen de ausferrita y ferrita pro-eutectoide en aleaciones DPADI. Como consecuencia, pocos trabajos han sido publicados sobre esta temática, y menos aún, sobre la relación de la fracción en volumen de ferrita con las propiedades mecánicas de un DPADI.

Por tanto, es el objetivo de este proyecto fin de carrera el identificar las características dentro de la microestructura de los DPADI que directamente afectan a la tenacidad a fractura de las aleaciones investigadas. Para llevar a cabo esta tarea, se propusieron varios tratamientos térmicos, en base a simulaciones y referencias en bibliografía, con objeto de desarrollar microestructuras del tipo DPADI a partir de varias fundiciones dulces (DI) con diferentes composiciones de elementos aleantes adecuados para la mejora de ciertos aspectos microestructurales durante la aplicación de los tratamientos térmicos como más adelante se discutirá. Posteriormente al desarrollo de estas aleaciones se llevaron a cabo estudios microestructurales con microscopio óptico (LOM) con ataque de nital y la técnica de ataque de color, microscopio electrónico de barrido (SEM), análisis de rayos X (DRX), ensayos de

resistencia a impacto con probeta sin entallar y estudio de superficies de fractura con microscopio estereoscópico y SEM.

Este proyecto ha sido desarrollado para la industria Sueca del sector del automóvil y la industria que lo rodea. Esta englobado en un proyecto más grande cuyo objetivo básico es la reducción de pesos de vehículos desarrollados por el sector. El presente trabajo es una continuación de la tesis de master de Caroline Glondu, la cual se basa en tratamientos térmicos para desarrollar ADI convencionales. En este proyecto se ha obviado la parte teórica desarrollada ya por la ingeniera Gloundu sobre aleaciones ADI convencionales y se ha centrado en el desarrollo de aleaciones DPADI, pero se recomienda como complemento la lectura de la misma.

Método experimental

Para llevar a cabo el estudio de la relación de las propiedades mecánicas de los DPADI con la microestructura y por consiguiente la realización de este proyecto, varias fundiciones dulces con diferentes composiciones y procesos de elaboración fueron suministradas por compañías suecas. Para realizar los tratamientos térmicos y teniendo en mente los ensayos a impacto posteriores que se les iban a realizar, se cortaron probetas estandarizadas tipo de ensayo Izod a partir de tres anillos de fundición diferentes. Estas probetas tenían una base cuadrada de 10mm de lado y 55mm de largo y no fueron entalladas según la norma por especificaciones en torno al proyecto por parte de los diferentes actores implicados.

El primer paso crucial de este proyecto fue, por tanto, caracterizar cada uno de esos materiales base para establecer sus composiciones y revisar posibles defectos de la fundición. Como se discutirá a lo largo de los diversos capítulos del proyecto, las condiciones de partida de la fundición de hierro son determinantes en los resultados de propiedades del material, en concreto sus propiedades mecánicas.

Estas propiedades iniciales de la fundición base, en principio, pobres para los estándares que se desean conseguir, no se verán modificadas posteriormente de forma sensible a mejor si el material para desarrollar ADI utilizado es de baja calidad. Existen parámetros críticos como el número de nódulos de grafito, su densidad, su tamaño, su homogeneidad, existencia de micro-porosidades (debido a contracciones durante el moldeo), etc. que afectan de forma severa en detrimento de las propiedades mecánicas de los materiales. Estas propiedades no pueden ser corregidas a posteriori de forma eficaz durante los tratamientos térmicos llevados a cabo para desarrollar ADI.

Hay otros defectos también importantes como la heterogeneidad de elementos aleantes en la matriz que pueden llevar a la formación de segregaciones de fases indeseadas dentro de esta, precipitación de fases perniciosas para con las propiedades a desarrollar o la formación de carburos que son uno de los principales responsables de la fragilización y perdida de tenacidad en los ADI. Estos defectos hasta cierto punto si podrían ser corregidos de forma más o menos efectiva durante los tratamientos térmicos posteriores, pero nunca está de más intentar partir de las condiciones más óptimas para evitarse complicaciones innecesarias. En este sentido, la observación de la presencia de carburos ya desde el estudio de la microestructura de la fundición base, es un mal indicio que posteriormente será difícil de corregir y que denotará una mala calidad del material de partida. Corregir todos estos defectos

implicaría elevar la temperatura por encima de las normales para los tratamientos ADI, lo que siempre supone un incremento en los costes de proceso y además tiene otros efectos en la microestructura que limitan todo el potencial de la aleación tras el tratamiento térmico.

Con respecto a la composición de las fundiciones dúctiles de partida, conocer el porcentaje de cada uno de los elementos aleantes es crucial para proponer las condiciones de los tratamientos térmicos y visionar la formación de las diferentes fases según que temperaturas y la posible formación de carburos perjudiciales. Los distintos elementos aleantes y su porcentaje en la mezcla modifican en especial el denominado carbono equivalente, parámetro que representa de forma estimativa el equivalente de C para una aleación exclusivamente formada por Fe-C como consecuencia de la influencia de otros elementos. Esto nos ayuda a situarnos en un diagrama de fases binario bien estipulado y estimar las diferentes fases que se van formando, sin necesidad de recurrir a diagramas de fases más complejos.

Como se discute a lo largo del texto, la adicción de elementos aleantes tiene, entre otros, dos cometidos importantes. El primero es conseguir una fundición base con las características adecuadas (cuya importancia ya fue discutida en párrafos anteriores) y el segundo propiciar la formación de las diferentes fases deseadas durante los tratamientos térmicos de ADI, siempre buscando un aumentando las propiedades de estos materiales. La complejidad del diseño de la composición de estas aleaciones se hace patente cuando se descubre que muchos elementos que se añaden para mejorar alguna de las características, pueden ser perjudiciales para el desarrollo de otras. Por citar algún ejemplo, el molibdeno que se adiciona para aumentar la templabilidad y evitar la formación de perlita, sobretodo en secciones de dimensiones elevadas, puede añadir por otra parte el efecto negativo de formación de carburos en los bordes de grano. Esto es debido a su elevada tendencia a segregarse hacia estas regiones y formar carburos a partir de ciertas concentraciones.

La composición de elementos aleantes del material también juega un papel importante en elaboración de simulaciones con programas de ordenador de las diferentes etapas del proceso. La simulación del sistema es una herramienta importante que ayuda a no dar palos de ciego durante el diseño del proceso experimental y a movernos en torno a resultados que presumiblemente se ajustarán a los reales, sin necesidad de perder tiempo llevando a cabo experimentos de largos periodos de duración. Así, se pueden ahorrar tiempo y esfuerzo y se consigue converger a planteamientos cercanos a los óptimos de forma sencilla y relativamente eficaz. En concreto se elaboraron simulaciones sobre los diagramas CTT y TTT de la aleación y porcentajes de las diferentes fases presentes a distintas temperaturas. Las simulaciones se llevaron a cabo mediante los programas JetMatPro y Thermocalc que basan sus cálculos en principios termodinámicos de la energía libre de Gibs y análisis neuronal de redes. Ambos programas necesitan los datos de composición para tales propósitos, de ahí la importancia de conocerla. Las composiciones se suministraron por la propia empresa de fundición y sus porcentajes fueron corroborados con caracterización por técnicas XRD de difracción de rayos X y SEM/EDX de microscopía electrónica de barrido acoplada a un sistema de detección de rayos X secundarios.

Después de llevar a cabo las simulaciones y tener una idea de los posibles resultados, se diseñaron y se desarrollaron los experimentos apoyando los datos de las simulaciones, con información encontrada en textos bibliográficos sobre la temática, trabajos anteriores y la experiencia personal previa. Tomando estos conocimientos como base, se analizó la aplicabilidad de nuevas metodologías para desarrollar microestructuras novedosas DPADI así como el planteamiento de un proceso de optimización de parámetros clave de proceso en

consonancia con los nuevos descubrimientos que fueran arrojando los experimentos realizados.

Con todo ello, los ensayos realizados tuvieron dos objetivos principales: obtener los valores ideales de los parámetros de proceso para maximizar la tenacidad a fractura y resistencia a impacto de la aleación y adaptar esos valores a procesos óptimos de producción industrial donde entran en juego factores como la rentabilidad y que hacen que los óptimos en este caso difieran de los ideales. En el segundo caso puede que no se obtenga la máxima tenacidad a fractura desarrollada en laboratorio, pero si valores que puedan ofrecer un producto competitivo con un equilibrio entre propiedades y costes. Especialmente importantes son los resultados de calidad, ya que hoy en día las empresas, sobretodo en el marco europeo, otorgan a éste parámetro un valor prioritario. Como consecuencia, no se busca tanto un resultado sobresaliente, si no un proceso que produzca homogeneidad en las mediciones de las propiedades. Este hecho se tendrá en cuenta a la hora de analizar los resultados y proponer los mejores tratamientos encontrados.

Los factores que se analizaron durante los ensayos realizados fueron tiempo y temperaturas de las distintas etapas de proceso. En resumen, primeramente se elaboraron ensayos a ciclos incompletos donde se realizaban simplemente etapas parciales del proceso y donde se mantenían muestras del material a temperaturas en el rango adecuado y durante un tiempo que se mantenía constante durante todos los ensayos para después enfriar bruscamente e ir observando la evolución de la microestructura con la temperatura. Se hizo por consiguiente un estudio de la evolución de las fases con la temperatura dando soporte a las predicciones de las simulaciones.

Una vez comprobado que las simulaciones se ajustaban de forma aproximada a la realidad, se realizaban los tratamientos térmicos completos. En concreto se elaboraron dos tratamientos térmicos completos de ADI a las temperaturas de austenización de 900º C y 950ºC, cuatro tratamientos DPADI con temperaturas de austenización completa para dos niveles, 900º C y 950º C y temperaturas de austenización intermedias para otros dos niveles 775º C y 800º C y por último un tratamiento DPADI modificado siguiendo el proceso Yang. Todas las temperaturas de *austempering* se eligieron a 360º C. Los tiempos de cada de las diferentes etapas se fijaron en una hora. En el texto del proyecto se describen los experimentos de forma más detallada.

El proceso Yang consistió en bajar por debajo de la temperatura de austemperizado durante el temple sin llegar a alcanzar la temperatura de formación de martensita (260º C para el material según estimaciones), mantener esa temperatura durante 5 minutos y posteriormente realizar un proceso de *austempering* convencional a 360º C. Para este proceso se eligieron las temperaturas de 900º C y 800º C respectivamente como las temperaturas de las dos etapas de austenización para la formación de DPADI. Con el proceso Yang se perseguía la formación de una microestructura DPADI mejorada con tamaños muy pequeños de los dominios de la ausferrita, lo que teóricamente debiera haber desembocado en una mejora sustancial de las propiedades. En el texto del proyecto se detalla este último proceso de forma más extendida y se discute y se valora su eficacia.

Ya durante los primeros experimentos se apreció la posibilidad de que la manera en la que estaban siendo cortadas las diferentes probetas de ensayo (en la dirección radial del anillo) podría estar influyendo, como así se comprobó posteriormente, en los resultados obtenidos. Esta influencia se debía principalmente a la heterogeneidad microestructural y composicional

que presentaría el anillo de fundición, tras su estudio, en sus diferentes regiones. Esta heterogeneidades, se cree, son consecuencia directa de las considerables dimensiones del anillo y de gradientes de temperatura durante el enfriamiento por su disposición durante el proceso, apilándose éstos de diez en diez anillos con diferentes fronteras térmicas que impedía la correcta evacuación del calor. No era el objetivo de este proyecto el discutir sobre el enfriamiento de los anillos de fundición y en general sobre su proceso de fabricación, pero si se discutiría con la empresa encargada de la fundición y se aconsejaría sobre la mejora del proceso.

Como consecuencia de estas apreciaciones se planteó un estudio de la influencia en las propiedades a tenacidad de impacto de probetas que fueron cortadas en las diferentes regiones del anillo y siguiendo diferentes direcciones como se detalla durante el proyecto.

Conclusiones

Tras el desarrollo experimental y la recopilación de resultados se pueden sacar tres conclusiones destacables. Una de ellas tiene que ver con la calidad del material de partida, la segunda con la dependencia de la obtención de muestras según que región de un anillo de material base de partida y la tercera, la quizás más destacable pues el autor no tiene constancia de que se hayan obtenido resultados similares con aleaciones ADI, el descubrimiento de una microestructura y su relación con la mejora de ciertas propiedades del material.

Del estudio microestrutural de los materiales base, dos fundiciones dulces ferritico-perlíticas con diferentes composiciones de elementos micro-aleantes, se deduce que las calidades de estos materiales base no son las adecuadas para conseguir las propiedades óptimas de tenacidad tras los tratamientos térmicos para desarrollar aleaciones ADI y DPADI si nos ceñimos a las recomendaciones generales de la bibliografía, sin embargo se obtuvieron resultados prometedores durante los ensayos de impacto tras la aplicación de tratamientos térmicos, aunque no lo homogéneos suficientes según los estándares requeridos. Aún así, el proveedor certificó que las fundiciones suministradas cumplían con los requisitos estándares estipulados según normativa para fundiciones dúctiles. Es reseñable que partiendo de condiciones no idóneas se obtengan buenos resultados pues se puede deducir que mejorando los defectos de partida, los buenos resultados debieran a su vez mejorar de forma apreciable.

Los requerimientos básicos que no posee la aleación base, que se han mencionado de forma breve durante la introducción, se explican con más detenimiento a lo largo del texto de este proyecto. En concreto, y en especial para la primera de las aleaciones que se estudió, se aprecian heterogeneidades tanto en el tamaño de los nódulos de grafito como en la distribución de elementos aleantes en las diferentes regiones intergranulares con la consiguiente apreciación de segregaciones. Estos dos aspectos están muy relacionados ya que son interdependientes unos de otros. Ya que el carbono equivalente, como se argumenta en el texto, juega un papel principal en la precipitación de las diferentes fases, estas heterogeneidades son ampliamente perjudiciales para la obtención de una distribución homogénea de fases con las características requeridas tras los tratamientos térmicos. En particular, se apreció una configuración dendrítica en la distribución de nódulos de grafito, según se describe en la bibliografía sobre las teorías de enfriamiento de las fundiciones dulces nodulares. Estas formaciones dendríticas tan claras y extensas en tamaño son consecuencia de un enfriamiento inadecuado.

Además, en las aleaciones base se apreciaron otra clase de defectos como micro-cavidades debido a contracciones durante el enfriamiento. Estas micro-cavidades son puntos potencialmente peligrosos para la iniciación de fracturas lo cual son altamente perniciosas si el objetivo que se persigue es obtener buenas propiedades de tenacidad a fractura. Además se apreció la existencia de micro-fracturas en la primera de las fundiciones que no se sabe si son propias del material base o fueron creadas durante los procesos de preparación de las muestras para la observación de la microestructura (por un corte excesivamente rápido que indujo a tensiones térmicas dentro de las muestras).

Sin embargo y en comparación con el primero, el segundo material base que se utilizó para llevar a cabo los experimentos, presentaba características mucho más idóneas para los propósitos requeridos, aunque estas características aún diferían de las idóneas. En concreto, la distribución de nódulos de grafito se apreció mucho más homogénea con menos tendencia a formar segregaciones, y el número de micro-cavidades parecía más reducido.

Estas deficiencias en las aleaciones base de partida son difíciles de corregir con los tratamientos térmicos posteriores. Se puede plantear alargar el tiempo y aumentar la temperatura de austenización, aunque esto haría que se produjera una crecimiento excesivo de los granos de austenita lo cual tampoco es beneficioso ya que es a raíz de estos donde empiezan a precipitar las diferentes fases posteriores durante el enfriamiento y por tanto el tamaño de los granos de austenita está relacionado con el tamaño posterior de las diferentes fases y su distribución en la microestructura, aspecto que a su vez influye en las propiedades. Por ejemplo, está demostrado que el tamaño de la ausferrita afecta a las propiedades mecánicas de los ADI y que preferiblemente se requieren tamaños pequeños de esta fase para obtener buenas propiedades de tenacidad. Además, la ferrita pro-eutectoide de los DPADI se desea que precipite en los bordes de grano de esta austenita recristalizada tras el tratamiento de austenización. La ferrita pro-eutectoide está relacionada con el anclaje de dislocaciones que están a su vez relacionados con el crecimiento de fisuras, con lo que su presencia en la microestructura es muy apreciada para la mejora de las propiedades mecánicas de los ADI. Cuanto menor sea el tamaño de estos granos de austenita recristalizada, mayor será la red de ferrita pro-eutectoide que precipite y más interconectada estará ésta, por lo que se puede esperar una mejora sustancial de las propiedades mecánicas por el aumento de zonas limitantes al crecimiento de fisuras.

Enlazando con lo anterior y relacionando las malas propiedades microestructurales de los materiales de partida con un posible enfriamiento realizado de manera incorrecta, se centro la atención en el proceso de fabricación de los añillos. Se llegó a la conclusión que debido a su tamaño podrían existir heterogeneidades microestructurales y de composición en las diferentes regiones del anillo debido a los procesos de colada y gradientes de temperatura durante el enfriamiento. De la información recabada de los responsables de la empresa encargada de la realización de los anillos, se deduce que la zona con mayor velocidad de enfriamiento es la correspondiente a la superficie de radio máximo, siendo la base y la zona superior, así como la zona del radio interior las segundas que sufren una velocidad de enfriamiento mayor, quedando las zonas centrales y de interior del anillo como los puntos donde se ha producido un enfriamiento más lento.

Según se estaban cortando las piezas para los primeros ensayos de tenacidad de impacto de piezas sin tratar o con tratamientos térmicos de prueba, la zona central o de rotura de estas probetas coincidía con la zona de enfriamiento más lento. Mediante estudios de

microestructura, estas zonas centrales son las que presentaban una microestructura más desfavorable con las propiedades a medir, por lo que se planteó el estudio de las mismas propiedades en probetas que hubieran sido extraídas de diferentes zonas del anillo para ver si éstas se veían afectadas de forma significativa. Se realizaron cortes longitudinales en la dirección tangente a la radial en las zonas exterior, interior y central, y cortes en la dirección radial y se compararon sus propiedades a impacto, así como las superficies de fractura y las microestructuras. Se comprobó que había una diferencia significativa en los valores obtenidos a tenacidad a impacto entre las probetas que se habían obtenido de zonas exteriores y probetas que se habían obtenido de zonas interiores, siendo los primero más elevados que los segundos. Tras un estudio de las superficies de fractura y microestructural de las diferentes muestras, se planteó como posible causa una mejora en la microestructura, tanto en homogeneidad como en tamaño de dominios microcristalinos, en las piezas exteriores. Estas presentaban menores porcentajes de carburos precipitados y eran más homogéneas lo que provocaba una rotura dúctil sin presencia de clivajes, factor que si se detectó en las superficies de rotura de piezas extraídas de la zona intermedia del anillo.

Si bien la precipitación de carburos supuso el principal inconveniente para no obtener las propiedades en sus rangos más prometedores a partir de las aleaciones de partida y tras los tratamientos térmicos propuestos, una de las conclusiones más relevantes de este proyecto fue la detección de una microestructura novedosa que podría estar salvaguardando y minimizando el efecto pernicioso en las propiedades de tenacidad en las aleaciones DPADI. A pesar de no conseguir una abundante precipitación de ferrita proeutectoide en los bordes de grano, microestructura que se perseguía como uno de los objetivos de este proyecto, la escasa cantidad que precipitó lo hizo rodeando a los carburos. Este hecho, se presupone, proporcionó una protección frente al inicio y al avance de las fracturas y de absorción de energía de impacto tan precaria en los frágiles carburos, frecuentemente puntos de iniciación de estas fracturas.

Tras los ensayos a impacto se comprobó que, en comparación, los resultados para las aleaciones DPADI desarrolladas en los laboratorios de la universidad eran muy similares a los obtenidos de una aleación ADI realizada en condiciones de una ambiente industrial. Sin embargo la homogeneidad y reproducibilidad de resultados con las aleaciones DPADI fue mayor que con las de ADI tradicionales. Como conclusión se estimó que estas diferencias poco significativas se deben a que hay una fuerte influencia de las malas calidades del material base de partida que podría estar enmascarando los mejores resultados esperados con las aleaciones DPADI. Además, las condiciones durante los tratamientos térmicos para desarrollar el ADI de manera industria, fueron mejor controladas y más homogéneas en todo el proceso derivado de la mayor estabilidad térmica de hornos con mayores capacidades y que el proceso se pudo hacer en una línea de continuo sin enfriamientos bruscos derivados del traspaso de las probetas por los diferentes hornos en el laboratorio.

Futuras investigaciones

Tras la realización de este trabajo se propuso el desarrollo de nuevos anillos con procesos y composiciones mejoradas con la finalidad de minimizar las deficiencias detectadas en los anillos utilizaos. En concreto se revisó los contenidos en Si, Ni, Mo y Mn ya que estaban fuera de los rangos recomendados por el sector y son en cierto modo responsables de algunos

de los defectos observados en el material, sobretodo en lo referente a la formación de carburos, principales responsables de no haber obtenido las mejores propiedades a tenacidad.

En cuanto a la caracterización de propiedades mecánicas, solamente se han ofrecido datos sobre ensayos de tenacidad de impacto. Se debieran hacer estudios más exhaustivos con ensayos de tenacidad a fractura. Estos al final no se llevaron a cabo por falta de tiempo y complejidad a la hora de mecanizar y preparar probetas destinada a tal fin a partir del anillo suministrado.

A día de hoy, se tiene constancia de que en base a este proyecto se han desarrollado nuevas aleaciones con resultados muy prometedores, mejorando de forma sustancial los obtenidos en este trabajo.

Improving the Fracture Toughness of Dual-phase Austempered Ductile Iron

JAVIER HIDALGO

No. 2008:5
Masters Thesis: 27/2008
Department of Materials and Manufacturing Technology
Chalmers University of Technology
SE-412 96 Göteborg
Sweden
Telephone: + 46 (0)31-772 12 50

Printed by Chalmers Reproservice
Göteborg, Sweden 2008

Improving the Fracture Toughness of Dual-phase Austempered Ductile Iron

JAVIER HIDALGO

Department of Materials and Manufacturing Technology

Abstract:

Dual Phase Austempered Ductile Irons, DPADI alloys have a microstructure with a combination of ausferrite and pro-eutectoid ferrite along with graphite and residual/retained austenite. To reach this particular microstructure ductile iron is austenized in the austenite-pro-eutectoid ferrite region before being carried though an isothermal heat treatment somewhere between the bainite-start and martensite-start temperature. The special austenization procedure makes DPADI prime candidates for applications that require a high fracture toughness resistance like suspension components. The aim of this study is to identify features in the microstructure of dual-phase ADI that directly affect the fracture toughness of the investigated alloys. To do this alloys subjected to various ADI heat treatments have been impact tested and thereafter analysed by light optical microscopy, X-ray diffraction and hardness testing. From Thermo Calc Modelling and experimental investigation of the austenite to pro-eutectoid transformation zone, it was found that an austenitization temperature of 790°C resulted in a microstructure, which avoided perlite formation. In the investigation of industrial ADI heat treatment it was found that the last and first to cool regions of the sample geometry had an impact toughness of around 70 and 100 J, respectively. Furthermore a comparison of conventional ADI and DPADI heat treatments showed that the DPADI heat treatment had an impact toughness of 90 J with a scatter of ±15 J, whereas the conventional ADI heat had the same impact strength with >±20 J scatter. This reduced scatter was attributed to the encapsulation of the detrimental Mo-rich carbides by pro-eutectoid ferrite, after light optical and scanning electron microscopy. Moreover, it was observed that detrimental reductions in impact toughness resulted in areas where slag inclusion, carbides or voids were present. Consequently, it is recommended that more attention is directed to the ductile iron casting process to safeguard the success of the ADI heat treatment

Preface

This diploma thesis is based on work carried out in the Department of Materials and Manufacturing Technology at Chalmers University of Technology, during the late autumn of 2007 and early spring of 2008. The work is performed in cooperation with the Swedish ADI industry.

Acknowledgements

I want to take advance of the following lines to express my gratitude with all the people which contribute to the success in finishing the present work.

My first mention and special thanks are destined to my supervisors in Sweden, Henrik Borgström and Doc. Kenneth Hamberg from the department of Materials and Manufacturing Technology of Chalmers, for their guidance and experience on the topic. Their constructive criticism and discussions during the work served me to achieve a high level of understanding and as a continuous motivation even when the results weren't as satisfactory as expected in the first instance. I wish also to thanks Prof. Lars Nyborg, from the department of Materials and Manufacturing Technology of Chalmers, to give me the opportunity to carry out this work and my supervisor in Spain, José Manuel Torralba from the Materials Engineering and Science of Carlos III University, Madrid, for giving me the opportunity to study abroad and for supporting me with this work and helping me with setbacks during my stay in Sweden.

I also want to mention the staff at the department of Materials and Manufacturing Technology who despite of not being involved directly in this work, still unselfishly helped me with my tasks. To all of them thanks, but I'm especially grateful for the support provided by Dr. Yiming Yau and Urban Jelvestam during the most demanding experiments. I also appreciated the precious time stolen from Bengt Stenborg from ESAB who conducted the impact toughness measurements.

It was priceless all the affection and support received from my parents, Alfredo and María Teresa, to which I couldn't find better regard than dedicate them this work, culmination of my Industrial Engineer Specialized on Materials degree. In addition all the patient and understanding showed by Elena Gil Molina during last months helped me as an extra motivation to finish my work. I want to dedicate to her this work too.

Javier Hidalgo García

Table of Contents

1. Introduction

Austempered Ductile Irons (ADIs) comprises a family of Fe-C alloys with a characteristic microstructure that provides them with suitable properties for many industrial applications. These properties include high strength, high ductility, high toughness, low mass, good wear resistance and good machinability all possible at a lower price compared to common steel and aluminium. This is the result of its microstructure that consists of spheroidal graphite in a matrix of bainitic ferrite and a carbon-saturated austenite, which is also referred as an ausferrite microstructure. To reach this particular microstructure ductile iron is carried though an isothermal heat treatment somewhere between the bainite-start and martensite-start temperature; the austempering heat treatment.

ADI have been recognised as a potential engineering material since its discovery in the early 1960's, but due to its complexity, it is believed that it has not been exploited to its full potential yet. Therefore, additional research into this field is well motivated. An example of this is the innovative dual phase austempered irons, DPADI, that has a greater ductility than the conventionally heat treated ADI, due to its microstructure with ausferrite and allotropic or proeutectoid ferrite along with spheroidal graphite and carbon-saturated austenite. This makes DPADI prime candidates for applications that require a high fracture toughness resistance like suspension components.

Even if a lot of studies have been devoted to the control of austenite volume fraction and carbon content during the ADI process [1,2], only a few attempts have been made to control ausferrite and pro-eutectoid ferrite volume fractions in DPADI [3]. Consequently, few studies have attempted to relate ferrite volume fractions with the material's mechanical properties in DPADI.

Therefore, the aim of this study is to identify features in the microstructure of DPADI that directly affect the fracture toughness of the investigated alloys. To do this, alloys subjected to various isothermal heat treatments have been impact tested and thereafter analysed by light optical microscopy, X-ray diffraction and hardness testing. The present work is a continuation on Caroline Glondu's master thesis [4], which was on common ADI heat treatments.

2. An Overview of Austempered Ductile Irons

ADI is the acronyms of Austempered Ductile Iron, concerns a big family of materials within the ductile irons with a common exponent, the austempering heat treatment. This heat treatment leads to properties like, high strength-to-weight ratio, ductility and toughness, fatigue strength, good wear resistance and machinability, all achieved at a lower price compared to common steel and Aluminium [5].

Therefore, ADIs are suitable to cover wide range of applications and requirements. Essentially ADI is gaining more and more acceptance among the automotive, trucks, military, railroad, and construction sector, being a competitive alternative to conventional metals and alloys. Such materials include conventional ductile irons, cast and forged aluminium and many cast and forged steels. Consequently, the interest for ADI research and development today is nearly as high as it was during the time of its discovery.

2.1 Main Characteristics

The most important characteristic of ADI is that its yield strength is over three times that of the best cast or forged aluminium. In addition, even if ADI weighs about 2,4 times more than aluminium it is 2,3 times stiffer and considerably cheaper. Compared to steels, ADI usually has a higher specific strength, despite of having about 10% lower density. Nevertheless, most of the time ADI alloys are superior to its engineering material counterparts, if price is considered.

In addition, ADI fracture toughness and fatigue properties, equals or betters that of forged steels. Typical values for fracture toughness ranging 55-102 $MPa \cdot m^{1/2}$ [1] at room temperature, but it is believed that values higher than 100 $MPa \cdot m^{1/2}$ could be obtained, for special ADI alloys like Dual Matrix ADI. Consequently, big expectations motivate an exhaustive investigation into factors related with these properties, which is the main incentive to carry out this thesis work.

2.2 Uses and Applications

Since the discovery of ADI in the early 1930's, only a small fraction of the total production of ductile cast irons, DI, is used in ADI applications. Total wide-world production was estimated in 1998 to approach 100000 tonnes annually, which corresponds to 1% of the total DI production. Today this figure is basically unchanged, despite of a greater confidence in the ADI material.

This fact seems disheartening, since excellent and competitive ADI properties may reflect a higher level of acceptance within the industrial world. To increase the acceptance for ADI, component manufacturers need to gain more experience from producing large series of parts. The monetary risk factor, associated with new material introduction, frequently pleads on conservationism attitudes if material do not perform well enough; large cost when correcting problems is associated, and many times manufacturers think is not worth to afford the experience required. In ADI case, there is a lacking of knowledge concerning machining optimization parameters and cutting tool materials selection, just to mention a few.

Nevertheless, ADI is currently winning market shares, because of new researches and an attractive cost ratio mixed with a wide versatility in design possibilities. The majority of this

market share increase has been seen in the automotive industry, which is finding in ADI the perfect candidate to fulfil a great amount of its components requirements. Therefore it comes as no surprise that approximately 40% of the demand ends up in light vehicles, heavy trucks and bus components.

Suspension components, wheel hubs, brake callipers, knuckles, sway bar components, differential gear, engine and accessory brackets, engine mount, crankshafts, and control arms, are some common examples of ADI components in the automotive industry. Is important to remark that all these components use to be completely mechanized to create free-defect surfaces, or at least they are commonly mechanized in all areas where the stresses are high. Machinability is thereby a much desired property as well, and ADI fulfil this requirement in a great extent.

Gears represent some of the best known, most widely publicized and high potential uses of ADI, replacing typical forged steel with highly satisfactory results. Crankshaft is another potentially significant application for ADI. Studies conclude that ADI crankshafts exhibit properties comparable to or better than the best forged and heat treated steel ones, both for fatigue loads and torsion forces support requirements. Relevant importance is also given to friction elements, with a clear ADI potential, due to its abrasion resistance.

To conclude this overview of ADI applications, remember that ADI is widely used to produce high strength parts replacing components made of steel and aluminium. Even though toughness and elongation are primary requirements for high load applications, further improvements on these properties with DPADI, would be a step forward in order to widen the ADI applications. If this is done, apart from mechanical advantages, weight optimization could also be achieved. Reduction of weight allows not only developing more potent vehicles, but also helps to reduce oil consumption with the inherent benefit of saving money for the final client and contributing positively to the reduction of CO_2 emissions. All of these factors could empower the ADI industry, and those companies that invest in ADI research could obtain a privileged benefit if the promising results can be obtained and implemented.

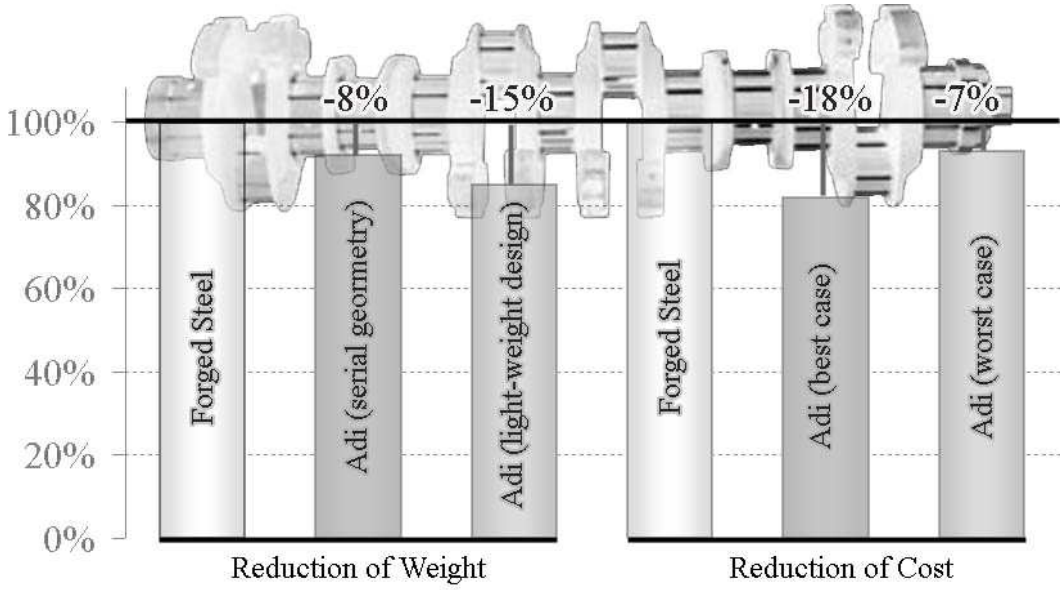

Figure 1 ADI crankshaft mass and cost comparison with conventional steel crankshaft. ADI crankshaft shows superior dynamic properties compared to forged steel, summed to acoustics and damping behaviour comparable to actual production component for Chrysler Motors. Interpreted from [6]

3. Material Aspects in Austempered Ductile Irons

Most studies underlie the importance of ADI heat treatments to achieve suitable final properties, but sometimes forget to address the importance of a good base material to ensure that these are also repeatable and reliable. Unfortunately, cast iron is one of the most complex alloys that can be cast, thus it cannot be treated as a simple Fe-C-Si alloy. In the present work the stable iron-graphite eutectic form (with spheroidal graphite), the so-called ductile iron, is going to be studied and used to develop ADI materials with high levels of fracture toughness. Is not the aim of this thesis work to study cast iron solidification, but to better understand the posterior steps of ADIs mechanical properties, a brief overview will be given to elucidate the process and the final cast iron microstructure.

In addition, a good casting control is essential to obtain good results to avoid resulting casting defects that would otherwise impair the requirements set on the ADI component. Therefore, as most cast solidification defects cannot be corrected through heat treatments some recommendations must be fulfilled in order to achieve a suitable base material. These recommendations include [5,7]:

- Produce a casting lacking of surface defects, especially in high stressed areas, that could induce to lower its resistance to static and dynamic loading.
- A nodularity greater than the 90%, meaning that at least the 90% of the nodules should have spheroidal shape (type I or type II)
- A minimum of $100 \cdot mm^{-2}$ nodule account
- Consistent chemical composition, homogeneous and stable from batch to batch.
- Essentially free of primary carbides, porosity and inclusions.
- Consistent pearlite/ferrite ratio
- A control of inoculation, poring temperature, etc. during DI production → Close control of the process parameters in the foundry.

3.1 The Ductile Irons

Fig. 2 shows the wide family of cast iron representing the most important members and classifies them depending on graphite shape and matrix type.

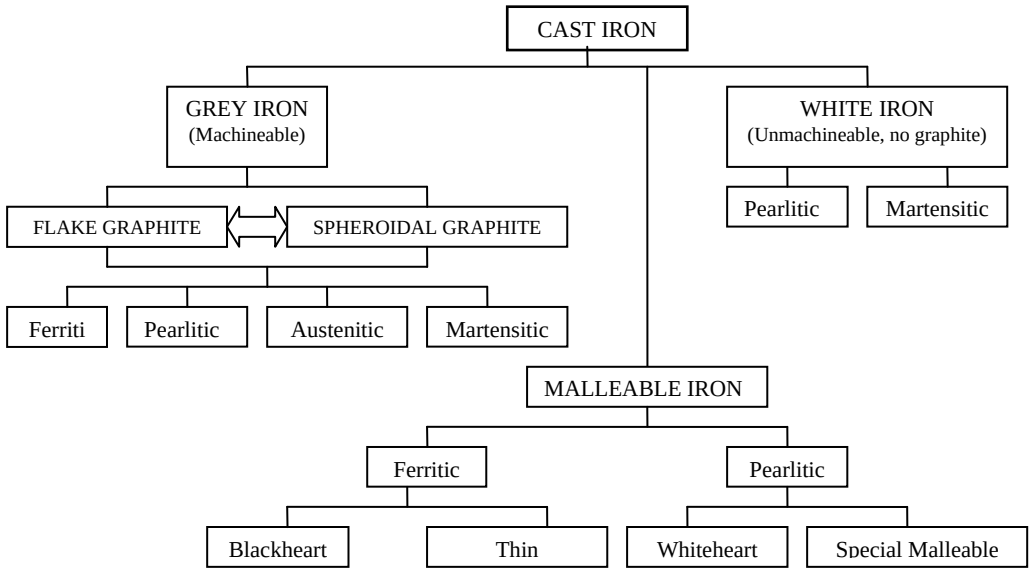

Figure 2 Cast iron family tree.

The microstructure, in which the cast iron melt solidifies, depends strongly on two main factors: cooling rate and chemical composition. Moreover, the silicon addition facilitates graphite formation and in conjunction to the amount of carbon also the presence of Perlite. The graphite formation is also dependent on the cooling rate; if this is decreased the tendency to form graphite will increase as seen in Fig. 3.

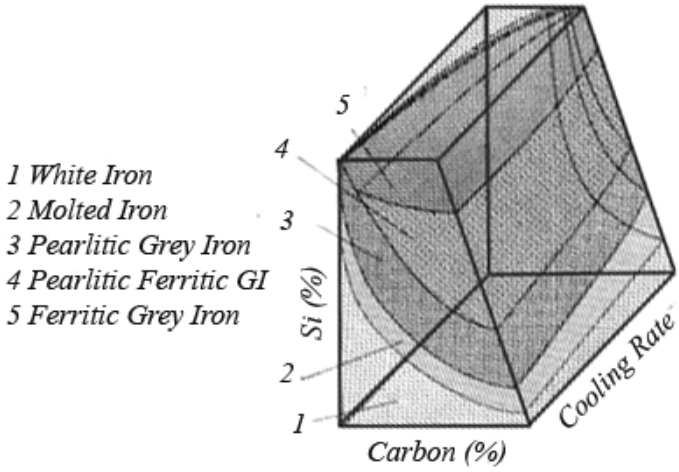

Figure 3 Different types of irons depending on Si%, C % and cooling rate. Interpreted from [8]

3.2 Casting Requirements

In this section a brief overview of casting requirements will be given.

Graphite Shape

The graphite morphology of iron is affected by the melt composition and the solidification velocity. The graphite morphology changes from lamellar, LG, to compacted, CG and finally spheroidal, SG, when an increasing trace amount of Mg or Ce is added to the melt. Note that the influence of other alloying elements is not considered here. The graphite morphology affects the toughness and fatigue resistance of cast iron and hence ADI. Increased notch effect is observed for irregularly shaped graphite nodules, which can be detrimental for the mechanical properties, like the fatigue resistance. However, a nodularity exceeding 90-95% can be achieved in foundries that produce high quality castings.

Nodular Count and Segregations

The number of nodules per unit volume is another important quality parameter. This parameter reflects the segregation that may occur within the cast structure. From practical point of view segregation means that there are composition gradients in the structure. This composition gradient could imply consequences during posterior heat treatment in the different matrix constituents' composition and distribution, which is related with carbides formation that is detrimental for mechanical properties. Therefore, segregation induced during solidification should be avoided for most cases apart from when it is an advantage for the structures development. Furthermore, high silicon content in conjunction to the inoculation effect of Ca, Ba, Al and Bi in welding and a fast cooling rate, is related to an increased nodule count as well as a reduced graphite size [9], which are beneficial for the properties of cast iron that is used for ADI.

Casting shrinkage

This type of casting defect refers to the total volume reduction of a casting, due to partial reductions at each stage of solidification [10]. They result from an abrupt change in section size, from an isolated heavy section, which cannot be fed. An unsuitable composition for a given section or pouring too hot or too cold [11,12] could also cause casting shrinkages.

Inclusions

Inclusions can be defined as a non-metallic and/or intermetallic phases embedded in the matrix [10]. In almost all circumstances in metal casting, they are considered to be detrimental to the performance of material; with some properties being more sensitive to their presence like elongation than other properties like as tensile strength. These inclusions always appear in the eutectic s. In these regions the amount of segregation ring elements are high

Porosity

This defect is a characteristic of being porous, with voids or pores. They result from trapped air or casting shrinkages [10].

3.3 Cast Iron Solidification Theories

The solidification mechanisms of a ductile iron and the resulting microsegregations are some aspects of its metallurgy that still remains not thoroughly understood, despite significant research efforts. Recent etching techniques like hot shakeout [12] combined with colour etching have allowed new solidification theories to be developed in this field. Concretely, three theories exist, two are classical and the last has been proposed by Boeri and Sikora [13]. Solidification theories are significant to propose mathematical models that allow predictions on the grain size and nodules distribution in the casting process.

Uninodular model (UN)

Some studies, especially those who focused on modelling of microstructure and segregations, use the early model proposed by Patterson and Scheil, which explains the solidification process as units formed by SG nodules created first in the melt and then enveloped by austenite shells[14]. Measurements of the graphite's radii and γ shell, show that the ratio between these radii remain constant ($r_\gamma / r_{GR} = 2.3$). A large number of mathematical models to predict grain size and segregation dispersion are based on this model, but actual observations indicate that this model fail to predict these variables [13,14,15].

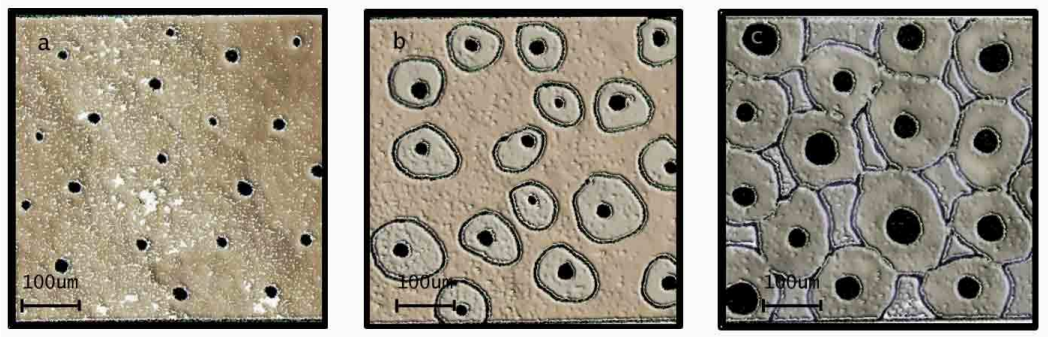

Figure 4 Uninodular Model solidification schema. Based on [13]

Multinodular model (MN)

This model is the favourite of amongst solidification experts who believe that a cluster of austenite dendrites and graphite nodules interact to form the solidification units. These units are described as engrossed austenite dendrites, which contain several graphite nodules. Based on the observation of microsegregation patterns, the MN model coincides quite well with actual observations made after the use of new etching techniques. However, these still have weak points that require further explanation.

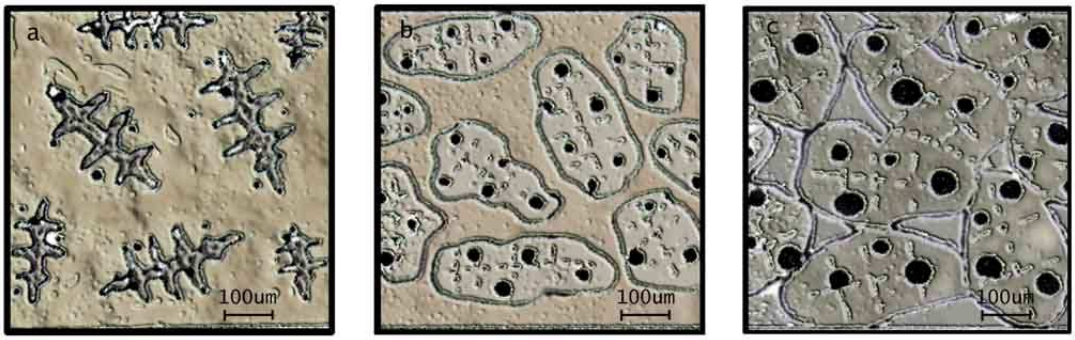

Figure 5 Multinodular Model solidification schema. Based on [13]

Independent nucleation model

The independent nucleation model, IN proposed by Boeri and Sikora [13], tries to address and correct the weak points of the MN model. According to this model, the solidification begins with the independent nucleation of austenite and graphite from the melt. Thereafter the austenite dendrites grow and envelope most of the graphite nodules. Further graphite growth is controlled by the diffusion of carbon from the liquid to the nodules, trough the austenite.

Figure 6 Independent Nucleation solidification model. Based on [13]

3.4. The Alloying Design of Austempered Ductile Iron

The composition of an ADI cast is similar to ductile irons, apart from that it is harder to propose a correct percentage for the alloying elements, because of the ADIs heat treatments. Designing an ADI alloy without sub-optimising is a complex task. When selecting a composition, elements that adversely affect casting quality, those that generate undesirable graphite morphologies, promote the formation of carbides and inclusions, or shrinkages should be limited. Moreover, a composition selection should consider posterior heat

treatments and thus the final ADI microstructure, as this determines the mechanical properties. For example, perlite should be avoided in the final microstructure as it is brittle. Therefore, particular elements like Mo and Ni are added to the melt to suppress the perlitic reaction so that austenite can transform into bainite instead, which improves the hardenability.

The ADI process depend principally on the carbon diffusion (the carbon equivalent), which also dictates the carbide formation of some elements and also segregations. Other considerations, like the section size and the type or the severity of the austempering, must be also taken in account when determining the alloying elements. When allowing, it is also important to notice that the properties after austempering depends as much on the process parameters as the compositional threshold of the alloying elements. Furthermore, some of the elements used in the cast are considered to be "strategic" elements, whose price variation could mean that they could be replaced by other materials if their market price is too high. Only the minimum amount of alloys required to fulfil the requirements should be employed. Excessive alloying only increases the cost and difficulty of producing high quality Ductile Iron for ADI [1]. Moreover, distinctions are made from those elements that help to obtain a proper cast and those that control the hardenability of the iron and the properties of the transformed microstructure. The principal ADI alloying elements are summarized below.

Silicon promotes graphite formation. It decreases the solubility of carbon in austenite so the rejected carbon concentrates in the melt to allow the graphite nucleation. This element also increases the eutectoid temperature, and inhibits the formation of bainitic carbide. With higher silicon contents the ADI impact strength increases and the ductile brittle transition temperature is lowered. This can be explained by greater graphite nodule count and smaller graphite nodule size, lower presence of carbides and higher ferrite content induced by the high silicon content [16].Silicon should be controlled closely within the range 2.4~2.8 % to achieve the desired carbon equivalent.

Manganese is an inexpensive substance that strongly increases hardenability. Its addition is useful to prevent perlite formation, especially in thick section. However, a too high content causes it to segregates to intercellular regions [8,17], where it forms carbides and if the segregations concentration is sufficiently high, could lead to shrinkage and unstable austenite. To maximize the mechanical properties and reduce the sensitivity of the ADI to section size and nodule count, it is advisable to restrict the manganese level in ADI to less than 0.3%. One way to achieve this is to use high purity pig iron in the ADI charge [5], which offers the advantage of diluting the manganese in the steel scrap to desirable levels as well as controlling undesirable trace elements. Moreover, it has been well documented [17] that manganese, like carbon, shifts the isothermal diagram to the right, which increases the incubation time for bainite transformation

Molybdenum is the most powerful hardenability enhancer in ADI apart from carbon. Typically it is required in heavy sections castings to prevent the formation of perlite. However, like manganese, it segregates at cell boundaries during solidification to form carbides, which decreases both tensile strength and ductility. Therefore the molybdenum content should be restricted to less than 0,2 wt% in heavy section castings and avoided if necessary due to its cost.

Copper addition to ADI doesn't significantly affect hardenability on its own, but in combination with manganese and molybdenum, there is a useful increase in the maximum section size that can be austempered successfully [18]. No significant effect on the tensile

properties is observed when copper addiction in these percentages, but an increment of ductility at austempering temperatures below 350ºC. This could be explained because of copper doesn't segregate us much as other elements like Mn, and it partitions preferentially into the solid phase [1]. Copper is usually added in amounts ranging from 0,5 to 0.8 wt%.

Nickel has the same function as copper in ADI. For austempering temperatures below 350ºC nickel reduces tensile strength slightly, but increases ductility and fracture toughness. Additions of nickel usually vary form 0,5 to 2 wt%.

Other elements like chromium and vanadium could also be added also to improve hardenability; however, this is not common since these are strong carbide-formers.
As discussed earlier, it is important to use an optimum amount of alloying elements to obtain the required austemperability and to suppress or minimize segregations. It is also crucial to consider the sample geometry to be austempered to avoid perlite formation, for that reason, the critical bar diameter, must be estimated according to equation (1) [19]:

$$D_C = 124 \cdot C_{\gamma^o} + 27 \cdot (\%Si) + 22 \cdot (\%Mn) + 16 \cdot (\%Ni) + 25 \cdot (\%Mo) + 1.68 \cdot (10 - 4 \cdot T_{a2}) + 1$$
$$+ 2 \cdot (\%Cu)(\%Ni) + +62 \cdot (\%Cu)(\%Mn) + 88 \cdot (\%Ni)(\%Mo) + 11(\%Mn)(\%Cu) + \quad \textbf{(1)}$$
$$+ 127 \cdot (\%Mn)(\%Mo) - 20 \cdot (\%Mn)(\%Ni) - 137$$

Where T_{a2} is the austempering temperature and C_{γ^o} is the carbon content of the austenitic matrix. The carbon content depends on the austenitising temperature (T_γ) and the iron. This dependence is reflected on equation (2) [19]:

$$C_{\gamma^o} = \frac{T_\gamma}{420 - 0.17 \cdot (\%Si) - 0.95} \quad \textbf{(2)}$$

Most studies concluded that high carbon equivalent irons must be used to avoid significantly as-cast carbide precipitation, which decreases the strength, ductility and machinability. A high carbon equivalent is related also with the increment in the nodule count [16].

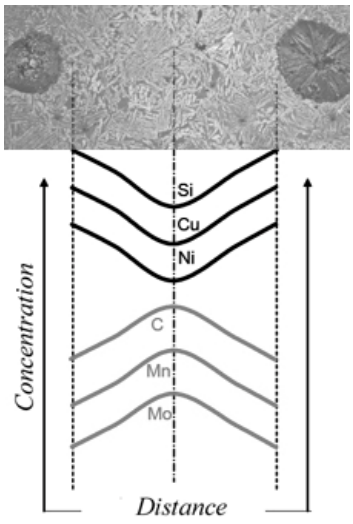

Figure 7 Common elements distribution between two graphite nodules. Interpreted from [7]. These patterns of elements concentrations will modify the carbon content within different areas of the matrix creating inhomogeneities in the microstructure.

4. Ordinary and Dual-phase Austempered Iron Microstructures

In this chapter, ADI and DPADI microstructures are presented and compared.

4.1 Phases Found in Austempered Ductile Iron Microstructures

Austenite is normally a high temperature phase consisting of carbon dissolved in iron, which is formed in the first steps of the heat treatment when the temperatures exceed the austenizing temperature. Its stabilization in the matrix and its presence in the final microstructure, depend on its carbon content. The carbon content of the austenite is the result of carbon diffusion mainly from the graphite nodules during the initial stages of austenization, but it is also affected by the posterior rapid cooling to the austempering temperature. The carbon supersaturation of austenite depresses the start of the austenite-to-martensite transformation far below room temperature and leads to that part of the austenite remains untransformed after the isothermal heat treatment, even if the majority of the austenite transforms into acicular ferrite. Therefore, high carbon contents are needed to stabilize austenite, but the presence of some alloying elements aids this stabilization further. The untransformed austenite is also referred as “residual austenite”, or high-carbon stabilized austenite. In austempered ductile irons, stabilized austenite, in volume fractions up to 40% in lower strength grades, improves toughness and ductility and response to surface treatments such a fillet rolling.

Bainitic ferrite can be distinguished as two types; lower and upper bainite. They differ by the metallographic and morphologic aspect, which is a consequence of the ADI conditions like austenitization and austempering temperatures and times, but also by the austenite grain size. The type of austenite present in the final ADI microstructure will determines static and dynamic fracture toughness at different temperatures [1], as well as other mechanical properties, affected by the chemical composition.

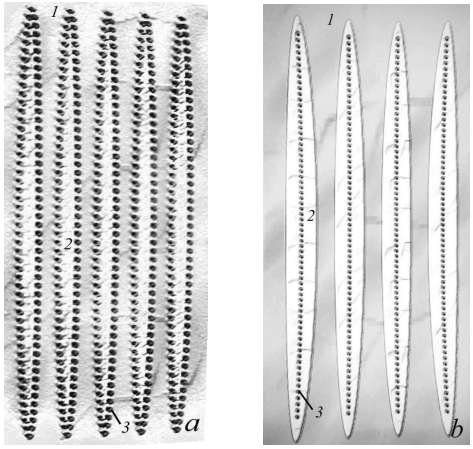

Figure 8 a) Upper Bainite, b) Lower Bainite. 1) Austenite, 2) Ferrite, 3) Carbide. Interpreted from [4]

Both, upper and lower bainite, are an aggregate of acicular ferrite and carbides, but the difference of these two structures reside in one hand in the location of precipitation of carbides in the structure, and in the other hand, in the amount of untransformed austenite.

As showed in Fig. 8, Lower Bainite consist in plate-shaped bainitic ferrite unit arranged in sheaves with the carbides forming about 40-60 degrees angle lattice (depending on the cast iron and the process carried out) from the growth direction at the centre of bainitic ferrite, whereas upper bainite consists on needles or lath of bainitic ferrite, often arranging in

sheaves, containing rod-like carbides which are orientated in the direction of the lengthening growth and at the edges of bainitic ferrite.

Graphite Nodules are usually spheroidal in shape, due to its natural growth habit of the graphite in liquid iron, but its morphology can range from spheroidal shape to flake. The shape plays a significant role in determining cast properties in cast irons; graphite flakes acts like cracks within the iron matrix, while graphite spheroids acts like "crack-arresters". In fact, typical ADI casts are based on spheroidal graphite, SP, which lead to their low density. Using SEM analysis it was determined [14] that SG nucleates on duplex sulphide-oxide inclusions with a diameter approximately 1 μm. The graphite nodule core is made of Ca-Mg or Ca-Mg-Sr sulphides, while the outer shell is made of complex Mg-Al-Si-Ti oxides. Even if it is not entirely clear, is believed that rejection of C and Si by the solidifying austenite imposes a high solute undercooling on the proximity of the γ phase, favourable for graphite nucleation [14,42].

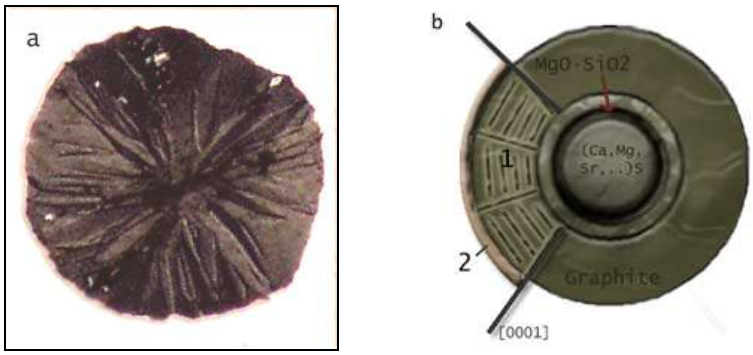

Figure 9 a) LOM observation of a spheroidal graphite nodule, b) Schematic of a graphite nodule shell. 1 indicates inner graphite shell with typical layer growth, 2 is the outer shell with different microstructure.

4.2 The ordinary Austempered Ductile Iron Microstructure

The common austempered ductile iron microstructure contains spheroidal graphite (resulting from the cast iron) embedded in a matrix which is generally a mixture of phases generated in an especial heat treatment. The most desirable phase of an ADI is normal referred to as "Ausferrite", but is also called "Bainite" in some references because of its metallographic similarity with this later. The Ausferrite consists of a mixture of bainitic ferrite, also called acicular ferrite, and a high-carbon retained austenite. The importance of this structure and the presence of stable austenite in the microstructure related with some mechanical properties will be discussed.

There are other constituents in the ADI microstructure. Martensite, carbides and perlite could appear and their presence could degrade the mechanical properties. Also cementite, which is a non desirable phase for fracture toughness, could appear.

The proportion of these main phases depends on many variables like the chemical composition of the cast ductile irons, but it has have been demonstrated that it mostly depends on the "Austempering" heat treatment. Bainitic ferrite is typical generated from austenite during the austempering process after a quick quenching below the bainite-start temperature. Of course the resulting microstructure will be influenced by the process time and temperature, but this is discussed later.

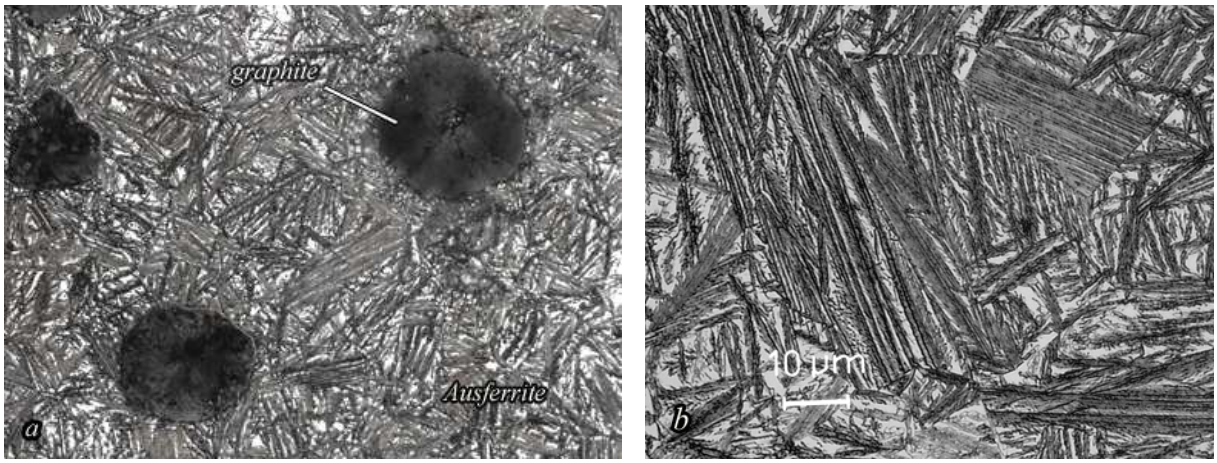

Figure 10 LOM microscopy of an ADI. a) The graphite nodules are totally imbibed by ausferrite microstructure. b) Enlargement of ausferrite areas; the ferrite needles growth till find a grain boundary.

4.3 The Dual-phase Austempered Ductile Iron Microstructure

Dual Phase austempered ductile iron, DPADI, is commonly referred to a special ADI microstructure obtained after some special and unconventional austempering processes. It can be described as ausferrite matrix containing networks of allotropic ferrite. This mix of phases has been proved to have improved fracture toughness compared with normal ADI where "only" ausferrite phase is present [3].

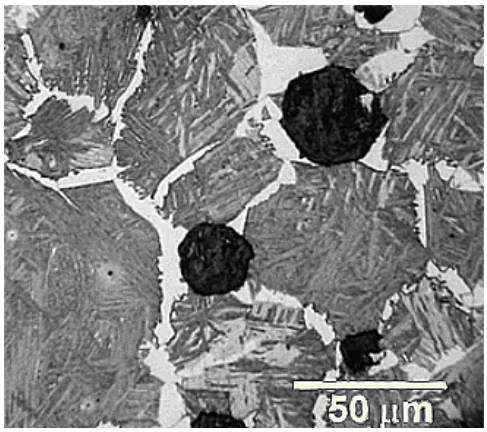

Figure 11 Dual Phase ADI microstructure [20]. The bright white zones are ferrite, the grey areas are ausferrite, and the black rounded shape dots are the graphite nodules

Having a look on the phase diagram for Fe-C-Si, Fig. 12, and focusing on the binary system Fe-C (cutting slides from different concentration of Si) a region called "the intercritical interval" can be seen where ferrite, austenite, and graphite coexists. This region is limited by both, the upper and the lower critical temperatures, which define the beginning of the transformation of austenite into ferrite during cooling. The position and extension of this interval is significantly modified by chemical composition of the alloy, thus a particular determination of this interval should be carried out experimentally or by modelling for each alloy composition. Moreover, this composition and/or temperature interval should be explored in order to achieve various novel microstructures, which could provide a wide range of properties that are competitive or better than those found in conventional ADI microstructures.

Recently some authors [21] have reached a very special DP (dual phase) microstructure with continuous and well defined ferrite networks morphologies seen in Fig.11. Here the ferrite precipitates at the former grain boundaries of recrystallized austenite, instead of around the graphite nodules, which is likely to lead to improved mechanical properties. Consequently, these microstructures could be fruitful in obtaining microstructures with improved levels of fracture toughness.

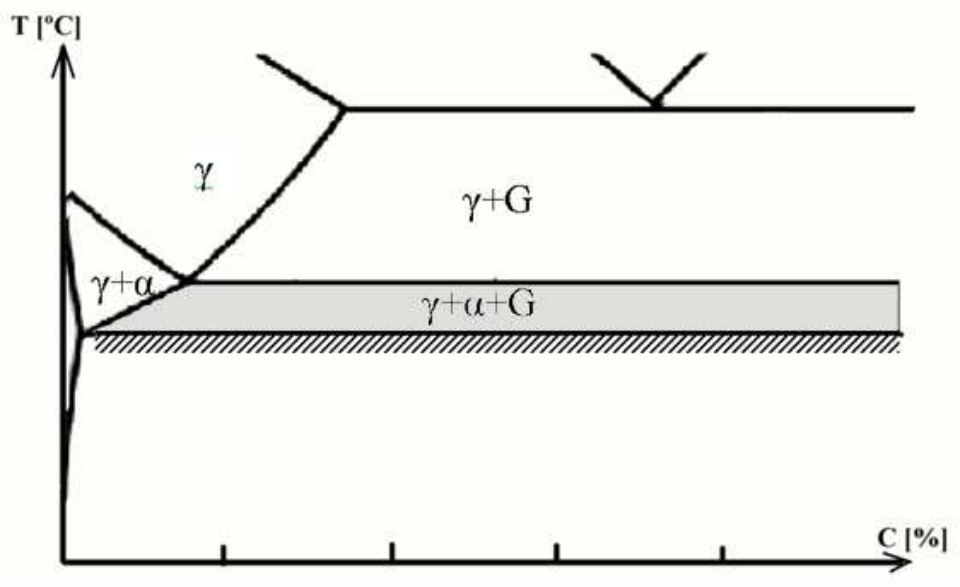

Figure 12 Fe-C-Si equilibrium phase diagram for a fixed Si percentage. The grey area delimits the intercritical interval where ferrite is formed

5. The Heat Treatment of Austempered Ductile Irons

In this chapter on overview of the heat treatments used to transform ductile iron into austempered ductile iron will be provided.

The previous work by Glondu [4] provides more extensive information for conventional ADI heat treatment, and the optimization of the austempering temperatures for a particular ADI alloy. That work has served as a valued guideline during this present work and as a valuable source for planning the experiments. However, it is not the intention of this present work to repeat what has already been covered in that work, but to provide further enrichment to the topic at hand. Therefore, it may prove necessary to consult Glondu's work if information is perceived to be missing form the present chapter.

5.1 The Ordinary Austempered Ductile Iron Heat Treatment

Many industrial heat treatment practices of ferrous alloys involve a complete austenization process in the beginning, followed by a heat treatment such as annealing, quenching, normalizing, austempering, etc, depending on the iron composition and desired final properties.

The process carried out to achieve the Ausferrite microstructure in ductile iron is called austempering. The complete heat treatment consists of four main stages: 1) austenization, 2) quick quenching to austempering temperature, 3) austempering, 4) cooling to room temperature as shown in Fig.13. Some variations in the complete cycle are sometimes made by adding intermediate processes if it is necessary for the final properties.

The most relevant step and where the transformation into Ausferrite occurs, is known as austempering. During this step, transformation occurs among a certain range of temperatures, between 400 and 260°C, through an isothermal heating during certain time. This temperature range covers the entire zone between the perlite-start temperature and the Martensite-start formation. But in order to obtain a suitable microstructure all the steps must be carried out carefully, because of the influence of temperature, time and cooling velocity affects the final microstructure and thereby the mechanical properties.

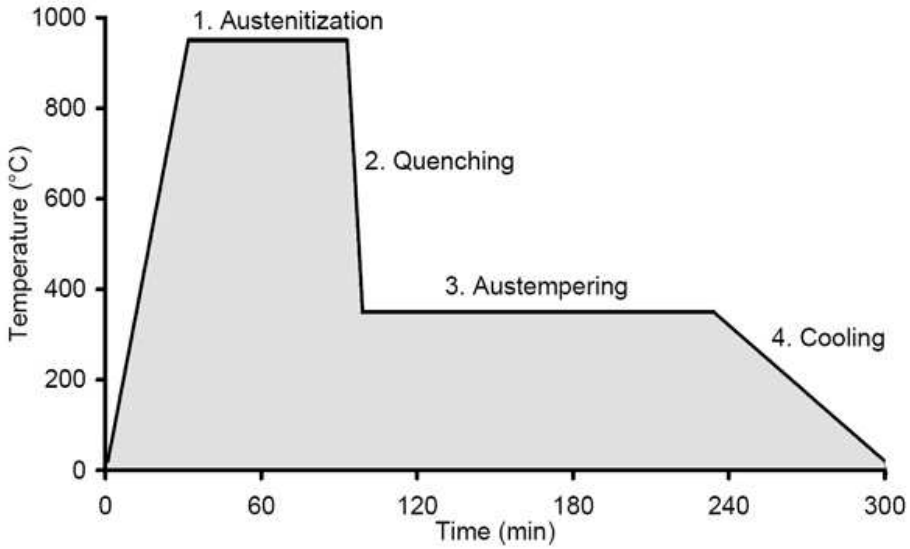

Figure 13 Illustration of common ADI heat treatment stages

Economical optimization should also be present in ones mind to save process costs and energy. In this way, the study of all the process parameters is important, and different results could be obtained for the ideal heat treatment and the best implementation for industry sector. To do this a brief review of each step and variables during the process will be presented.

5.1.1 The Austenization Process

During austenization, the cast component is heated between 850 and 950º C for about 15 minutes to 2 hours. The optimum temperature and time depend on the chemical composition of the ductile iron and the process variables.

The objectives of this stage is to create a carbon saturated austenite matrix, to dissolve the carbides present in the ductile iron and to even out elements with segregation tendencies throughout the matrix. In parallel, the process should ensure a control of the austenite grain size to safeguard the mechanical properties. Moreover, a high carbon content in the austenite matrix makes it possible to stabilize the austenite during the cooling steps, which would otherwise evolve to another phases during the cooling process. If carbon is successfully saturated in the austenite, it can be detected as “retained austenite”, which is present in the final ausferrite microstructure. If this is achieved, it will give a positive contribution to the fracture toughness parameter. The high carbon content will also increase hardenability as discussed previously. Furthermore, it is important to minimize the amount carbides in the matrix, as they are responsible for the degrading of the mechanical properties.

The austenization temperature and time determines the matrix carbon content because the diffusivity and the solubility of C within matrix increase with the temperature; variable time is also involved. Moreover, the graphite nodules and the carbides in the ductile iron will either serve as a source or sink of carbon depending on the temperature range.

The austenitization temperature determines the graphite dissolved and the dissolution rate. This temperature should be selected to ensure sufficient carbon transfer from the graphite nodule to the austenite matrix. A too low austenitizing temperature should cause an incomplete austenitization and may affect to the mechanical properties, by the presence of cell boundary cementite/carbide. If the austenitizing temperature increases, the amount of retained austenite increases along with the carbon content. At high austenitizing temperatures the diffusion of the carbon is faster and the concentration of impurity elements at the austenite grain boundaries is lower.

The austenitizing time should be the minimum required to ensure that the casting has been completely transformed to carbon saturated austenite. It must be the sufficient to ensure the reduction of microsegregation of alloying elements and long enough to eliminate the risk of cementite phase in the austenite. Long austenizing times should be avoided because of the risk for abnormal austenite grain size growth. Large grains, entails a coarse acicular ferrite structure [1] at the end of the process, whereas a fine structure should, in theory, maximize toughness properties.

5.1.2 The Quenching Process

Quenching is the second stage of the ADI-treatment, where the casting is quenched to an intermediate temperature from the austenitization temperature. In this step, caution has to be exercised so that the cooling rate is fast enough to avoid the perlite nose in the Isothermal

Transformation diagram, TTT, found in Fig. 14. Furthermore, the ADI alloy must not be quenched below the Martensite start temperature (Ms).

Therefore, in view of optimum mechanical properties, literature suggests that, in this stage the whole structure might consist of a combination of residual austenite and acicular ferrite (or bainitic ferrite) with no pearlite [1]. This can be achieved either by calculating the critical bar diameter (Dc) for a particular ADI composition using equation 1 or adjusting the chemical composition to avoid segregation during quenching for a particular specimen diameter. The higher the amount of the alloying elements, the higher will be the possibility of the segregation of them [22].

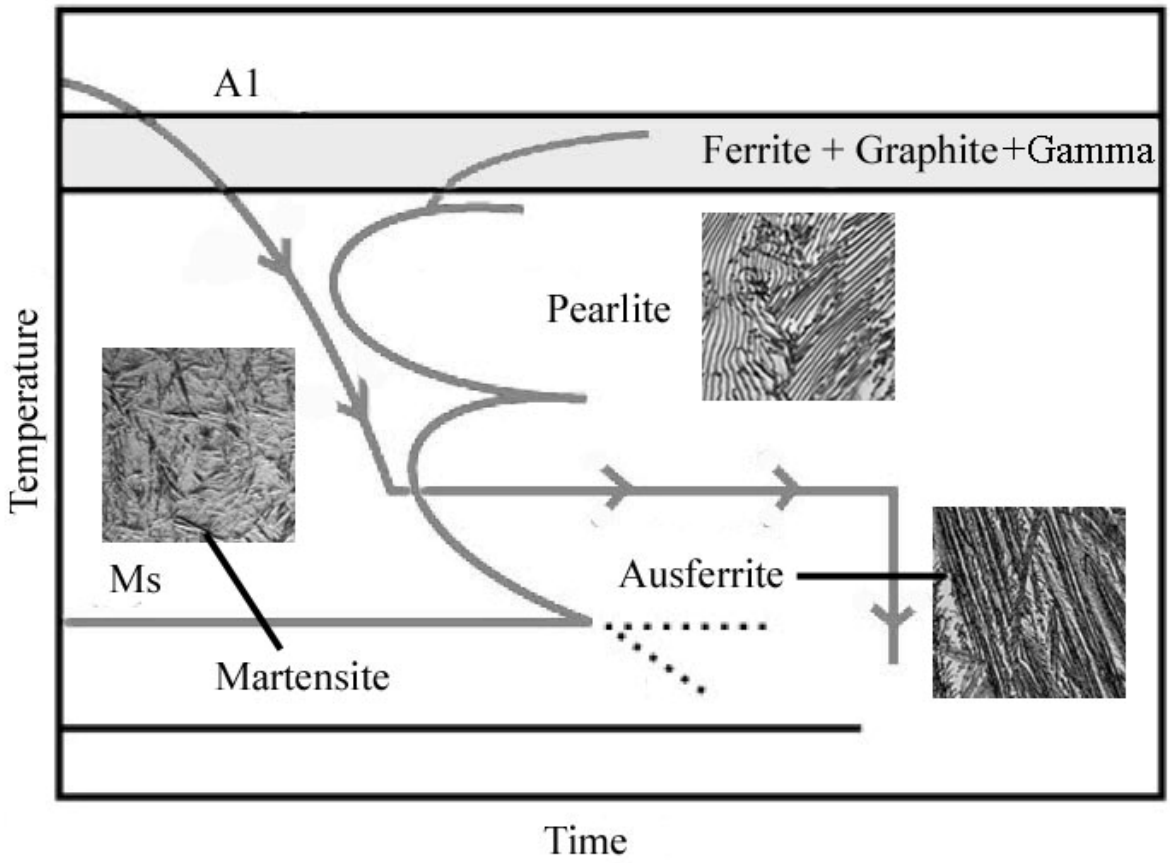

Figure 14 TTT diagram for an ADI alloy. The pearlitic nose is avoided increasing the cooling rate.

A good cooling media frequently used in this stage is molten salt bath. It allows rapid and efficient heat transfer with a uniform low viscosity among austempering temperatures range. Furthermore it dissolves easily in water which is positive for posterior surface removing operations. However, there are two drawbacks with this cooling media: It is endowed with health hazards and it pollutes the environment. The use of water could also be possible, but not advised as the resulting rapid cooling rates increases the risk of vapour entrapment [23]. Another issue with water is that the austempering temperature is too close to the steam saturation temperature of around 375°C.

5.1.3 The Austempering process

Austempering time and temperature, in addition with local concentration of allowing elements, were demonstrated to play a determinant role when carbide precipitation in the ferritic and retained austenitic component of ausferrite occurs [1,17,24].

During austempering, a two-stage phase transformation reaction takes place in ADI. In the first reaction, austenite (γ) decomposes into ferrite (α) and high carbon content or transformed austenite (γ_{HC}):

$$\gamma \rightarrow \alpha + \gamma_{HC} \quad \textbf{(3)}$$

If the casting is held at the austempering temperature for too long, a second reaction takes place, which causes further decomposition of the high carbon austenite into ferrite and ε-carbide:

$$\gamma_{HC} \rightarrow \alpha + \varepsilon \quad \textbf{(4)}$$

Best combinations of mechanical properties (tensile strength and ductility) are obtained in ADI after the completion of the first reaction but before the onset of the second reaction. This time period is so-called “process window”.

The presence of ε-carbide must be avoided due to this phase brittles the material so operating around the process window is essential. Another important function of the ADI alloying elements is to enlarge the process window.

Time and temperature are determinant for the formation of different types of ausferrite and for the percentage of retained austenite and its carbon content which are key factors for fracture toughness, as will be discussed on further chapters.

5.1.3 The Cooling Process

At the end on the isothermal transformation the final microstructure is achieved and consequently the heat-treated material is ready to cool down. The final cooling is as important as other parameters such as austempering conditions or chemical composition, so caution has to be paid it. In the ADI literature the sample was usually air cooled to room temperature, because this was the most economical [1]

.

6. Mechanical properties of Austempered Ductile Irons

Last chapters have introduced some important concepts related with mechanical properties, such as composition and phases dispersions of as-cast iron, heat treatment variables, and concentration of constituents. All summed influences ADI microstructure, and so ADI mechanical properties. To summarize, ADI´s mechanical properties are due to its special ausferrite matrix and depends mostly, not considering other factors, on the relative amounts of acicular ferrite, retained/residual austenite, the nodularity of the graphite and on the morphology of the phases. Everything that helps to increase volume fraction of stabilized austenite and lesser amount of acicular ferrite, creating a coarse matrix, will be in benefit of high ductility but against high strength. As discussed earlier, other important factors are the carbide and the formation of other non desirable phases like martensite. High ductility is in some sense synonymous of good fracture toughness, and this property is what expected to get better during this work, but if possible, high strength should accompany too in achieving a competitive properties mix.

Table 1 Grades of ADI materials

GRADE		TENSILE STRENGTH	0,2% YIELD STRENGTH	ELONGATION	IMPACT ENERGY	TYPICAL HARDNESS**
ASTM A 897M-90	DIN EN 1564	R_m [MPa]	$R_{p0,2}$ [MPa]	[%]	[J]	HB
	1	800	500	8	260-320	
1		850	550	10	269-321	100
	2	1000	700	5	300-360	
2		1050	700	7	302-363	80
	3	1200	850	2	340-440	
3		1200	850	4	341-444	60
	4	1400	1100	1	380-480	
4		1400	1100	1	388-477	35
5		1600	1300	-	444-555	-

6.1 Remarkable mechanical properties of Ordinary Austempered Ductile Irons

6.1.1 Fatigue Properties of Ordinary Austempered Ductile Irons

ADI is considered an engineering material with excellent fatigue properties, as well as high fatigue limit and high fatigue strength. The fatigue limit of an ADI is in the range of 200-500 MPa. These values depend on the chemical composition, heat treatment, loading type and number of cycles defined for fatigue limit.

The fatigue limit of ADI is not proportional to the tensile strength or hardness, but is related to the toughness and retained austenite content [25,26]. Retained austenite content is connected with the carbon content of the austenite; the higher the carbon content the higher the retained austenite content. Large amounts of retained austenite are related at the same time with the creation of more barriers for fatigue crack growth and are believed they extend component fatigue life. Additionally, small austenitic grain size is suitable for the high fatigue strength of the specimen [27]. Thinner and shorter acicular ferrite-retained austenite bands have been demonstrated to grow if small austenite grain size is achieved during austenitization stage. This is, accordingly, increasing the number of anchors for the dislocation motion and making more difficult the formation of persistent slip bands.

Thus, maximum fatigue strength and fatigue limit are associated with heat treatments that lead into high levels of retained austenite, low recrystallized austenite grain size and therefore maximum ductility. Consequently, lower austenitization temperatures are usually associated with improved fatigue resistance because of the narrower grain growth compared with higher temperatures. In contraposition, less carbon will spread among the matrix with low austenitization temperature levels, so there might be a compromise in austenitization temperatures to achieve optimum fatigue values. Moving to the austempering temperatures, high austempering temperatures lead to an increase in the fatigue limit of the specimen, up to a certain point. Austenite content increases with austempering temperature [34] and fatigue limit increases with the amount of retained austenite, but this happens with some limitations. A large amount of retained austenite would undergo martensitic transformation (very harmful phase in ADI) under plastic deformation in ADI .

The high fatigue strength of the ausferrite structure is also strongly related with the graphite nodule size, nodule count, nodule shape and its interaction with the matrix. Fatigue strength and fatigue limit could be optimized by decreasing the size of the graphite nodules [28].The effect of the graphite nodule count on the fatigue limit seems to be more significant in ADIs alloys rather than other types of ductile irons [29]. The fatigue limit and the tensile strength of the ADIs have been observed to increase with an increment in nodule count, so that presence of alloying elements that decrease the nodule count such as Ti, is not very recommended. ADI with low nodularity tends to have more graphite nodules with non-spheroidal shape. Non-spheroidal shape introduces higher stress concentration factors as compared to spheroidal shape.

In addition to the disadvantages of low nodularity, the presence of martensite phase and carbides reduces the fatigue strength, as happens with fracture toughness, so a special care should be taken to reduce or avoid their formation or precipitation.

6.1.2 Fracture Toughness of Ordinary Austempered Ductile Irons

General considerations about fracture toughness

Fracture toughness, commonly denoted K_c, can be defined as the inherent resistance of a material to failure as result of the propagation of a pre-existing crack when a static load is applied. Fracture toughness has units of $MPa \cdot m^{1/2}$.

This pre-existing crack could be artificial and conscientiously handmade when this property is tested, but normally is an isolated surface micro-defect that degenerates in a planar dislocation, or an inclusion or defects in the matrix such as voids, faults and etc, where the crack find a favourable way to growth. For that reason a grade of variability on the results testing the same material is introduced. However statistics demonstrates that the values can be ranged between well defined intervals when several experiments are conducted. .

The term toughness by itself refers as well to the ability of a structural material to resist shock or impact; its ability to absorb energy before fracture. But this property when dynamic loads are applied is also so-called impact toughness.

Literature about the fracture toughness of Austempered Ductile Iron includes static and dynamic fracture toughness measurements, designated by K_{IC} and K_{ID} respectively which abide to normalized ASTM standard tests methods registered in E1820. The sub-index I

indicates that fracture was produced primary in mode I as shown in Figure 15. This is typically used in standardised tests, because mode I is the most severe failure mode and it is easier to model by analytical theories.

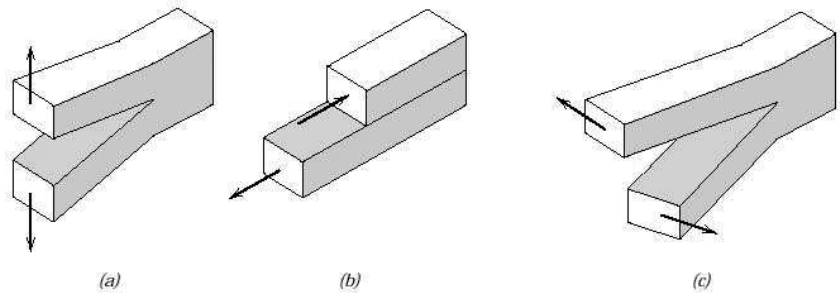

Figure 15 Different Crack Modes: a) Mode I, b) Mode II, c) Mode III. In reality the crack mode is a combination of these three modes

Equation (5) is a generic analytical expression that allows roughly estimations on the values of fracture toughness. It is based mainly on Saint-Venant's principle and others elasticity and resistance on materials theories. Is not the objective here to develop them only indicates this general expression has a strong shape dependence factor $Y(\theta)$. Also depends on the length of the initial crack "a", and the strain σ.

$$K_C = Y(\theta) \cdot \sigma \cdot \sqrt{\pi \cdot a} \quad \textbf{(5)}$$

Experiments reveal, for general materials, there is also a dependence on the velocity of the load application and the temperature as well as the material factors, which are not included in this equation.

Remarking last phrase and applied for ADI's, literature shows that the static and dynamic fracture toughness values are affected by the ADI matrix type and the chemical composition of ductile iron, but also by the process temperature and the velocity of load application [1,30].The ADI fracture failure neither for low nor high temperatures doesn't follow a perfect elastic behaviour. Such implications bring up the necessity of different ways of measuring fracture toughness considering different material work temperatures and material characteristics. Due to that last, it has introduced experimental calculation of K_{IJ}, which is defined as fracture toughness value measured in highest testing temperature and can be analytically calculated by Equation (6).

$$K_J = \left[\frac{E \cdot J}{1 - \nu^2} \right]^{\frac{1}{2}} \quad \textbf{(6)}$$

Where E is Young's modulus and ν is Poisson's ratio for the material. Moreover J characterizes the elastic-plastic field in the vicinity of the crack tip and is the area under the load-displacement curve

To end this brief overview about fracture toughness there are three fracture's categories: ductile, brittle and a mix of both that are present in materials.

Fracture failure mechanism in common ADI

In literature on steel, classical fracture mechanisms are described as either ductile fracture with nucleation and growth of micro-voids, or transgranular and intergranular creep [31,32]. These mechanisms do not operate in a similar way for both ductile irons casts with spheroidal graphite and ADI materials. This can be explained as a direct consequence of the special features of the metallic matrix and the presence of spheroidal nodules of graphite, due to the high content of Si in the alloy, which modifies the plastic behaviour of the material and complicates the analysis of the fracture surfaces [30]. These analyses reveal that ADI fracture mechanisms for impact test resemble a quasi-brittle behaviour, which means roughly a mixture of ductile-brittle fracture. In all the literature reviewed in relation to ADI fracture toughness, commonly ductile fracture predominates among brittle for room temperature tests [1,33,34].

The matrix of ADI can withstand a certain amount of deformation before fracture during tensile or impact testing. However, the graphite nodules in the matrix cannot deform and hence are barrier to matrix deformation and give rise to crack initiation. Crack initiation could occur either with a graphite crack, with a void formation between the nodule and the matrix or both. In addition, carbides may precipitate in the bainitic ferrite laths or at the ferrite/austenite interfaces and these may also influence the fracture of ADI and produce characteristic features [33]. Other possible initiation points, as commented in earlier paragraphs, are cast and material defects, but in the following lines just only graphite nodules and carbides are going to be considered.

Graphite nodules can be treated as notches creating a discontinuity within the ausferrite matrix. Classical fracture theory could be applied around the graphite nodules boundaries supposing spheroid shape, so is predictable an increment of the strength about 3 times greater than the rest of the matrix around these areas.

Differences in deformation capacity between graphite and the matrix are responsible of microvoids formation, being considered the most probable point of initiation and fracture propagation. At this point, little can be found in literature on posterior crack propagation. Morevoer, the complexity of the ADI matrix raises uncertainness about the mechanism of crack growth during fracture crack.

A first consideration is that the bainite ferrite laths are packed in clusters in a well determined direction whereas these clusters don't follow a concrete direction within the matrix, so when a load is applied, we can find three different situations:

1. The longitudinal direction of a cluster is parallel to the loading direction.
2. The longitudinal direction of a cluster is normal to the loading direction.
3. The longitudinal direction of a cluster makes an angle with the loading direction.

The orientation of the clusters will influence the critical path of the fracture propagation. The third possibility above must dominate to create a random orientation, thus the material presents similar toughness properties in all space directions.
Crack will always follow the most favourable way. For situation 2, the ferrite/austenite interface can withstand the same external tensile strength and because of the atomic

mismatch, these surfaces are weak points suitable for crack propagation. Conversely, in situation 1, the more ductile austenite (compared to ferrite) can sustain more deformation before fracture, thus, the bainitic ferrite laths breaks first and the austenite deforms past the bainitic ferrite laths producing a rounded end in a plane perpendicular to the fracture [33]. Situation 3 is more complex, and can be treated as a combination of 1 and 2 and also depends on the angle. Furthermore, if carbides are considered, the model cannot be used to predict crack evolution. Consequently, there is a need to study the role of carbides on crack propagation further.

Microstructure vs. Fracture Toughness

This last conceptual explanation of fracture failure mechanism in ADI serves to understand better experimental results when this property is measured. Some study works about the topic found on literature [1,34], draw relevant conclusions about the relation of fracture toughness and ADI microstructure. They reflect the following microstructural features that are considered essential to maximize fracture toughness:

- Fine acicular ferrite with austenite present as thin film between the ferrite blades.
- Austenite content of around 25 vol.%.
- As high a carbon content as possible in the austenite. The higher the content the higher the fracture toughness.
- More than 1,8 wt.% in carbon content of austenite is required.

In general, ADI with a lower ausferrite (bainite) microstructure shows better fracture toughness properties than those with an upper ausferritic (bainite) microstructure. In contrast, upper ausferritic microstructures provide ADI with better tensile properties. These facts enhance refuted works on literature [1,13,34] which clearly shows that the optimum microstructure for obtaining maximum tensile properties and the optimum microstructure for maximizing fracture toughness differs greatly. A compromise between these two properties must be considered depending on the application.

Austenitizing and austempering temperatures play an essential role when optimizing fracture toughness. Changing the levels between high and low within the typical process window, leads in totally oppose effects in ADI microstructure for both processing temperatures. These temperatures are also interdependent on the final results and properties.

Fine acicular ferrite is related with its maximum fracture toughness and is obtained at low austempering temperatures [34]. In contraposition to those theories that believes ferrite needle grows along recrystallized austenite grain, the final ausferrite grain size seems to reduce with decreasing austempering temperature independently of the previous austenite cell regions. It could be said, derived from different sources [34,13], that ausferrite grows either till match the austenite cell boundary or it own nucleated grain so the needle size depend on both the austenitization and the austempering temperature. However to maximize the austenite content an increment of the austempering temperature is needed. This increment on austempering temperatures has found to lead to on increasing ductility but decreasing strength [34].

Related with these last issues, the following relationship has been demonstrated to be valid for ADI alloys [34]:

$$K_{IC}^2 \propto \sigma_\gamma \cdot (X_\gamma \cdot C_\gamma)^{1/2} \quad \textbf{(7)}$$

where σ_γ is the yield strength of the ADI, X_γ is the volume fraction of austenite, and C_γ is the carbon content of the austenite. The yield strength has also been demonstrated [35] to be dependant on the wide of the ferrite blade L, and varies as $L^{1/2}$. All Equation's (7) factors depend as well on austempering temperature. While σ_γ increases with decreasing austempering temperatures, $X_\gamma \cdot C_\gamma$ increases with increasing austempering temperatures. The optimum austempering temperature is the one that maximizes Equation (7).

In addition, the austenitizing temperature is also important in optimising the process. Concerning this factor, very little information can be found about the topic in litterature. However some results point to the conclusion that increasing austenitizing temperature leads on better dissolution of carbon in the austenite, but to the coarsening of the austenite grains [34,36]. This grain coarsening increases ferrite needle length and consequently decreasing fracture toughness in the posterior austempering stage. Despite a considerable increase in carbon content with high austenitizing temperatures tensile and fracture toughness properties were found to deteriorate [34]. One plausible explanation, apart from the increase in ferrite needle length, is the precipitation of phosphorus among the austenite cell boundaries, which has an embrittling effect.

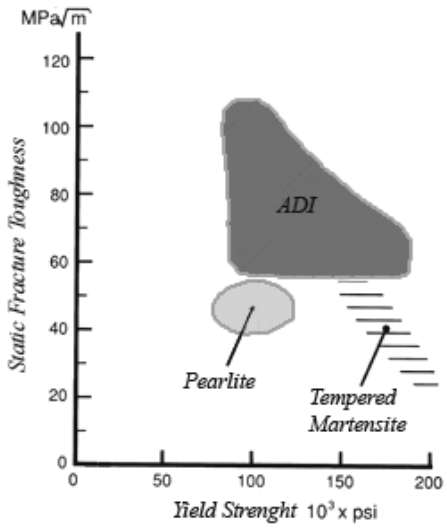

Figure 16 Different ADI alloys Static Fracture Toughness vs. Yield Strength. Interpreted from [7]

6.2 Other ferrous materials –How high fracture toughness is achieved

In the ferrous alloys market the demand of engineering materials which fulfil very particular and increasing customers' requirements is growing. During the last century, fracture toughness and fatigue arose as poorly known, but very determinant properties for component failure. Nowadays the mechanisms of these phenomena are the centre of ongoing research, due to their impact on safety. From this research high fracture toughness solutions can be found amongst multiphase steels such as dual phase steels and transforms inducted plasticity (TRIP) steels, and the so-called ADI.

Multiphase steels commonly refer to high-strength steels that have a ferrite microstructure surrounded, by grain boundaries, a dispersion of a hard phase which could be martensite or bainite or both. The material entity acts like a particle reinforced composite so the rule of mixtures applies, which relates volume fraction of the hard phase to different properties. This can be applied to estimate the expected behaviour for a certain load condition. An example of

application of this rule is reflected in equation (8) which calculates global strength for dual phase steel depending on volume fractions of ferrite and martensite.

$$\sigma_{DP} = V_F \cdot \sigma_F + V_M \cdot \sigma_M \quad \textbf{(8)}$$

Dual-Phase Steels are a high-strength low allow (HSLA) steels (max. 0,1 wt% C) characterized by a microstructure consisting of about 20% hard martensite particles dispersed in a soft ductile ferrite matrix. This microstructure is developed commonly after a continuous short time annealing in the intercritical temperature range to form ferrite-austenite matrix followed by a quick quenching to obtain ferrite-martensite mixtures. The martensite inherits the high carbon content of austenite, but this content must be limited to develop lath martensite instead of twinned martensite, which will deforms to a limited degree delaying the void formation in ferrite-martensite interface during strain [37]. Ferrite phase grows equiaxially into the austenite as part of the transformation mechanism. Some amount of retained austenite could remain untransformed in the final microstructure, but a transformation into martensite occurs if the material is subjected to stress or strain.

A special property of DP steels is the lack of yield point. This is due to the combination of high residual stresses and high mobile dislocations density in the ferrite, which causes plastic flow to occur easily at low plastic strains [38]. This property contributes to eliminate the Lüders band formation and ensures that a good surface finish is obtained after forming, which also contributes to a fracture toughness improvement.

In these materials, the absence of yield point, the early plastic flow at low strain, the distribution of phases (a brittle but strength core surrounded by a ductile phase), the amount of retained austenite and the manner in which it transforms upon plastic straining, combined are believed to be the responsible of high ductility and fracture toughness properties [37,38]. Furthermore, weight reductions demanded by the automotive industry could also be achieved through high specific strength.

Some researches in the DP steels field have explored the use higher carbon content, which leads to yield strengths over 1000 MPa while total elongation remains constant at about 20-30%[38,39]. Actual studies also show that significant reductions in processing cost for DP steel are possible for some manufacturing techniques [37] such as hot rolling, which does away with special heat treatments, thus leading to lower costs.

Transformation Induced Plasticity (TRIP) refers steels with a final microstructure based on bainitic and retained austenitic phases within a pro-eutectoid ferrite matrix. This microstructure is developed in a similar way as the DP steel case, but this time, the austempering is done in the bainitic temperature range. In these steels mechanical properties are dependant on volume fraction of phases, size, distribution and shape of their particles or grains [40]. Percentages of retained austenite higher than 15% have demonstrated to increase the product of strength and ductility from 1800 up to 2800 for TRIP steels in commercial 700 MPa grades [41]. Moreover, properties also depend on the bainite morphology, which can be controlled by holding times and temperatures in the heat treatment.

6.3 Mechanical properties obtained after Dual Phase ADI heat treatments

Several different processes can develop DPADI structures. This text will revise three of those heat treatment found on the literature that seemed to be the most interesting for the purposes of the present work. They will be referred as HT1, HT2, HT3.

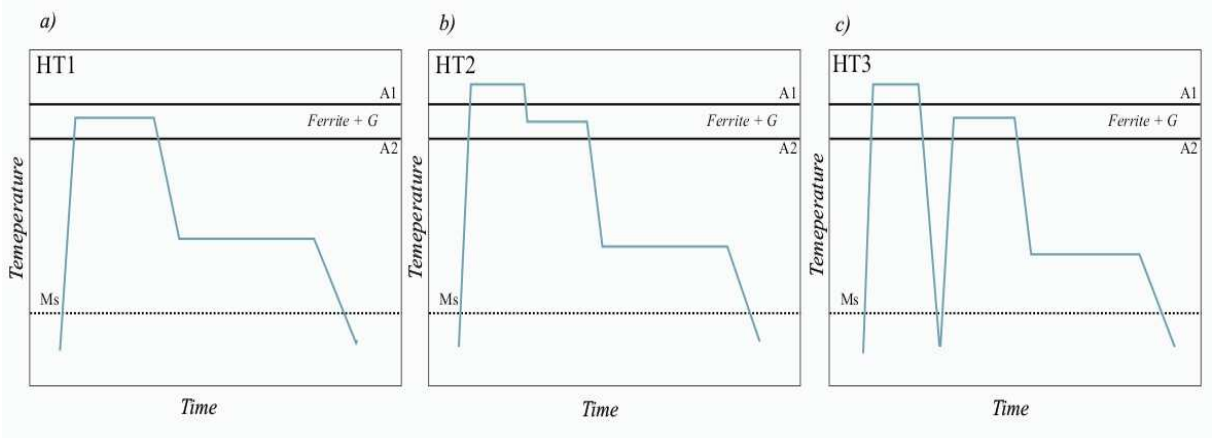

Figure 17 Different types of processes for develop dual phase ADI microstructures

The different processes are explained below and a graphical representation is shown in Figure 17:

HT1: is a heat treatment based on a partial austenization in the intercritical interval, defined by A1 and A2 temperatures, where the ferrite formation starts. Thereafter a quick quenching to the austempering temperature precedes the austempering dwell and cooling.

HT2: is a two steps austenitization process where a complete austenization is performed above the upper critical temperature before a second austenization in the intercritical interval. Thereafter a quick quenching to the austempering temperature precedes the austempering dwell and cooling.

HT3: In HT3 a typical austenization-quench cycle is performed before a partial austenization in the intercritical interval, defined by A1 and A2 temperatures, where the ferrite formation starts. Thereafter a quick quenching to the austempering temperature precedes the austempering dwell and cooling.

The intercritical temperatures austenitization step is carried out to cause ferrite precipitation. The interval temperature is between 750 and 860°C, for lower and upper temperature, respectively, but this also depends on the ductile iron composition. Note that in normal ADI heat treatments the complete austenitization process is carried out above the upper intercritical temperature.

As discussed in typical ADI, ausferrite phase optimization is a key issue on fracture toughness. In DPADI it is also a crucial factor that must be optimized along with the ferrite precipitation.

In addition, ausferrite properties have shown to be easily modified through the selection of the austempering temperature, but ferrite formation results are very sensitive to temperature and time variation [3]. The amount of ausferrite varies with the increment of pro-eutectoid ferrite

precipitation, and when it decreases, it was observed that the tensile strength, deteriorated while the ductility increased. The best ausferrite percentage that shows reasonable values of both tensile strength and ductility is around 80% [3]. Consequently, a good process control of the ferrite precipitation is a vital determinant in the case of DPADI. Therefore the continued section will be dedicated to the key issues of pro-eutectoid ferrite precipitation process and its implications on fracture toughness.

First issue fact is related to the disruption/dissolution of the graphite morphology, which degrades mechanical properties, by increasing the sources of potential crack initiators. This has been observed [42] in the case of ferritization heat treatment above the austenitization temperature, that the graphite spheroids partially dissolves into the matrix, thereby loosing their nodularity i.e. their spherical shape, whereas in the case of heat treatment below austenitizing temperatures, hardly any dissolution occurs. Moreover, Matrix constituents' inclusions have also observed to be introduced within the graphite nodule after the austenitization steps. Therefore, inclusion and graphite dissolution are detrimental factors for fracture toughness properties.

In addition, the influence of prior austenite microstructure has recently been demonstrated [36] to play an important role on the transformations during the post-cooling ADI phases. Thus, the ductile irons microstructure need to be adjusted in order to fulfil specific requirements, as mentioned earlier.

Another possible cost saving procedure would be the application of the ADI heat treatment during casting cooling. Despite of avoiding post casting heat treatment it would require the removal of the cast mould prior to salt bath quenching, which is not possible to do industrially today. However, there is another possibility to performance DPADI microstructures and is to use already as-cast material to carry trough the DP ADI heat treatment.

Nevertheless, both DPADI heat treatment procedures start in the solid state, after nucleation of liquid phase or after a heating reformed austenite phase. Another issue is that the austenite differs drastically in each case and also determines the different phases' precipitation behaviour and the mechanical properties [36].

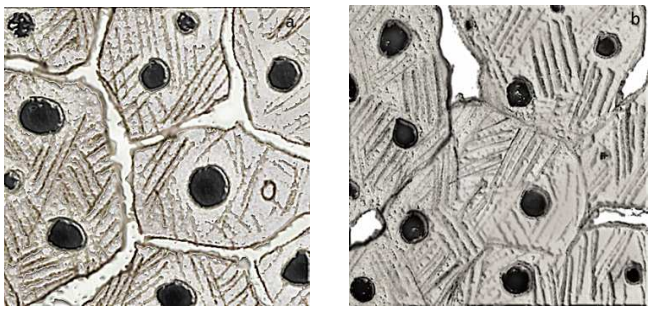

Figure 18 Several sorts of ferrite precipitations.

The one formed directly from the liquid phase on the cast iron, referred as non-recrystallized, shows a dendritic grain growth soaking graphite nodules. In this case, and having the ferrite precipitation as useful example due to discussed implications, ferrite nucleates and preferentially grows in contact with the graphite nodules, developing the bulls' eye configuration. In other hand, the austenite formed after reheating, referred as recrystallized,

nucleates in a larger number of sites provided by the as-cast microstructure. In this case grain boundaries provide active nucleation sites for most diffusional transformations during cooling, as could be ferrite precipitation.

After these last considerations, differentiation between different DP ADI commented on 5.2 is going to be discussed. Basically all the mechanical properties differences come trough the different microstructures develop, but in all cases an improvement on some mechanical properties was observed compared with conventional ADI.

In HT1, allotropic ferrite formed shows a dispersed precipitation within the matrix, whereas in HT2 the ferrite precipitation occurs at the grain boundaries of the recrystallized austenite. This last success was proved [3] to result on an interesting combination of strength and ductility, better than in HT1. Depending on process variables combinations of elongations over 24% and yield strength around 600 MPa could be obtained .However, no fracture toughness study has been made for this promising microstructure, neither a deep investigation on the heat treatment parameters optimization, thus is a motivation for further investigation during this master thesis experiments. If HT2 described microstructure is obtained, it could be assumed a combination of the best on multiphase steels, which was the ferrite, and the advantage of the substitution of brittle martensitic or bainitic cores for ausferrite. However, graphite is still a disadvantage of DP ADI compared with multiphase steel in terms of potential crack iniciators.

In HT3 the properties improvement are not so related with the allotropic ferrite site precipitation. The martensitic microstructure introduced by quenching [43] provides a large number of precipitation sites for the acicular ferrite to form, and thus a uniform fine ausferrite microstructure is obtained. Moreover, the stability of retained austenite in the final microstructure is increased due to the fact that allowing elements concentrate in the austenite phase during the holding in the ($\alpha+\gamma$) temperature range, showing a lower posterior carbide precipitation which also depend on the increment on the holding time among this range.

That last effect on ausferrite formation reminds what happened during Yang process referred in Gloundu's work [4]. This method consist in an added step on the normal ADI heat treatment, which is just only a quenching to the martensitic temperature upper range instead of the normal one, followed by a reheating to the common austempering temperature [24]. Higher toughness was expected because of a dense ausferrite microstructure which suggests fine ausferrite formation. Previous works experiments [4] were not satisfactory in developing promising Yang improved fracture toughness properties which just only suggest perfecting the method for the concrete ADI composition. Is the author believe, and motivated also by HT3 results, that Yang process should be tried in combination of HT2 to improve fracture toughness properties in resulting DP ADI

7. Materials, Modellings, Experiments and Characterization

This chapter introduces the experimental procedures utilised to characterise Austempered Ductile Irons studied, and at the same time describes the experiments conducted.

7.1 Procedure

The experimental part of the present work aimed for checking and improving on the previous work by Glondu [4] in relation to fracture toughness of austempered ductile irons.

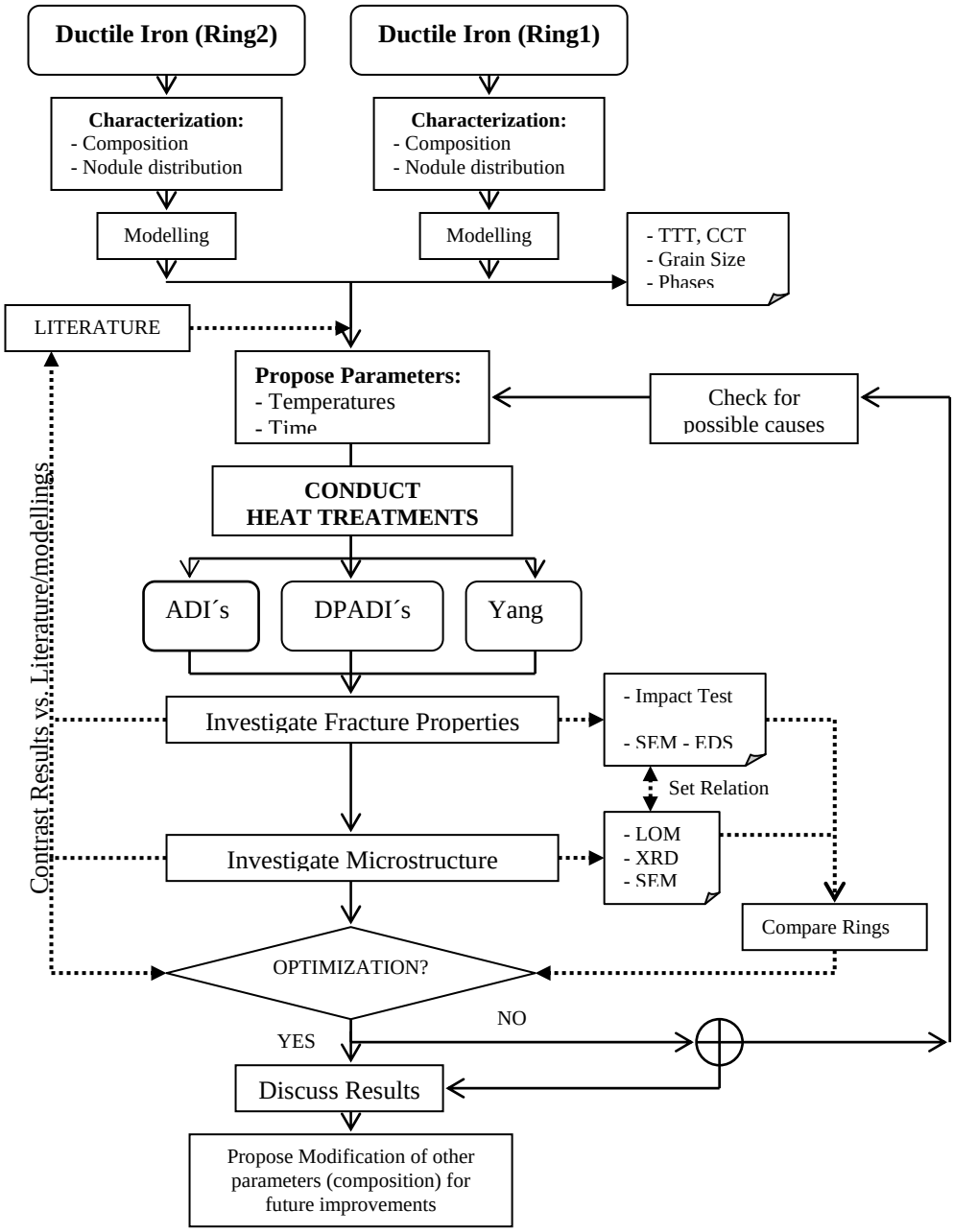

Figure 19 Flow chart of experimental procedures for ADI fracture toughness improvement.

A flow chart explaining the experimental procedures for ADI fracture toughness improvement is shown in Figure 19.

For conducting experiments, different cast ductile irons supplied by Swedish companies have been used. First is important to make a characterization of those materials in order to ascertain compositions and check for possible cast defects. As discussed in earlier chapters, conditions of the base cast iron are determinant in the mechanical properties results. Properties won't be improved with posteriors heat treatments if the base material to develop ADIs is of a poor quality.

Composition of the alloy is also necessary to run modellings. Modellings became an important and helpful tool for not shooting in the dark during all the experimental process design and to have a rough idea of what would be the phase composition and the grain size in the microstructures developed.

After running modellings and having an idea about possible results, experiments were designed and conducted based on fracture toughness issues found on literature, previous works and personal experience. Taking them as a basis, the applicability of some novel methodology to develop improved microstructures as well as the optimization of some key parameters according with new discoveries, were analysed for the supplied industrial cast alloys.

The trials had also two main objectives: to come up with ideal parameters for maximized fracture toughness and primary to present an optimized process for industry. The main difference between both results is the consideration of economical parameters which for example would result on reduced optimal times during different heat treatment stages. Concerning that last, proposed methodology has been subordinated to the industry high performance and expectations for results, which doesn't mean an unconscious procedure was carried out; a better planning and a harder and intense work was needed instead.

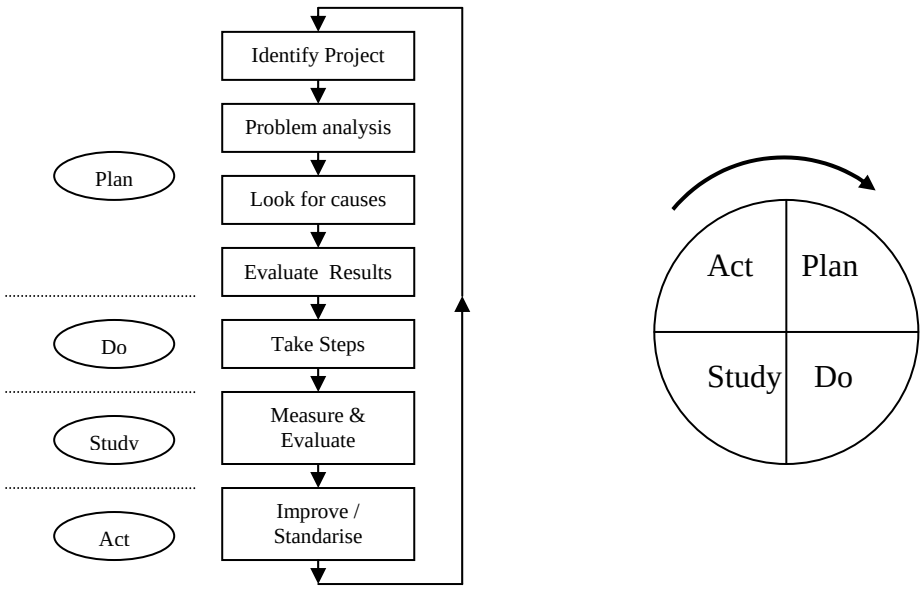

Figure 20 PDSA-Clycle for solving problems in the continuous improvement work presented by Deming. Interpreted from [44]

As the process of properties optimization depends on many factors and hasn't really a master recipe, an iterative methodology has been proposed to sharpen the results. This consists on trial and error experiments based on earlier modellings that either narrows the parameter

range to the optimum in every iteration or end up in the conclusion the heat treatment applied doesn't entail better results that others obtained with previous works. This methodology was intended to be and implementation of the "learning cycles" (Figure 20 shows PDSA-cycle) commonly applied on Swedish and others top industries to achieve quality; in what are so-called leaning processes or Total Quality Management (TQM)[44]. Those cycles also include a packet of simple but effective statistical and management tools that allow to fast and easily propose decisions and analyse results in a reliable way. Furthermore, they complement quite well the scientific rigor with the constantly changing industry demands and requirements for rapid solutions, making this methodology ideal to be applied for this work.

7.2 Materials used in experiments

Different ductile iron and ADI alloys had been used to conduct the experiments. Two of these ductile iron alloys, mainly used during this work, came from two rings previously cast by two different Swedish industries; since now thy are going to be referred as R1 and R2 (ring 1 and ring two respectively). The rings have an internal diameter of 370 mm, external diameter of 500 mm and a thickness of 25 mm. The process carried to develop these casts was not specified by the foundry, either the compositions. A composition analysis was carried out to determine the percentage of elements in the melt. The results are reflected on Table 2. This table also shows the material composition of one particular cast founded on literature [4], so a comparison of different work results might be done. This as-cast material is going to be referred as CM.

Table 2 Outline of the chemical composition of the samples (wt.%)

	C	***Si***	***P***	***S***	***Cr***	***Mo***	***Ni***	***Cu***	***Mn***	***Sn***	***V***	***Ti***
CM	3,58	2,51	0,031	0,006	0,02	0,36	0,36	0,75	0,36	-	-	-
R1	3,46	2,57	0,036	0,005	0,03	0,39	0,34	0,77	0,36	0,005	0,005	0,012
R2	3,65	2,13	0,026	0,009	0,05	0,27	0,35	0,82	0,34	0,013	0,023	0,009

Coming back to what was presented in earlier chapters in relation with cast composition (see), some elements concentrations are not within the recommended standards for ADI alloys. Principally the carbide formers, manganese and molybdenum, for all the rings were added in rather high proportions (higher than 0'3% and 0'2% respectively) which brings up the suspicious of the presence of segregation areas, carbides and other cast defects such as shrinkages in the final microstructure. Another remarkable appreciation is the low content of nickel. This element which increases the ductility, insignificantly affecting the tensile properties, is for all the rings lower than the 0'5% minimum recommended. It might be though that the high content in copper, reaching the 0'8% maximum advisable, would compensate the scarcity of nickel since they have the same effect on the material.

Table 3 Carbon equivalent for different rings

Cast	Ceq
R1	4,12
R2	4,18
CM	4,22

In parallel to composition determining, characterization of other cast irons' parameters was made. Light Optical Microscopy, in combination with computational algorithms, allows analyzing graphite nodule count, size, shape and distribution. Moreover, a characterization of cast defects is also included on the material analysis. These parameters will be determinant on the mechanical test results since they affect strongly to the properties and cannot be corrected with the heat treatments carried out. As consequence of cast defects, heat treatments could result inefficient and significant useless for any positive result interpreting. The characterization of them becomes crucial not only to determine the quality of the material but also to correctly analyse and interpret the results. Wrong conclusions could come up and some interesting methodologies could be rejected if these analyses are not carried out.

There are more complex techniques to determine internal defects like ultrasonic test (interior defect) and magnetic particle test (surface defects), but these kind of inspections are time consuming. Consequently, important experiments were repeated to reduce experimental scatter and samples having very high or low impact toughness were investigated for the presence of defects.

In addition to those last ductile irons, some samples coming from a third ring (denoted as R3) were taken to mechanical properties evaluation. This ring, having the same composition of R2, underwent a normal ADI heat treatment in a controlled industrial process with following parameters: Austenitising temperature and tine 860ºC-1h, austempering temperature and time 400ºC-1h.Those parameters values are being actually used as optimized values for that particular alloy and its industrial possibilities and applications. The results with this alloy were taken as a reference to compare with the novel heat treatments and microstructures developed during this work and to measure the success or not of the experiments carried out.

Density of the different sort of samples is another interesting parameter to be measured. This allows supplying values related to the mass which is more useful when designing elements in some different industries, especially automotive an aerospace. Therefore it is recommended that density measurements are conducted in future work.

7.3 Modelling

Today, computational modelling has become an essential tool for researchers in several science fields. They are based on the phenomenological description of a process and the subsequent proposition of a model that allows roughly reflecting the reality. Usually a more complex model is narrower to the real solution result, but at the cost of more time and/or money. When a model is created and validated, an algorithm is proposed and implemented in computer language.

In materials field, iron foundries and casting designers use computational modelling because they permit, for casting and other processes, the establishment of prediction either of the microstructure of the heat-treated material, its mechanical properties or both. This is helpful and useful to meet the final properties of the material without carrying out any experiments.

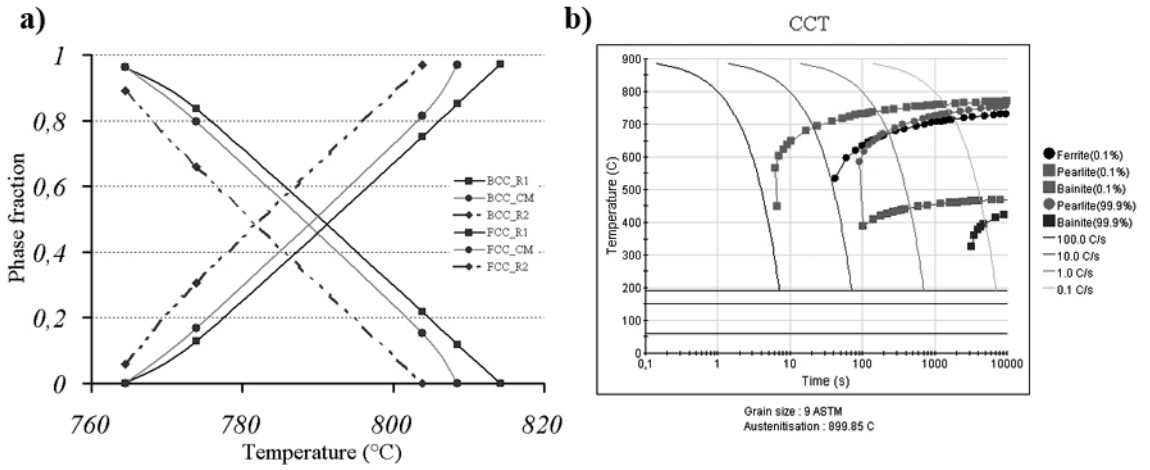

Figure 21 a) Thermo Calc TCW4 modelling of the phase fraction vs. temperature for R2. b) JMatPro-4.1, R2 CCT diagram generation for 900ºC

In the current work two different software applications were used, JMatPro-4.1 and ThermoCalc TCW4. ThermoCalc software works by using Gibbs free energy for the models. JMatPro does too, but also has an empirical database which helps checking the outcomes. This database is limited for just only some particular alloys. Both applications make possible obtaining TTT and CCT diagrams resulting from cooling the alloys. Time-temperature transformation (TTT) diagrams measure the rate of transformation at a constant temperature, while Continuous cooling transformation (CCT) diagrams measure the extent of transformation as a function of time for a continuously decreasing temperature. The most relevant functions of these diagrams for the present work are the estimation of phases for a concrete holding temperature and time, and the possibility of checking the cooling rate to avoid the formation of detrimental phases such as perlite or martensite. Phases composition can also be assessed directly with ThermoCalc TCW4 software, not only size it up from TTT and CCT diagrams.

Although modelling is helpful tools for basically saving time (creating proper TTT and CCT diagrams is a costly affair) and money (no need of experiments) , people should keep in mind that they are generated based on a model, which means the results are not going to be exactly the same when the real process is carried out. Therefore, predictions from modelling have to be considered carefully because nothing guaranties that they will coincide with real experiments. To validate modelling results some quick test are advised to be done with a particular alloy, or just compare them with the first trials to check whether it is advisable trust the modelling or revise the model. However modelling can provide valuable starting points for the experimental trials.

For ADI alloys, previous works [8,45] have focused on the elaboration of a model that can be able to predict some characteristics of the final ADI material. In those works, neural network method and phase transformation theory were used to establish relations between input parameters and the output parameter to model.

7.4 Experiments

7.4.1 Preliminary Study

Three ADI different heat treatment cycles have been conducted for R2 alloys as seen in Figure 22. These heat treatments will be referred to ADI, DPADI and Yang. For R1 alloys only DPADI heat treatments were conducted. The purpose of these first experiments is to investigate the materials possibilities after have been subjected to different heat treatment conditions and to establish a starting point for further optimizations.

The ADI process is a normal four-step ADI-heat treatment, also called "conventional single-step austempering process" and it was already described in paragraph 5.1. The DPADI process consists in a two-step austenitization stage for developing dual phase microstructures in ADI. This process was as well described in paragraph 5.2 and referred to HT2 heat treatment. Finally, the so-called Yang process is a normal DPADI heat treatment with a sort undercooling prior the austempering to 260ºC during 5 minutes, followed by a reheating to normal austempering temperature and finishing with a normal austempering stage.

To conduct heat treatments several furnaces were used during the process. A Carbolite tube furnace was used for full austenitization stages. It was provided with an argon protective atmosphere to avoid or delay the maximum possible the surface oxidation, and graphite degradation due to the impinging oxygen. The furnace is supplied with a digital Eurotherm temperature control device. The intermediate austenitizing at interval temperatures was done in a Carbolite box furnace. For this furnace, there was no possibility to use a protective atmosphere. The furnace is supplied with an Ether Mini temperature control device with a NiCr/NiAl internal thermocouple. Finally a molten salt bath was used for the isothermal transformation during the austempering step and for the Yang's process. The salt used during the experiments was AS 140 from Durferrit. The molten equipment is a Max Sievert with Eurotherm temperature control.

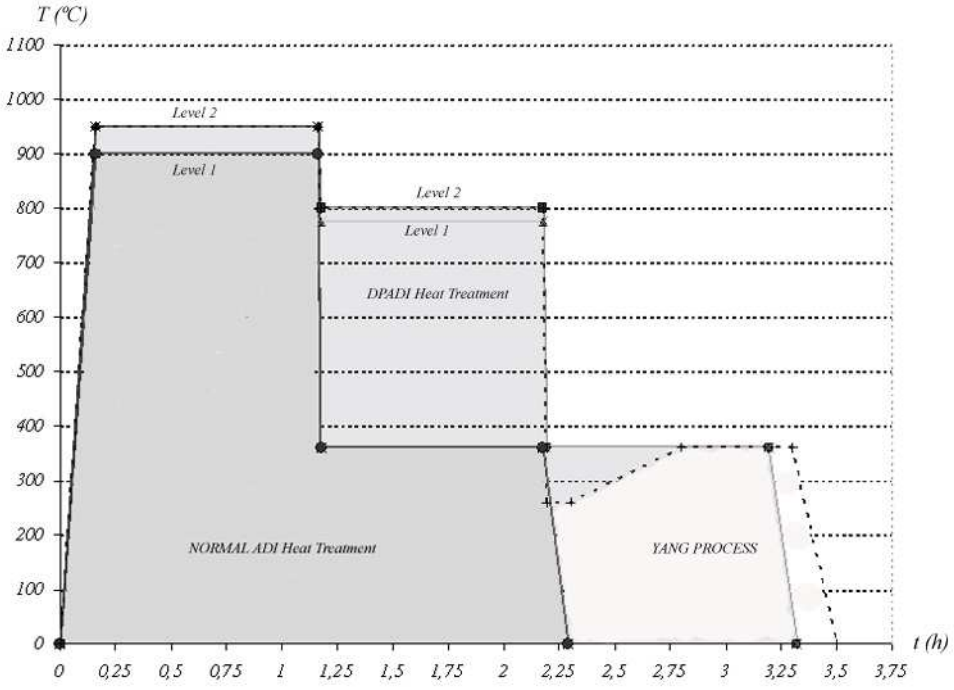

Figure 22 Representation of the different sort of heat treatments carried out.

All the furnaces were calibrated before experiments realisation and extra thermocouples and external instrumentation (Fluke 53II Thermometer) aided to steadily control the temperature during the experiments. Despite of this the, temperature variation for tube oven during experiments was estimated to ±3º C due to imprecise sample positioning near the thermocouple. For the box furnace, temperature variation was estimated to ±5ºC. For the salt bath temperature variation was estimated to ±5ºC. The measurement error was around ±1°C.

Full austenitization stage: two variations in austenitization temperatures were done, 900 and 950°C, in all processes except Yang process for which only one trial was conducted at 900° C. This big gap between two levels was chosen with the belief of totally different results achieving for grain growth and carbon content in the austenite, thus conclusive conclusions would be drawn. Modellings were carried out with these temperatures to previously check them feasibility in the process, having a rough estimation of grain size and carbon content parameters that allows envisioning the possible implications over the whole process.

A one hour time for austenitizing step was chosen based on previous experiments over rings' samples and on industry trends. This time is not necessary the optimum stage time, but is enough time to allow relatively good carbon diffusion within the matrix for different temperatures. This was tested previously for different temperatures before any decision were taken.

The process time was fixed for all the experiments. In one hand it was considered interesting to fix time parameter to solely analyze temperature dependence in the evolution of segregation areas and grain growth, but as previous results [4] has shown little variation was found.

Intermediate austenitization stage: For DPADI heat treatments, two intermediate austenitizing temperatures levels were also tried; 775 º C and 800 º C. These temperatures weren't chosen by chance. Modelling gave approximately the amount of different phases expected for each temperature along the interval temperatures range, as it can be observed in Figure 23. After modelling, and based on literature recommendations about phase composition related with mechanical properties, it was consider interesting, as an starting point, investigating these temperature levels.

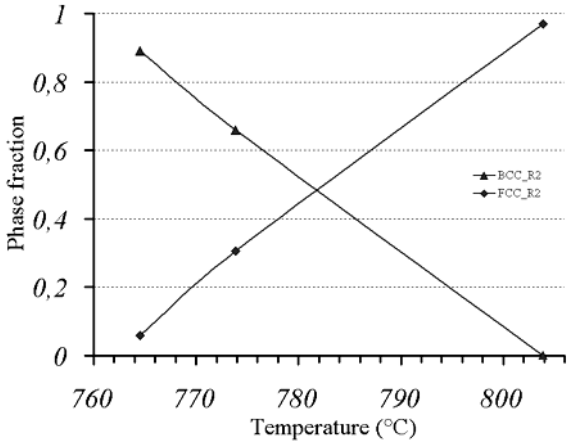

Figure 23 Thermo Calc modellings for austenite-ferrite phase fractions with T for R2

Austempering stage: Previous works results [4] suggested that optimum austempering temperature is somewhere around 360ºC. This optimum temperature is for maximizing fracture toughness in similar alloys than the ones used during the present work. As well, an optimum time of two hours is proposed. For all the experiments the 360º C temperature was kept, but the austempering time was reduced to one hour. The reasons for this can be explained as more or less austempering optimization issue is already well known among the literature, so to improve existing results about this topic many efforts should be put for just only a little improvement. At the same time, novel processes and new influencing parameters are trying to be ascertained. There is nothing stipulated and no cost analysis for this was done, but the author believes that a total process time of three hours or less (for the samples' thickness) would be a reasonable time to make DPADI alloys competitive with the normal ADIs. As all the austenitizing processes for DPADI was fixed in two hours, there were only one hour left to realize the austempering. Not using the optimised time is also interesting because if good results finally happened, they can be improved extending the austempering time if it is cost advisable. Supporting this decision, industry actually is using for normal ADI-processes one hour austempering time. Therefore, for the normal ADI heat treatment and for the special Yang process, the austempering time was kept in one hour too, but also to allow an easier comparison of the results.

Apart of the experiments explained above, some extra quick experiments were conducted in this preliminary study. The motivation for these experiments is contrasting experimental results with the modelling results for full austenitization and intermediate austenitization temperatures and, at the same time, coming up with a clearer image of the material microstructure performance, saving the more time possible.

For R2 samples, experiments consisted on a simple single-step heating at several temperatures in the range of 950 to 765 º C. All R2 samples were held for half an hour, enough time to heat them up, reach the desired temperature and to maintain it for a minimum of 15 minutes before a quick tempering.

A different study was made with R1 samples. They were subjected to a two stage austenitizing process. The first step was a full austenitization for one hour at 900ºC. Then, for the intermediate austenitization temperature two different temperatures were tried, 800 and 830ºC for one hour each. To conclude the heat treatment a quick quenching to room temperature finally is made.

7.4.2 Optimum process proposition.

After the preliminary study, the outcomes brought up the possibility of improving the process parameters to achieve better results concerning fracture toughness properties. However, DPADI experiments were not such as successful as expected compared with literature conventional ADI experiments. It was concluded, as will be discussed in next chapters, that a more appropriate temperature values combination for DPADI shall entail outstanding results.

As well, a dependence on the samples extraction position within the ring was observed, so for the new experimental trials the best areas (which resulted to be the inner and outer areas) were chosen to test the full potential of the material.

For these experiments only R2 was used due to its distribution, size and nodule count of graphite nodules resulted to be pretty much suitable for achieving a significant improvement on the impact test properties.

During the preliminary study, three heat treatments had relative high impact test values that denoted a starting point to optimize fracture toughness. Based on these results, replications for two of the heat treatments were conducted for checking the reliability and robust of the results and to see if there were any differences when a better area is chosen. These include, the industry heat treatment (860ºC-1h austenitization, 400ºC-1h austempering) and the 900ºC-1h austenitization and 360ºC heat treatment were retested.

In addition, a new dual phase heat treatment was proposed to be experimented as a summary of all conclusions deduced from the preliminary study. Motivations for the selected parameters will be discussed on further results section. This heat treatment consisted in a 950ºC-1h full austenitization stage followed by a 790ºC-1h intermediate austenitization stage and ended with a 400ºC-1h austempering.

7.5 Characterisation

A wide range of diverse techniques are able to characterise the microstructure and mechanical properties of the ADI materials subjected to the experiments. In this paragraph the ones used during the present work are going to be revised.

7.5.1 Study of the ADI-materials' final microstructure

The main technique used for microstructure analyses was Light Optical Microscopy (LOM). It provided a general overview of the samples' matrix nature in a relatively fast and inexpensive way. However the complexity of ADI microstructures is difficult and tedious even for expert eyes. Therefore, supporting LOM, X-ray diffraction (XRD) in addition with colour etching were used to investigate the content of phases, while Scanning Electron Microscopy (SEM) coupled with Energy Dispersive X-ray spectroscope (EDX) was used to get high magnification images and to get a chemical analysis on the heat-treated samples.

All of these techniques require some standard preparation before starting the analysis. Rough surface polishing with silicon carbide or diamond micro-powder grinding papers is the first step for material preparation. Each sample can be mounted in a plastic (Bakelite) holder for helping the polishing, if necessary. Successive grinding with 180, 320, 400, 500, 600, 800, 1200 and 2400 sandpaper allows first coarse removing surface oxides and external layers and second a continuous surface refinement on each step. Then the material surface is ready for a fine polishing with diamond paste of 3 μm and 1 μm. Before this, an intermediate stage is recommended for ADI to obtain a posterior perfect finish. This stage consists on alumina paste polishing of the samples. It prepares graphite-iron interfaces for diamond polishing, keeping away from bad finishing with scratches remaining in those interfaces and from shabby graphite nodules images.

For either light optical microscopy or scanning electron microscopy, a 3% nital etching solution was used during around 3 seconds to reveal the phases in the microstructure. The optimum etching time differs depending on the heat treatments and microstructures. A light etching of approximately two seconds is recommended first. Then a further attempt of one or two seconds might be done. Notice that graphite nodules are commonly degraded if the etching time exceeds a limit, and there is also a risk of over etching, which would force to

repeat the entire polishing process. For the colour etching 2% Nital and 2s along with a 225°C heat treatment is done to colour the oxides.

7.5.2 Study of the ADI mechanical properties

To investigate the mechanical properties of the experiments resulting ADI-materials, Impact Energy tests were performed. For conducting the Impact Energy test un-notched specimens were used. The specimens have a prismatic volume with a square base of 10 mm wide and 55 mm length. Charpy machine tested impact energy dissipated in Joules.

Crack surfaces were analysed with scanning electron microscopy to check the crack mode and XRD was carried out to look for presence of carbides.

In a first instance, samples were cut along ring's radial direction for conducting experiments. This cutting direction will be denoted by V. After first results, concerns about the dependence of the different possible ring's cutting areas and directions came up, so a study of this factor was proposed and executed. This study consisted on cutting samples from a unique ring (R3) but from different areas and directions and with these samples carrying out impact tests and crack surfaces analysis.

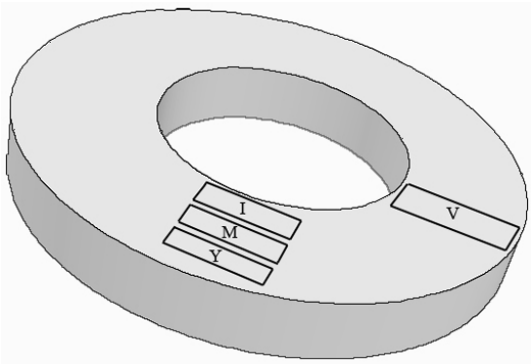

Figure 24 Different ring's cutting positions and directions

The samples extraction is schematized on Figure 24. Letter I refers the inner position and ring's normal cutting direction, while letters M and Y denote the middle and outer positions for the same normal direction. Letter V corresponds to the ring's radial direction.

8. Microstructure Analysis and Impact Test Results

8.1 Results of As-cast Ring 1 Characterization

This section has the aim of showing the analysis results of Ring 1 (R1) ductile iron alloy.

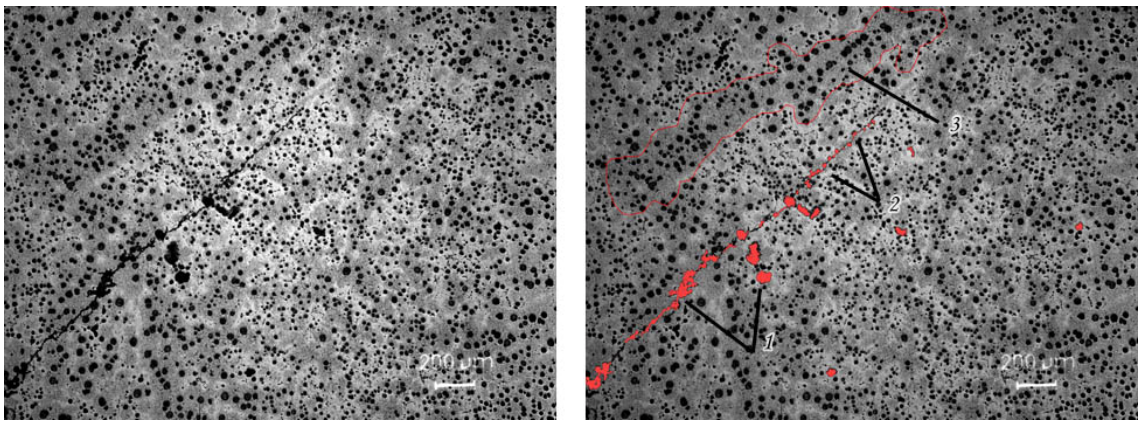

Figure 25 Defects founded in Ring 1. 1= Shrinkages, 2= Crack continues its propagation following a graphite nodule line, 3= inhomogeneities of size and nodule distribution.

The quality of the R1 cast material was questioned after its first LOM's microstructure analysis. Without entering in a more detailed study, Figure 25 shows conclusive details that allow asserting the presence of several serious deficiencies in the basic cast requirements [9,10,11,12]. First, heterogeneity for both nodules distribution and grain size of the graphite nodules can be observed. The presence of excessive large size nodules concentration areas (associated with dendrites growth) combined with smaller nodules ones will provoke, after heat treatments, an uneven distribution of the segregation regions as it can be appreciated in the light areas in Figure 19. In addition other defects are present like shrinkages that are suitable places for fracture propagation as it is remarked with red colour on Figure 25.

As it was discussed in earlier chapters, the raw material and its morphology (homogeneity, nodularity, nodule count, nodule distribution, defects …) influences the properties of the final performance ADI material. Therefore, it is significant to characterize all its relevant properties in order to envision possible consequences of poor quality in the fracture toughness results. Furthermore, initial microstructure will influence the results due to it progress to the final material's microstructure when is submitted to heat treatments.

Although bad as-cast material quality was presented for all Ring 1 samples, some heat treatment trials were conducted with them to appreciate the real consequences of poor quality and the potentials with this raw material. Ring1 samples were subjected to a 950ºC-1h, 800ºC-1h and 360 º C-1 h heat treatment trying to develop DPADI microstructures. In order to improve the carbon dissolution in the matrix and to reduce the segregation areas, 950ºC full austenitization temperature was chosen attending to the as-cast alloy previous experiments. The LOM images obtained after the microscopy study are resumed in Figure 26 and Figure 27.

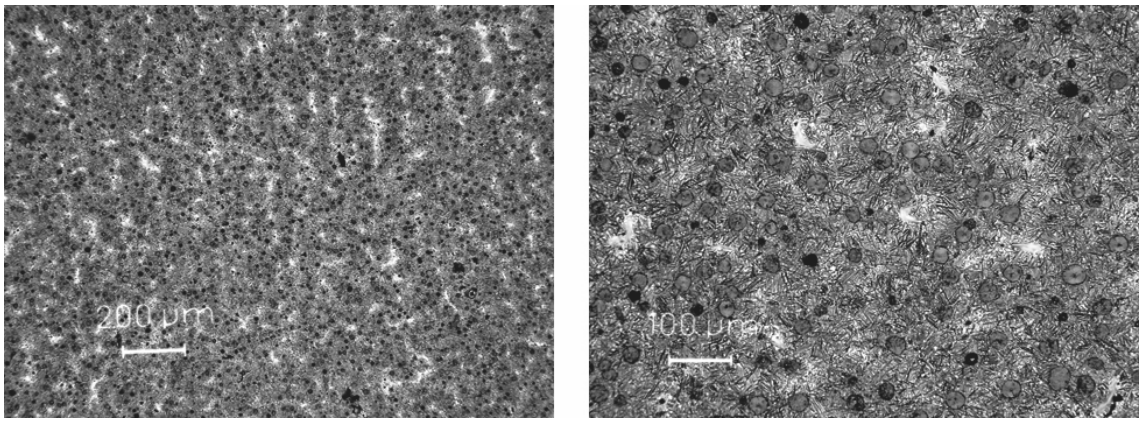

Figure 26 Segregation areas inspections

The first remarkable observation that can be made from Figure 26 is the very possible presence of ferrite in the cell boundaries delimited for the lighter grey segregation lines. The light white enhanced regions are coarse and wide enough to discard them as carbides and to identify them as ferrite, but this affirmation must be cautiously formulated. However, it can be also appreciated that the possible ferrite precipitations follow the dendrite branch trend line, which still is a handicap for the real opportunities of this material for toughness properties improvement. No martensite was found after a conscientious search which doesn't mean it was not formed. Unknown particles were also observed along segregation areas

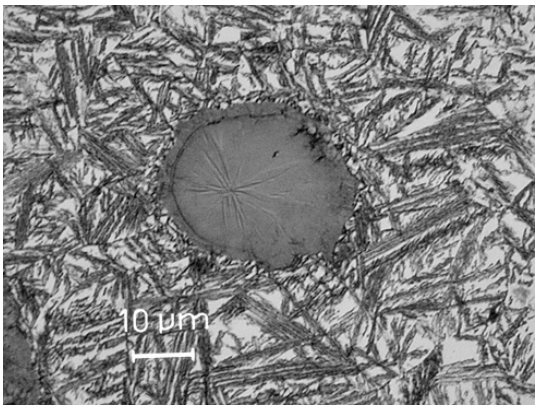

Figure 27 Magnification of the ausferrite structure. It can be appreciated clearly the graphite shell as a second layer surrounding the inner nodule.

Concerning the ausferrite characteristics, as can be observed in Figure 27, the grey needles represent the acicular ferrite. These needles are interconnected by ausferrite areas, distinguishable for its lighter grey colour. In the centre of the figure there is a graphite nodule. Its shape is not perfect nodular but it was a rare exception. Which is nice to observe is the inner and the outer shell of the graphite if the eyes are directed on its left half.

After heat treatments, impact test was conducted for three samples obtaining the values of 40'5J, 50'5J and 122J. The last 122J result is very promising considering the still remaining imperfections of the material, and brings lot of expectations of the possibilities if some corrections in the material deficiencies are made. Although the base material fulfils the stated demands, it was widely commented that there are still some weak points that could be improved to obtain better results in this work purposes. Those weak points would explain the big dispersion in results making the new material unreliable for a safety commercial use. A characterization process was carried out in order to explain the differences of impact values. The LOM microscopy didn't show big differences between samples except for the cell size.

For those poor results samples, a coarsening of the grain size was observed. A more rigorous investigation with XRD revealed a greater presence of carbides for those low impact test values samples which is a more convincing explanation for this large difference in values.

8.2 Results of the As-cast R2 Characterization.

Figure 28 shows R2 microstructure before any heat treatment. It basically consists in a predominant pearlitic matrix with occasional clear ferrite precipitations next the graphite nodules' interfaces forming the so-called bull eye configuration. Coarse and fine pearlite regions coexist along the whole microstructure associated with inhomogeneities in the carbon content and the cooling rates.

Isolated possible ferrite islands were rarely found in cell boundaries. Without a better analysis with other techniques (ex. colour etching), ferrite is easily misinterpreted and confused with carbides after etching with Nital. It is because of carbides also present a bright white colour when observing in LOM. A detailed study for the presence of carbides was, however, included within the scope of this work. It is probably the size and the shape as well as its positioning within the matrix that decides that they are likely carbides, but more experienced eyes could judge it in a different way. These early observations of possible carbides in the as-cast material represent a clear handicap of the raw material.

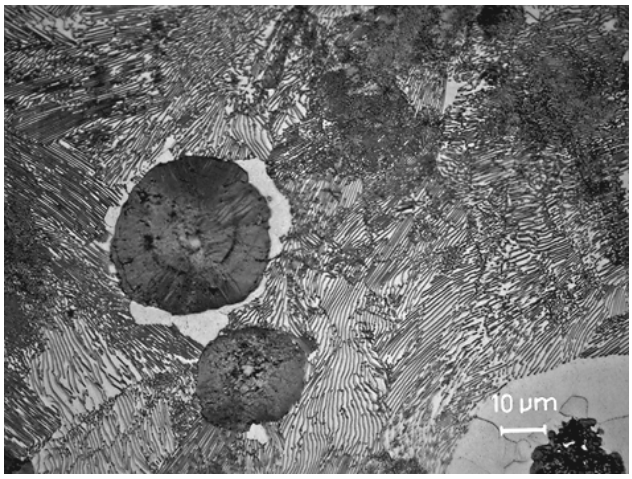

Figure 28 Ring's two Microstructure

An average value of 18 J resulted from the R2 untreated samples impact test. It is a very low value if it is compared with normal ADI materials which reach the 100 J. This brittle behaviour is understandable due to the presence of the pearlitic matrix and the ferrite precipitated on the graphite nodule interfaces.

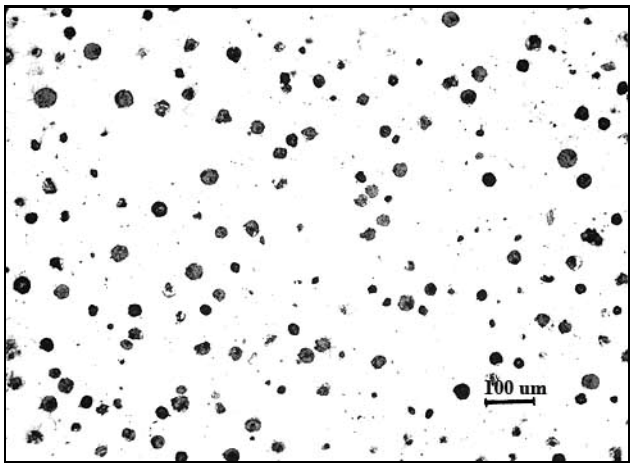

Figure 29 Nodule distribution for R2

The graphite nodule distribution for R2 can be observed in Figure 29. Contrasting with R1, R2 shows a more even concentration of graphite nodules with less tendencies of association in lines following the dendrite growth. Nevertheless, some of the nodules look like still having an excessive size, but not in a big percentage as occurred in R1.

As the nodularity and the homogeneity of the graphite nodules seemed to be better than for the ring 1, for further experiments, focusing on the use of R2 materials was considered the most logical idea because otherwise the results clearly had been conditioned to the poor quality alloy and the heat treatment and wouldn't make lot of improvements over the impact properties. Thus more detailed study was carried out for this alloy.

8.3 Results of the previous Investigations of Ring 2 Microstructural Possibilities

8.3.1 Modelling Results for Ring 2

For the same reason than for R1, modellings were run for R2 allow composition values. The resulting TTT and CTT diagrams are presented in Figure 30. In these graphics it can be observed that the pearlitic nose is very displaced into the left which reveals the risk of this alloy to develop pearlite if the quenching is not fast enough. If this would occur, it will be quite negative for the fracture toughness properties

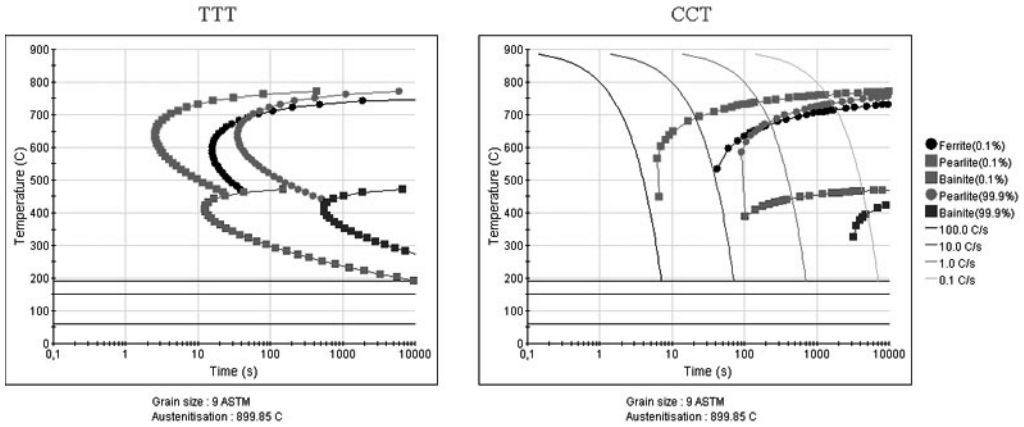

Figure 30 JMatPro TTT and CCT modellings for R2

In addition a modelling of ferrite-austenite phase fraction for austenitization interval temperatures was tried and it is showed in Figure 32, which will be commented subsequently.

8.3.2 Results of the Investigation on the Austenitization Regions for Ring 2

Figure 31 shows the microstructures developed during the investigation of the full austenitization temperature range. All the experiments consisted on heating the samples to their respective temperatures and then held them for 15 min after a quick quenching. The whole process lasted for around 30 minutes which is was consider time enough to make valid valuations with the results.

From the results, it can be asserted that very possibly the 850ºC temperature is not enough to dissolve properly the carbon into the austenite or to the complete austenitization of the matrix. It is concluded after looking at the low percentage of martensite areas (which means low carbon diffusion) and the ferrite still remaining and forming the bull eyes (see Figure 31.a). This result is not indicating that for longer holding times a better carbon dissolution won't be obtained, which probably will, but is telling that for this temperature there is a poor diffusion driving forces.

Increasing the temperature to 900 and 950ºC shows a greater and a more homogeneous dissolution of the carbon in the matrix. With the 900º C temperature it can be appreciated an inferior diminution of the segregation areas if compared with the 950ºC (see Figure 31), but in contrast, the cell size is greater for the 950ºC temperature. This discloses that a compromise between dissolving properly the carbon in the matrix (as well as reducing the segregation regions) and keeping a reasonable grain size shall be considered when choosing austenitization temperatures. This study served to propose the 950ºC and 900ºC temperature levels for further experiments.

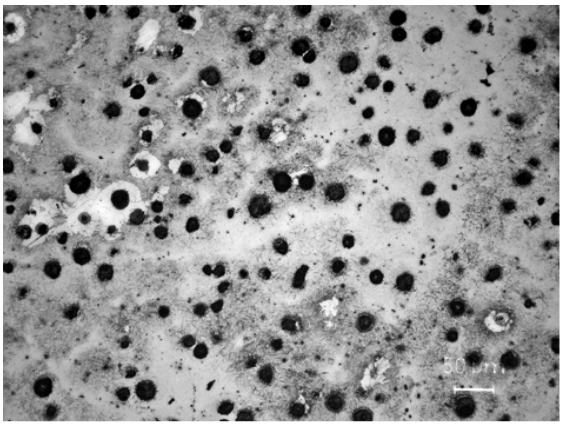

a) R2, 850º C, 15min

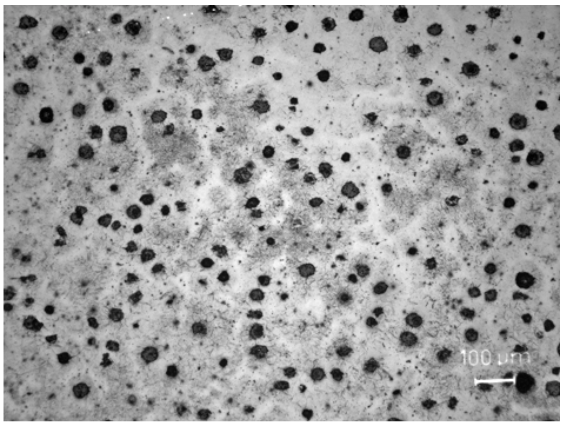

b) R2, 900º C, 15min

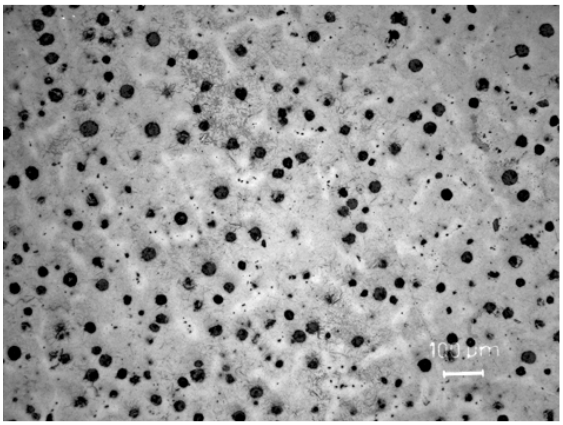

c) R2, 950º C, 15min

Figure 31 Microstructures developed during the investigation of the full austenitization temperature range.

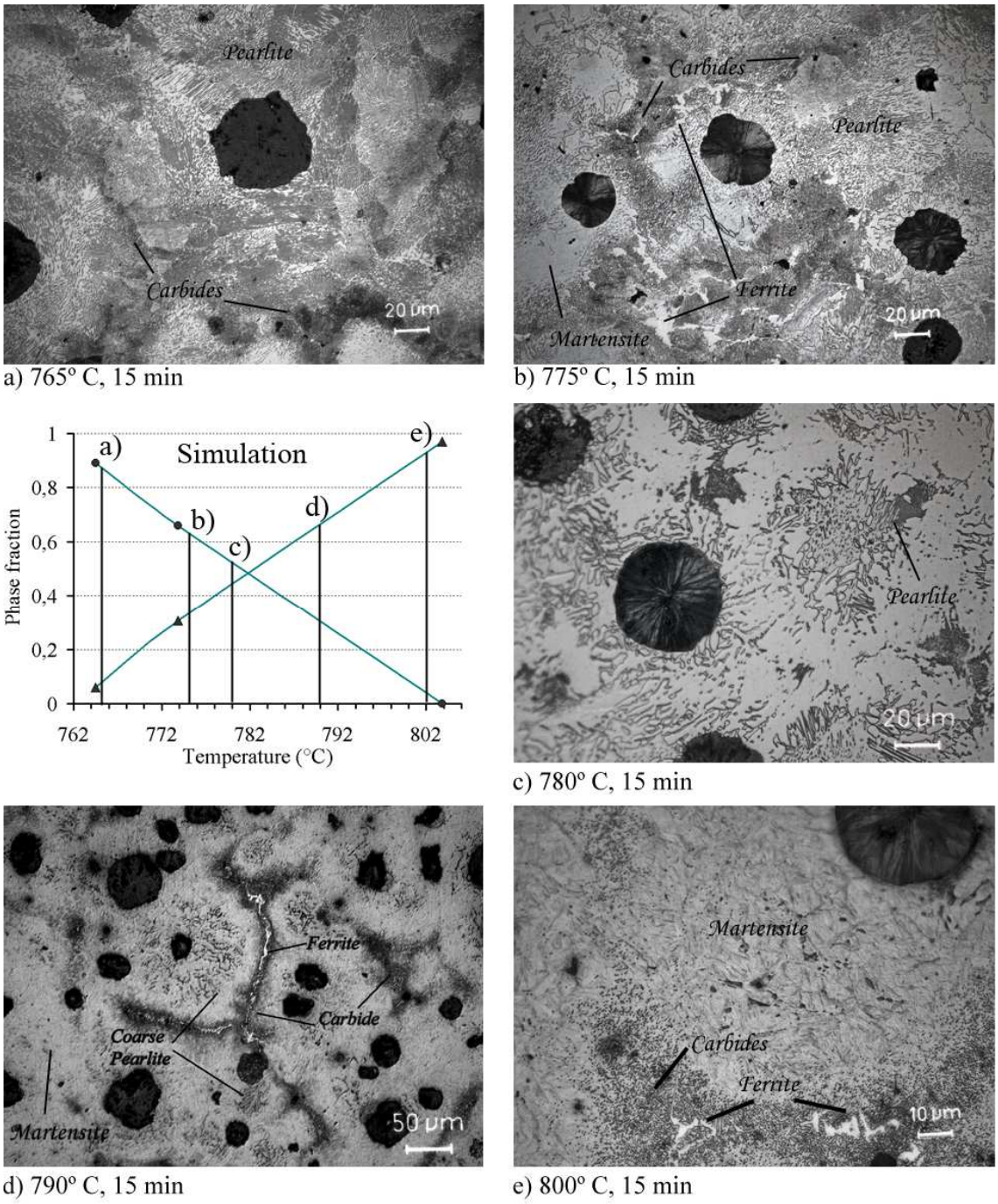

Figure 32 Investigation of interval temperatures for ring 2. The modelling of the austenite-ferrite phase fractions was made with ThermoCalc. On a), b), d) and e) what first was identified, and on the picture is marked, as carbides, a deep analysis brought out that phase is sorbite; what is marked as ferrite correspond to eutectic carbides imbibed by ferrite

Figure 32 shows the results of the microscopy characterization of the samples heat treated to investigate the austenitization interval temperature range for R2. All samples were heated to them correspondent temperature and then held for 15 minutes before a quick quenching. An evolution from pearlite (lower temperatures) to martensite matrix (higher temperatures) can be observed. It is clear that when gradually the temperature increases, pearlite areas start to soften following graphite nodule radial direction to the intercellular regions, keeping a remaining amount of coarse pearlite surrounding the nodules. This pearlite also remains near the cell boundaries but in this case instead of coarsening it gets fine. These results are quite

consequent with the TTT modellings (see Figure 30) which predict the cut of the pearlitic reaction somewhere between 780 to 790ºC after 900 sec.

More interesting resulted the outcomes from the ferrite phase fraction investigation and it precipitation on different areas to develop dual phase microstructures. The amount of ferrite decreases with temperature and allegedly, as it was deduced from the author interpretation of the images, it progresses from forming part of the pearlite to possible precipitate along intercellular regions and to its completely disappearance at the highest interval temperatures.
Certain controversy on the ferrite interpretation remains from these analysis. Considering what should happen during the interval temperature range, it is reasonable thinking that a rejecting of carbon mainly from the intercellular regions allows the ferrite forming within these zones. However, there is the risk of misinterpreting the pictures and confusing ferrite with carbides. It is also true that the intercellular regions are prone to carbide forming elements segregation, which makes very probable for this high alloying element cast forming carbides in that areas. Looking at Figure 32.d and Figure 32.e, the shape of the white light regions reminds the typical eutectic carbides one. Nevertheless, as predicted in the phase diagrams, ferrite would be present on the microstructure and there is no signal of it except the mentioned white regions or perhaps the light grey colour perimeter areas surrounding the white bright areas. To solve doubts, colour etching is proposed as the best and quickest alternative. Depending on what the micrographs really reveals, the microstructure developed in Figure 32.d could be very favourable for toughness purposes, in case of having ferrite, or a handicap, in case of having such amount of carbides.

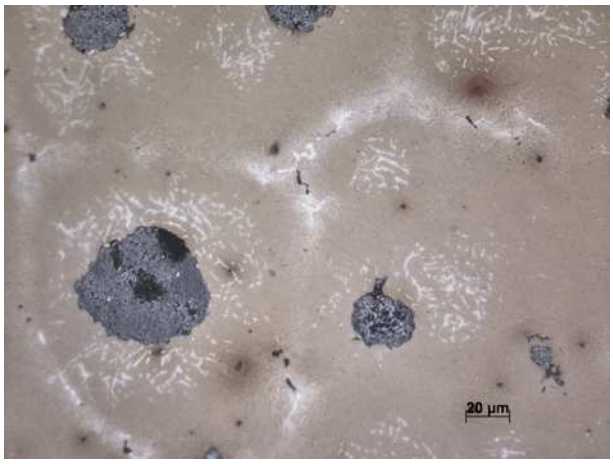

Figure 33 790ºC-15' etched and heat tinted with 1% Nital, 1 second and heated at 220ºC during 2 hours

An etched and heat tinted LOM image of the 790ºC-15' specimen is presented on Figure 33. The specimen was re-polished and re-etched with a soft Nital dissolution to undergo a colour etching heat treatment at 220ºC during 2 hour. The soft colour etching reveals the presence of different phases not appreciated with the normal etching. Dark white areas surrounding the graphite nodules can be identified as ferrite forming part of the remaining pearlite. In the normal etching it can be appreciated dark black spots following the branch configuration which was not clearly revealed with this colour etching. These lines can be identified as ε-carbide or cementite.

Focusing the eyes on the intercellular regions two phases can be clear distinguished. The brightest white one can be now clearly identified as eutectic carbide and the darker white adjacent can be identified as ferrite because it keeps the same tone and colour than the

identified ferritic areas nearby the graphite nodules. The cream colour areas represent the martensite areas. Black little spots regions revealed with normal etching can be identified as sorbite which is a special type of pearlite composed by little spherules of ε-carbide. That spots were softened with this colour etching making clear the real nature of the phase neighbouring the eutectic carbides.

Another interesting discovery resulted from these experiments. Ferrite inclusions were found in the graphite nodules as shown in Figure 34. It occurred globally for the 775ºC treatment during 15 minutes and then quenching, but also for other temperatures. These inclusions are referenced in literature [42] as being responsible of decreasing toughness properties of the material.

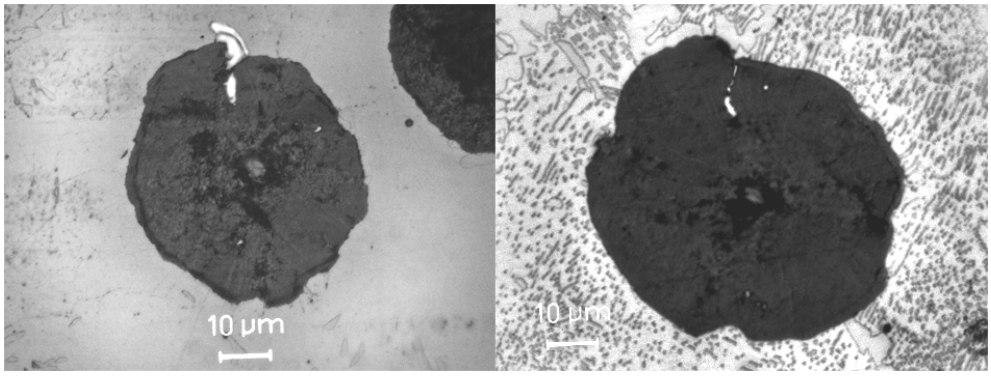

Figure 34 Discovery of ferrite inclusions in many graphite nodules for ring 2 and for 7750C during 15 min.

8.3.3 Result of the Study of the properties variation depending on distance for R2

Thinking on the possible casting process and for the relative big size ring it can be imagine some kind of microstructure and alloying elements heterogeneous distribution within the ring, due to the cooling process with presence of hot spots or the mould melt filling process. This can affect to the process of toughness optimization since the material after heat treatments couldn't be showing its full potential or giving a big scattering depending on which part of the ring is cut for samples. Assuming this possibility some experiments, as described in 7.5.2, were carried out. This study, as the best of the author knowledge, has never been reported with anteriority on literature which makes the results more interesting. The outcomes after impact testing these samples are reflected on Figure 35.

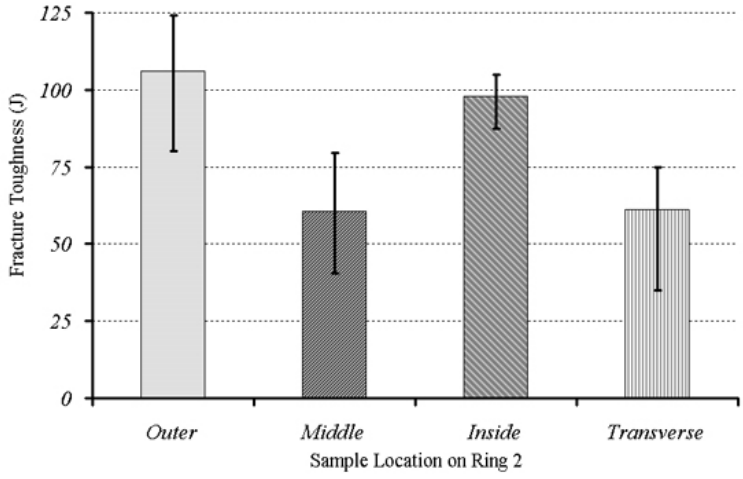

Figure 35 Impact test study for different sample location for R2

As can be observer on Figure 35 chart, there is a clear dependence on the sample location within the ring. The best results are obtained from the samples taken from the outer and inner radius regions. Middle and transverse samples show approximately the same impact values, which is reasonable because for both the fracture line will progress more or less from the same ring's region.

In order to investigate what is the cause of these variation on the impact test results depending on the sample location, further investigations on the fracture surfaces were made using the SEM. Figure 36 shows a comparison of two fracture surfaces corresponding to an outer (a) and a middle sample (b). The black spots represent graphite nodules.

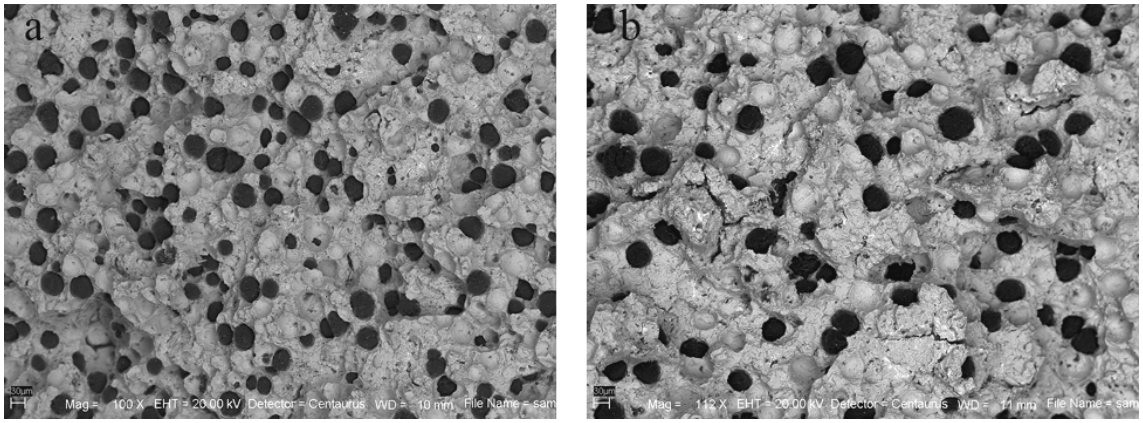

Figure 36 a) Surface SEM magnification for an outer sample, b) Surface SEM magnification for an middle sample

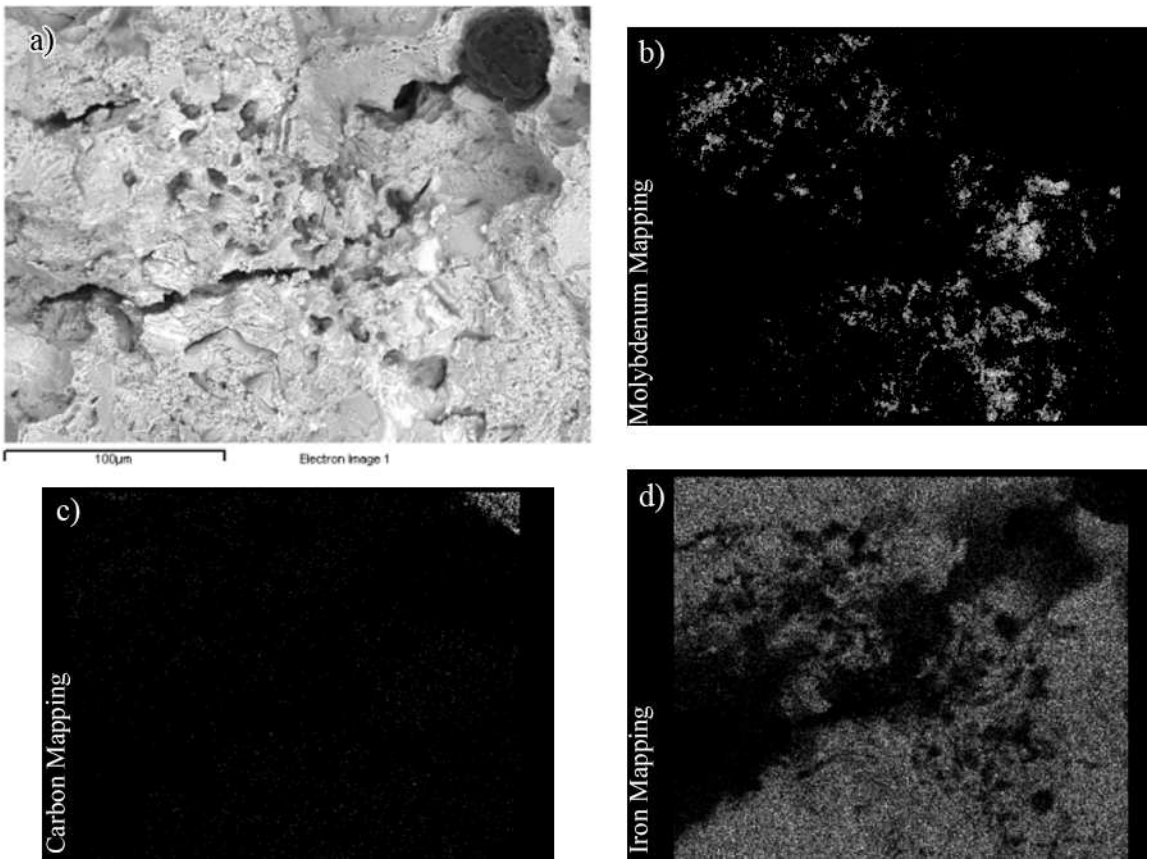

Figure 37 EDX mapping for carbide forming elements search for middle sample: a) scatter electron image, b) Molybdenum mapping, c) carbon mapping, d) iron mapping.

It was detected for the inner sample lot of microcracks among the entire fracture surface as can be appreciated on Figure 36.b. This surface also presents frequently cleavage regions. These issues are indicators of a brittle fracture and are consequent with the low impact test values for this sample. To deduce if these microcracks are caused due to the presence of carbides, more detailed analysis were made over these peculiar zones. A mapping searching for carbide forming elements is shown in Figure 37. It was detected the presence of high concentration molybdenum areas around the microcrack, which probably are associated with the formation of carbides.

If a comparison of Figure 37.a and Figure 37.b is made, the bright white areas near the right bottom corner of Figure 37.a could be identified as molybdenum carbide. Other unknown particles can be distinguished following the perpendicular direction of the biggest crack. This direction corresponds clearly with a segregation line on the cell boundary. The crack probably was initiated on the nearby graphite nodule (big black dark spot) and followed the most favourable direction which was the brittle carbide one.

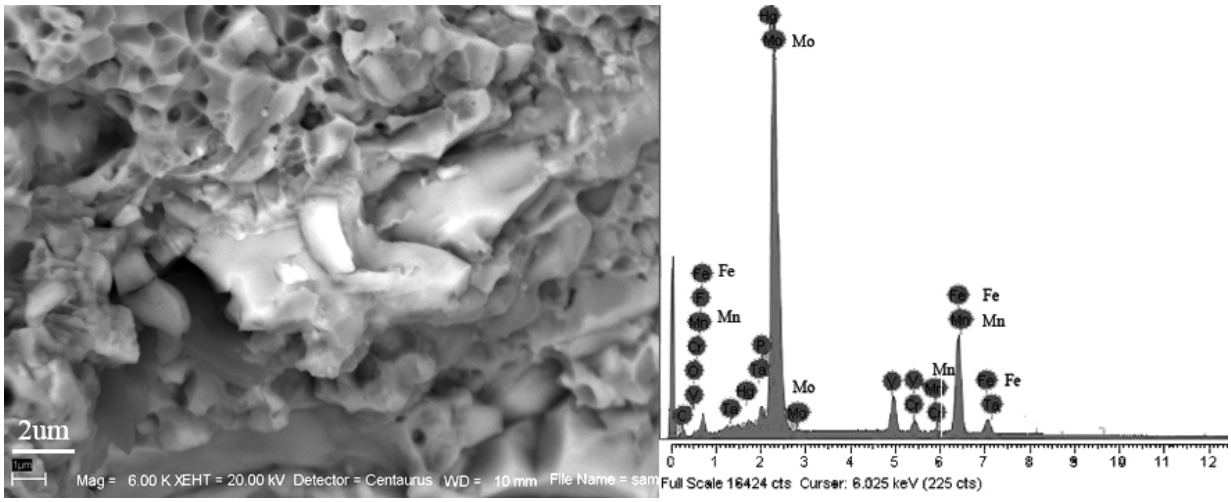

Figure 38 Magnification of a Mo carbide and its correspondent EDX analysis for middle sample.

A magnification of the areas surrounding the crack was made. In addition an EDX analysis over these areas was also carried out. Molybdenum carbide was identified as it can be appreciated in Figure 38. The carbide presents a brighter grey colour and can stand out for its more flat surface if comparing with the surroundings. The XRD analysis (on right) clarifies the nature of this particle which has strong peaks that can be attributed to iron and molybdenum standard peaks, even if the iron peaks some times are confounded with manganese peaks.

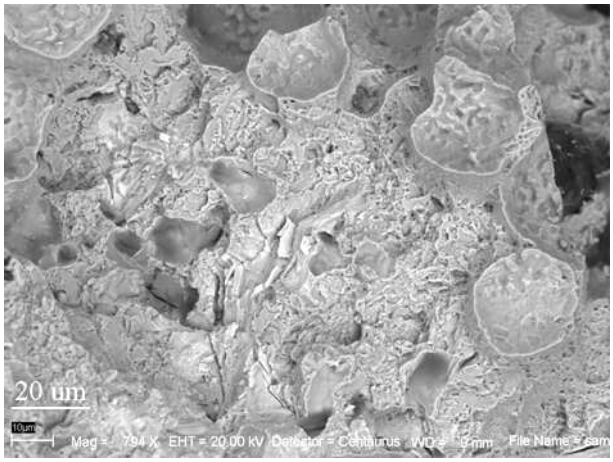

Figure 39 Outer sample fracture sample magnification

For the outer sample magnification of some regions (see Figure 39) was also made trying to look for the presence of carbides. No conclusive asserts could be drawn after the search. What is was observed is the more frequent crack propagation by dimples and in isolated cases cleavage fracture was observed. Figure 39 resumes what it was practically a constant among the surfaces areas examined. Ductile fracture is the predominant mechanism, combined with some brittle fracture that in the case of Figure 39 is associated with the presence of micro shrinkages as can be appreciated on this picture.

8.4 Results of R2 ADI heat treatments

8.4.1 Impact test results of the complete heat treated samples

After the previous study some experiments were proposed to develop ADI microstructures as explained in paragraph 7.4.1. The different experiment carried out are compiled in Table 4 and schematized on the Figure 40 chart. The samples were obtained from the transversal direction of the ring

Table 4 Impact data compilation for different experiments and R2 samples

	Code	T [ºC]	t [h]	T [ºC]	t [h]	T [ºC]	t [h]	T [ºC]	t [h]	IMP
ADI	**R2A**	900	1	-	-	-	-	360	1	33,8
	R2B	950								44,7
DPADI	**R2C**	900	1	800	1	-	-	360	1	70,5
	R2D			775						49,7
	R2E	950	1	800	1	-	-	360	1	48,9
	R2F			775						81,9
Y	**R2G**	900	1	800	1	260	0,6	360	1	24,1

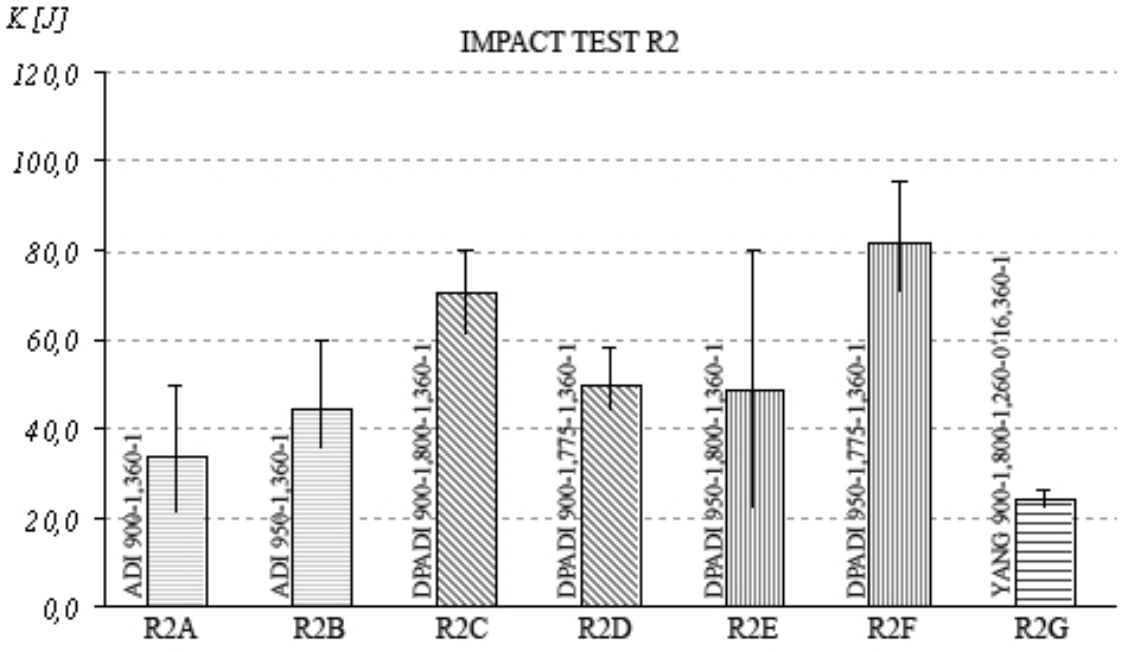

Figure 40 Chart with the impact test results for R2 experiment samples

The highest impact values occurs generally for those ADI batches that were austenitized at high temperature level (950º C), which is the case of R2B, R2E and R2D. This could be explained, before any other composition study, because of the possible higher carbon content on the austenite as the result of this higher temperature or a best dissolution of segregation regions. Comparing samples, normal ADI R2B resulted to be very competitive with some DPADI. It shows similar average impact test results than R2D and R2E, and clearly is more reliable than R2E.

The big variability present on R2E and in many other batches seems to be intrinsic to the material manufacturing processes. In this case, parameters like samples distribution along the oven of each batch could be a determinant factor since temperature distribution and flow have been demonstrated to be crucial and affect very sensitive the microstructure. The pieces, as earlier studies showed, are also subordinated to internal casting defects which can also explain the variability.

As earlier studies [4], Yang's heat treatment didn't evidence any improvement on toughness properties. This is probably because of the short one austempering time and low temperature that wouldn't permit the presumable martensite structures formed to turn into ausferrite during this stage.

There is a lack of information about DPADI alloys in literature, lack more evidenced when a relation between full and interval austenitizing temperatures in the final result. Some works [24,43] have demonstrated that those factors are related and influence in a large extent the fracture toughness properties. Even though, a factorial analysis for the DPADI samples was done trying to establish some relations of these temperatures with the toughness properties for the R2 alloy.

The study factors chosen for this investigative analysis of the results were full and intermediate austenitising temperatures, referred respectively as TA and Ta. The interaction between factors is referred as TA-Ta. A two-level variation of the factors was chosen. The different levels are represented on Table 5. These decisions allow interpreting the correlations between those last parameters with the impact results, L_k. Due to the number of levels was set in two and only two factors were intended to be studied, a full factorial design was recommended with four for the number of runs.

Table 5 Decision of the factors' levels

Level	Symbol	Full Austenitising Tempertature [º C]	Intermediate Austenitising Tempertature [º C]
Low	-	900	775
High	+	950	800

Table 6 shows the design matrix for the factorial analysis and the contrast for each factor L_k. To avoid noise factors and minimise the variation, and to estimate the variance of the contrast, s^2_{POOL}, three replicated experiments were made. These replicates are not genuine since the factors levels weren't changed on each run.

Table 6 Design matrix for the factorial analysis

i	TA	Ta	TA-Ta	y_{i1}	y_{i2}	y_{i3}	$\bar{y}_i$	s_i^2
1	-	-	+	58,3	46,6	44,2	49,7	37,94
2	+	-	-	95,7	79,4	70,5	81,9	108,88
3	-	+	-	80	70,5	60,9	70,47	60,80
4	+	+	+	80	44,8	22	48,93	569,21
L_k	2,66	-3,04	-13,43				$\bar{\bar{y}}_i = 62{,}74$	$s^2_{POOL} = 194{,}21$

The contrasts by themselves are not enough to decide whether they are significantly larger to consider their correspondent factors or iterations as active. Some comparisons with the contrasts normal standard deviation should be done. Consider a factor or iteration as active means that it has a strong influence on the results. To help analysing the results a normal probability plot with the contrasts was created and it is presented in Figure 41. A tendency line crossing the point (0, 50) is drawn to see how the contrast deviates from a normal distribution. Those factors or iterations which clearly deviate from this line are reflecting they will have in some extent an influence on the results, so they can be marked as active.

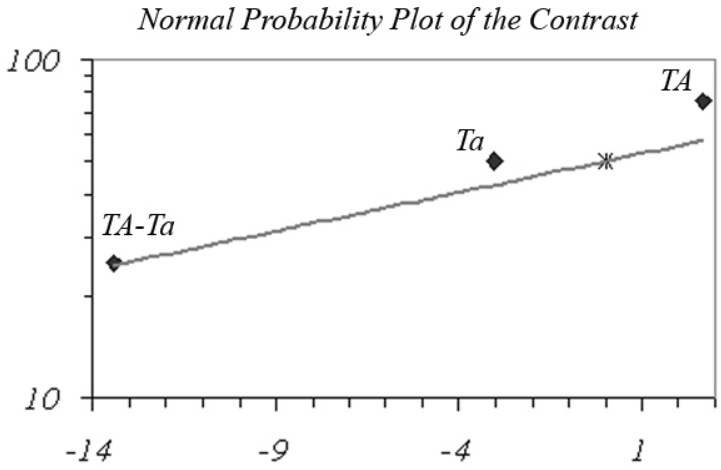

Figure 41 Normal probability plot of the contrast

From the normal probability plot of the contrasts, can be appreciated that none of the factors deviate an exaggerated distance from these line. In addition, the standard deviation of contrast resulted to be s_{pool}= 13’93. To consider a factor as active, its contrast must be larger than plus minus three times the contrasts standard deviation, fact that doesn’t occurs for any of the factors. That is meaning, in contrast with what literature narrates, that austenitizing temperatures have a poor influence on the fracture toughness properties. That would be reflecting that other factors, as could be defects on the cast, are influencing the results.

However some rough interpretations can be drawn from this study. Full austenitization temperature have shown to be the most influencing factor and as it has a positive contrast value, it should be set in the high level. In contrast, intermediate austenitizing temperature have less influence on the fracture toughness and as it has a negative contrast value, should be set in the low level. Interaction between T_a and T_A has been demonstrated, as founded on literature [34], that those variables don’t depend one from each other.

8.4.2 LOM Results of the Heat Treated Samples

Figure 42 shows a comparative of microstructures for three different dual phase heat treatments. The first relevant thing that can be observed, comparing with the study for interval temperatures, is the ausferrite evolution depending on previous microstructure and the ratio ferrite-austenite. When low interval temperatures were used, for example 775ºC, pearlite is developed in austempering previous steps. The resulting ausferrite phase seems to keep the pearlite tight lattices with long but fine ferrite needles imbibed in retained austenite as it can be seen on Figure 42.a.

The image corresponds to 950ºC-1h, 775ºC-1h and 360ºC-1h heat treatment. The ausferrite have, in this case, a high percentage of acicular ferrite. The compilation sequence between acicular ferrite and retained austenite is almost impossible to distinguish due to they are very close each other. However the needles length on average is quite large with a promethium of around 20μm what it was discussed to have a negative influence on toughness properties.

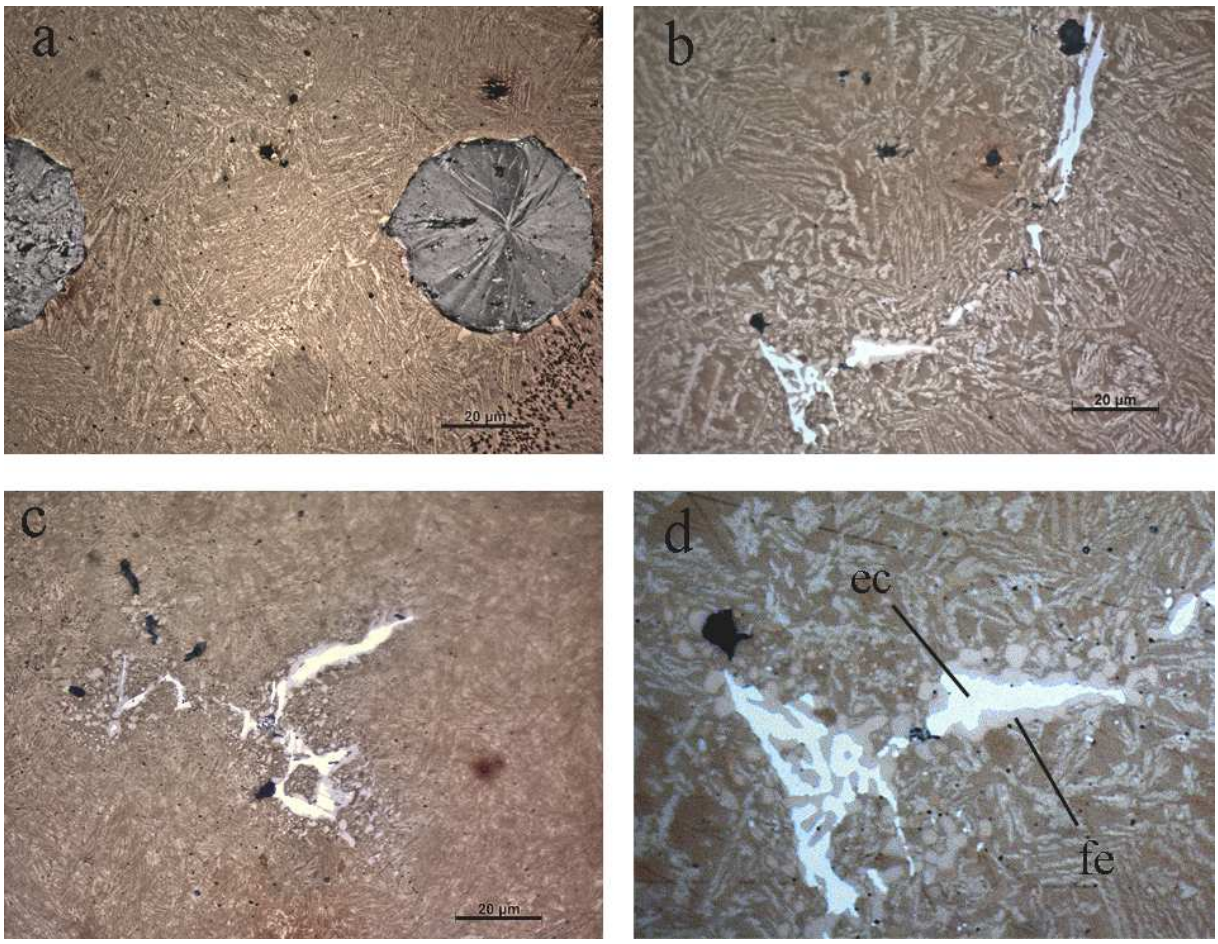

Figure 42 Colour etching with 1% nital at 220ºc for 2 hours. All the samples have same magnification: a) 950ºC-1h, 775ºC-1h, 360ºC-1h, b) 950ºC-1h, 800ºC-1h, 360ºC-1h, c) Yang Process, 900ºC-1h, 800ºC-1h, 260ºC-10', 360ºC-1h, d) detail of an eutectic carbide surrounded by proeutectoid ferrite.

For those samples austenitized in the high interval temperatures range, austenite was the predominant phase and there was no pearlite remaining. The ausferrite phase evolves directly from the austenite. Figure 42.b shows the microstructure resulted from the heat treatment 950ºC-1h, 800ºC-1h, 360ºC-1h. If it is compared with the previous microstructure, this one is coarser with a wider separation between acicular ferrite, in light pink cream colours, and

retained austenite revealed in dark brown colour. In addition the needles length was reduced. A peculiar observation is the ausferrite shape change depending on the matrix location. Near the graphite nodules, ausferrite present a more even orientation of laths and a more regular compilation. When the intercellular regions are approached, the orientation becomes uneven as well as the compilation and the needles extend in wide and short in length rounded them shape.

The Yang process (900ºC-1h, 800ºC-1h, 260ºC-10', 360ºC-1h) gave also interesting microstructure results. The LOM analysis of this process is relevant because of the samples subjected to this heat treatment presented the worst impact test results (20J). The components and characteristics of the matrix for Yang's samples can be appreciated on Figure 42.c. The ausferrite phase is in that case very fine and inexpert eyes could misinterpret it with martensite. It seems that in the early austempering stages, the ausferrite evolves from some martensite derived of the Yang's process undercooling. This theory is not contrasted, at the best of the author knowledge, but it would be attractive to investigate it deeply in further works. Nevertheless, the presence of martensite is not discarded and maybe is confounded with the ausferrite phase. The colour etching was very soft that didn't allow any distinction between ausferrite and martensite but the presence of both phases coexisting is very feasible looking at the CCT and TTT curves. The existence of martensite could be one of the reasons for the poor impact test results. Another explanation could be low austempering times that weren't enough to reduce the inducted strengths when quenching and undercooling. However, believing in those works that assure that the finest the ausferrite the better toughness results, and in spite of the low impact test values obtained, the microstructure developed during Yang process is still very promising. Perhaps Yang process is not recommended for high alloyed ADI which was also the conclusion of previous works.

For all the dual phase samples a remarkable discovery was made in relation to the eutectic carbides formed along the intercellular regions. This carbides stand out for them bright white colour in the pictures while what it is presumed to be ferrite maintains a soft pink cream colour among the whole microstructure. It can be appreciated that a phase similar to what it was identified as ferrite, when ausferrite phase was analysed, is surrounding the eutectic carbides. This fact is reflected on Figure 42.d which is a detail from magnification of Figure 42.b. No further investigation was made on the nature of this phase during this work, but in case of confirming the very probable ferritic composition somehow it can be considered as a good result because it would be meaning that a "protector" weak and ductile phase is created around a very brittle one, so theoretically the toughness properties would be improved due to that fact even with the existence of these carbides.

8.4 Optimum processes results

After previous studies and trials with different heat treatments and after clarifying the location properties' dependence within the rings, new experiments were proposed. For these new experiments the samples were extracted from the rings zones that showed better impact test results which were the inner and the outer radios transversal cuts. With this deliberation better results were expected, as so it happened.

A novel heat treatment was proposed to develop an improved DPADI material. It consisted on the 950ºC-1h, 790ºC-1h and 400ºC-1h stages. The austempering temperature was reached to 400ºC because of the thought that with 360ºC one hour wasn't enough time to fully austempering. The 790ºC temperature was the consequence of previous investigation for

determining the optimum amount of ferrite phase in the matrix. The whole treatment is consequent with the best impact test results obtained in previous trials. The 900ºC-1h and 360ºC-1h heat treatment was a replica of a previous trial and it was carried out to confirm whether improved properties are achieved if a good ring's cut is used.The 860ºC-1h and 400ºC-1h heat treatment was based on the industry current tendencies which presume to exceed the 100J during impact test for the alloys used during this work.

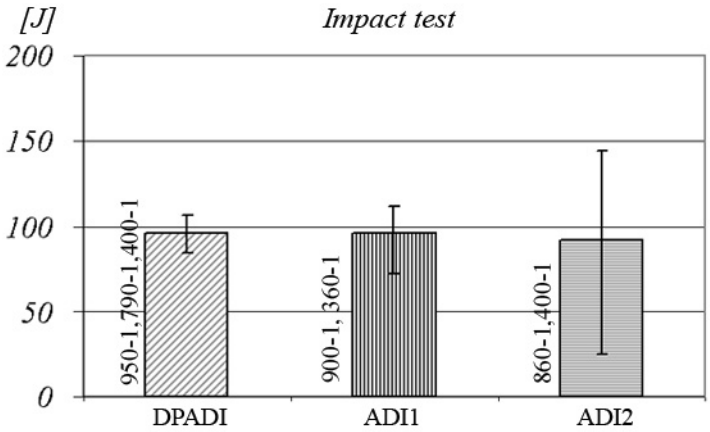

Figure 43 Impact test results for outer R2 samples subjected to different heat treatments

The outcomes of the impact test are presented on Figure 43 chart. It can be observed that there are not significant differences between the averages values for the different heat treatments, which are touching the level of the 100J. This is representing very positive results. Nevertheless, for one of the heat treatments, the 860ºC-1h and 400ºC-1h one, the variance of the values are intolerable making the heat treatment unreliable and thus unsafe. Further investigations on fracture regions with stereoscope microscopy for the 860ºC-1h and 400ºC-1h heat treatment and for the 145J and 25J samples, reveal the presence of elements inclusions and a higher amount of shrinkage regions for the poorest impact value sample. The presence of big element inclusions on small area impact test specimens introduces a risk factor for misinterpreting results due to those inclusions are very probable crack initiators and drastically brittles the samples, fact that is empowered for the high size/area ratio. So it is reasonable to neglect the 25J value and consider it useless for the reasons cited in spite of reducing the batch size to two elements.

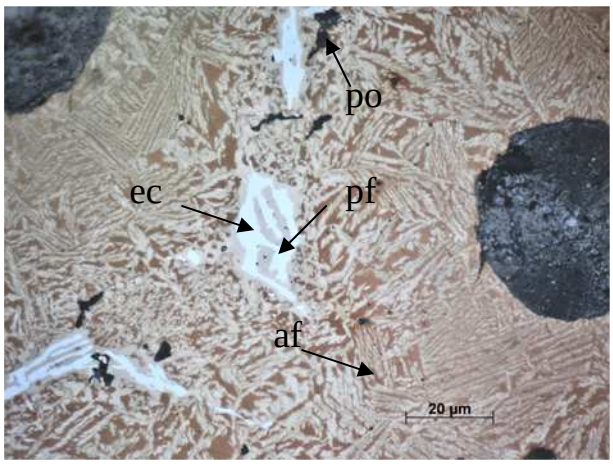

Figure 44 1% Nital heat tinted 950ºC-1h, 790ºC-1h and 400ºC-1h. ec: eutectic carbide; pf: pro-eutectoid ferrite; po: porosity; af: ausferrite

This inconvenient was assumed when the three elements batch was proposed for the experiments. Ideal batch's size would had been around ten elements, however the oven bulk wasn't big enough to assure homogeneity in heat application, and greater sizes than 3 specimens per experiment would had lead on excessive material mass to be heated, increasing the experiments times and also the risk of uneven heat evacuation when cooling.

Figure 44 shows a micrographic of the 950ºC-1h, 790ºC-1h and 400ºC-1h heat treatment. It can be observed the different ausferrite size and type following to graphite nodules lines. It is caused for the presence of elements segregations. The fine ausferrite found neighbouring the graphite nodules should be a constant along the matrix and the coarse ausferrite formed in the proximity of the cell boundaries shall be avoided as it could impair certain disadvantages for fracture toughness. The ferrite surrounding the carbides can be observed as well as the associated shrinkages. This fact was also observed for previous experiments when worst part of the ring was used for experiments. According to this, no real big differences between good oar bad cuts have been observed after microstructure analysis, but everything indicates that a difference exists.

9. Discussion of the results

9.1 About the quality of the as-cast rings

During the present work has been demonstrated that the quality of the as-cast rings used in the experiments, although being it within the normal standard demands, was not enough to achieve outstanding impact test properties. This is only meaning that with the actual industry standards can be obtained good results but there is a great potential for better ones if improved quality would obtained. Both rings, R1 and R2, presented several microstructure deficiencies and handicaps that were linked with the great scattering of the impact test results; defects that a more careful process design would correct.

For R1, inappropriate cooling rates of the ring could be causing inhomogeneities on the graphite nodules size. This affirmation is consequent with the observations of the perfectly clear dendritic growth during solidification. The dendrites are prone to concentrate the big size graphite nodules due to that nodules solidify during the first stages of the cooling and act like a carbon sink during all the process. However, the areas surrounding the dendrites take more time to solidify and the graphite nodules formed are smaller. This solidification way creates inhomogeneities that could be distinguished during different microscopy observations. In addition, some remaining segregation areas were observed too. These regions that follow the intercellular boundaries could be caused for an excessive alloying elements concentration within the matrix, especially and in concrete for this cast, Molybdenum and Manganese. The presence of shrinkages was also remarkable, being this another indicative of a bad cooling because their presence is related with ring's volume variation during solidification or badly gases evacuation. This cast defects made inefficient whatever heat treatment applied to maximize toughness properties, although with one of the sample the value of 100J was obtained for impact test; nevertheless the variability in results for different sample was still enormous as consequence of the inhomogeneities of the matrix making this alloy unreliable.

The results for nodularity and nodules distribution for R2 were more promising. That made suspect on better results with this alloy, as so happened, although this alloy was not exempt of a concerning huge presence of eutectic carbides along the cell boundaries. This undesirable fact was related with the existence of the Molybdenum alloying element massively concentrated along those regions too. Molybdenum is well indicated in heavy sections castings to avoid pearlite formation but is a very strong carbide forming element thus it use is recommended not exceed the 0,2 wt%. For R2 a 0,27 wt% was used so this is explaining the big amount of carbides. Another concerning fact, also derived from a high particular elements high concentration like manganese or the same molybdenum, was the frequently presence of micro-shrinkages in the places where carbides use to precipitate. Manganese concentration should not exceed the 0,3 wt% and for R2 is noteworthy crossing the limit with a 0,34 wt%. Excessive manganese is related with the formation of micro-shrinkages, but also with an increment of the incubation time of the ausferrite and less stable retained austenite. The presence of this micro-shrinkages combined with carbides, are a risky factor due to it is an ideal road for the fracture propagation.

Another handicap was observed for the R2. It was verified during a novel study, the location within the ring properties' dependency. This may be caused for different cooling ratios, gradients of temperature or elements composition inhomogeneities and it is bringing out, in addition with other factors, that the casting process need to be improved. In concrete, after impact test, the presence of micro-cracks was observed along the whole fracture surface for those samples extracted from the middle part of the ring. These micro-cracks were placed in

the segregation areas and they were probably associated with the presence of Molybdenum carbides. Micro-cracks weren't observed in the outer and inner ring locations which resulted to be the better areas to extract samples.

9.2 About the DPADIs compared with normal ADIs

Dual-phase austempered ductile iron microstructures were tried to be developed during this work. In concrete it was searched for ferrite precipitation along the cell boundaries with the thought this configuration would improve fracture toughness properties.

Heat tinted micrographics revealed that this configuration was achieved just only in some extend, but not in the level desired. Trying to explain this "partial unsuccessful" result with DPADI structures formation, is believe that inadequate casting alloying elements composition and characteristics for this particular case, would be degenerating in a very tough challenge for DPADI alloys developing. The possible most remarkable lack in relation with this is the low percentage of silicon. For R2, this element is presented in a low concentration, 2,13 wt% when the recommended amount is in the range of 2,4-2,8 wt%. This is not only obliging the use of a higher quantity of carbon to keep a suitable carbon equivalent, but also is probably inducing a lower ferrite content after heat treatments and the reduction of the ($\alpha+\gamma$) austenitization temperatures range, lowering also those temperatures. As well, the presence of carbide forming elements in the cell boundaries makes the carbon stay in eutectic carbide form. Consequently the necessary carbon rejection from these areas for the ferrite formation is limited and thus less ferrite than expected is precipitating along them.

However, it was discovered that this little amount of ferrite precipitation along wanted cell boundaries regions occurs imbibing the eutectic carbides formed. This peculiar find wasn't reported by any other study, at the best of the author knowledge, and it is believed that would imply advantages to the new material acting the ferrite like fracture anchor or a protector phase. The dynamic toughness results of the first experiments, when the transversal direction of the ring was used to obtain samples, showed a clear superiority of some of the heat treatments destined to dual phase microstructures forming in contrast with normal ADI ones. Considering the fact that after all heat treatments practically the same amount of precipitated eutectic carbides was observed, it makes suspecting that ferrite carbide's coat is a positive feature for optimizing fracture toughness for this concrete case.

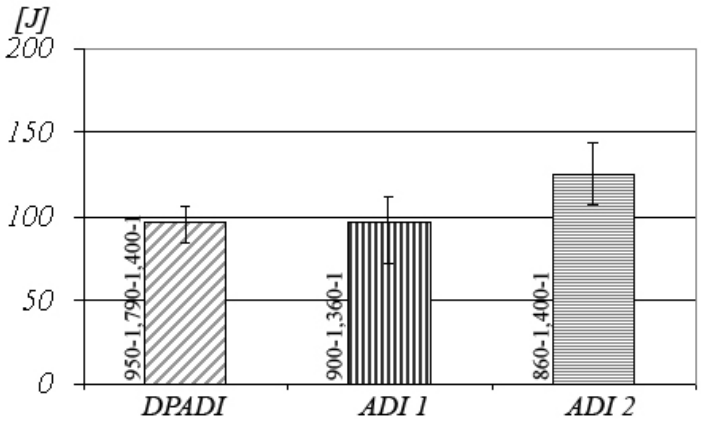

Figure 45 Impact test results for outer R2 samples subjected to different heat treatments, with corrected values for ADI 2

Further investigations with better cuts of the rings and better and optimized heat treatments showed similar results for both normal ADI and DPADI microstructures, which all exceeded the 100J during impact tests. Industrial normal ADI heat treatment 860ºC-1h and 400ºC-1h resulted to be the standing out process giving a maximum impact test value of 144'5J and a notorious 125J average value (after discard the 25J value, see Figure 45). Nevertheless, DPADI kept high impact values for all the locations of the ring which makes thinking in DPADI microstructures introduce reliability on the results maintaining a good level of fracture toughness. Although the differences between normal ADI and DPADI weren't so clear after final impact test results, it is believe that the handicaps founded on the as-cast materials are limiting the fully potential of both normal ADI and DPADI. A factorial study for DPADI showed that surprisingly temperature variation wasn't influencing the impact test results, which is also reflecting that other factors, as could be porosity or carbides (see Figure 42 and Figure 44), were having some effect. Very probably, with a better cast, those differences between diverse sort of ADI materials would increment favouring the DPADI type, in concrete in absence of carbides. One explanatory theory about the big success of the normal ADI 860ºC-1h and 400ºC-1h heat treatment, after not noticing high differences on the grain size or the carbides precipitated, is the slighter temperature gap between austenitizing and austempering temperatures which would be introducing less residual stresses when quenching. However a more consciously study had been needed to bring out more conclusive outcomes.

9.3 The (α+γ) austenitizing temperatures and microstructure evolution

Concerning the evolution of the previous phases to the ausferrite when intermediate austenitizing steps were applied, interesting results where observed. For those low (α+γ) interval temperatures where pearlite was formed, the resulting ausferrite have a much compiled pro-eutectoid ferrite-retained austenite laths, distributed homogeneously and following the old pearlite shapes. The microstructure developed after the 950ºC-1h.775ºC-1h and 360ºC-1h has these characteristics and resulted to be the best after impact test. With high interval range austenitizing temperatures a more common ausferrite was developed if compared with the one typically obtained in normal ADI. This occurs for the 900ºC-1h, 800ºC-1h and 360ºC and for 950ºC-1h, 800ºC-1h and 360ºC with also promising impact test values. The Yang process gave the lowest impact test results having the finest ausferrite microstructure that reminds the martensite one. The poor values obtained for impact test could be the result of martensite locations within the matrix which is just a supposition because they had not been identified properly. The observed microstructure makes thinking on very fine ausferrite and martensite confounded with that last phase (Figure 42.c). However, another explanation is the high internal stresses inducted with a big temperature gap cooling, from austenite temperatures to near martensite region temperatures combined with a short austempering time which was not enough to reduce these stresses.

After this microstructure studies, it seems that the final shape and size of the ausferrite depends of the previous phases developed during different heat treatments stages. This fact could be a novel discovery as it wasn't reflected in literature, at the best of the author knowledge. Nevertheless a better study shall be done to assert that the ausferrite evolves from its ancient predecessor phase during different heat treatment stages which could be pearlite, retained austenite or martensite, as it presumably happened during the experiments carried out.

10. Conclusions

The aim of this study was to identify features in the microstructure of DPADI that directly affect the fracture toughness of the investigated alloys. No massive ferrite precipitation was observed after DP ADI heat treatment for R2, probably for the high content of carbide forming elements which avoid the rejection of carbon during the intermediate austenitization process and a low percentage of silicon. However, the most outstanding discover was the precipitation of ferrite surrounding the undesirable eutectic carbides formed along the intercellular regions. This is concluded to be an advantage to those carbide-precipitated ADI materials that don't present these formations. This advantage was demonstrated during the transversal ring cut samples experiments. For that reason, DPADIs are believed to be at least more reliable materials compared with normal ADI, issue that shall lead into monetary saves to the industry and confidence in ADI alloys. Although, after comparing with normal ADI for good rings cuts, no conclusive differences after impact test results were detected, except a lower scattering for the DPADI. This could be meaning that no relevant features that imply improvements on the fracture toughness properties were developed in the DPADI, except more reliability.

A clearly dependence on the as-cast quality was detected, which is limiting the full potential of all heat treatments carried out during this work. In conclusion, an uncertain evaluation of the competitiveness between normal ADI and DPADI can be done. Both types of ADI had promising outcomes in the impact test results, but a modification on the conditions and the composition of the as-cast irons used for this work is recommended in order to reduce the deficiencies observed, mainly with the high percentage of carbides precipitations for all the heat treatments, the high level of shrinkages detected and the heterogeneities in the matrix such as graphite nodule distribution and shape. It shall as well be reminded of taking care of the properties' dependence on the location within the ring with a better casting process that avoid hot spot formation and promote a better evacuation and distribution of the heat.

If those disadvantages are saved, ADI materials will show very promising results that will make these alloys very competitive for fracture toughness. Probably better results with DPADI, making these alloys standing out the normal ADI ones, would be obtained after an improvement of cast qualities specific for that kind of materials.

11. Further Investigations

After this work, new alloys will be proposed to develop novel rings in order to minimize the deficiencies detected for the rings used. In concrete, a revision of the cast composition should be done for Si, Ni, Mo and Mn. As well the cast process shall be revised in order to avoid undesirable hot spot detected on the final microstructure. Further similar investigations than the ones conducted during this work are recommended to optimise the new materials, although the outcomes obtained in the present work shall serve as a reference for the continuous improvement process.

This study tried to include many different topics related to the fracture toughness properties resulting sometimes in a very weak analysis of particular issues, which makes the necessity of deep investigations on such as issues. The use of only three elements batch just only gave rough estimations of the real average values for impact test results, but there was a bulk limitation with the current laboratory ovens. The use of bigger devices to widen the batch size is recommended, and probably the help of the industry sector would be required

In concrete three relevant outstanding and novel topics are recommended to be reinvestigated more in detail: ferrite precipitation around the carbides, properties dependence on the ring location and evolution of the ausferrite from different phases. In addition, some test shall be done to check if the matrix residual stresses are dependant on the temperature gap when quenching.

Better researches on the different austenitizing temperatures and on the grain size related with fracture properties might be also carried out. It would be also interesting to run static fracture toughness test to determine K_{IC}, and tensile strength and hardness test in order to compare more seriously with the ADI literature.

Fatigue specimens should be tested in addition to the impact test results for R1 and R2 alloys to set the real potential of DPADI microstructures for industry uses.

BIBLIOGRAPHY

[1] Dorazil E. *High Strength Austempered Ductile Irons.* Series editor: E. G. West. Obe Howood series in metals and associated material. 1991.

[2] A. trudel and M. Gagné. *Effect of composition and heat treatment on the characteristics of austempered ductile irons*.

[3] A. Basso, R. Martínez and J. Sikora. *Development of Dual Phase ADI.* National University of Mar de la Plata. Science and Processing of Cast Iron VIII. Edited by L. Yanxiang, Shen Houfa, Xu Qingyan, Han Zhiqiang.

[4] Caroline Glondu. *Improving the Toughness of Austempered Ductile Iron.* Master Thesis. Department of Material and Manufacturing Technology, Chalmers University of Technology Göteborg, Sweden 2007. Chalmers tekniska högskola ISSN 1652-8913

[5] http://www.ductile.org/didata/Section4/4intro.htm

[6] M. Lahres, M. Grüner, C. Mohrdieck, H. Baur. *Strategies for ProcessingNew Engineering Materials for Automotive Powertrain Components.* DaimlerChrysler AG, Ulm/Germany; 14.th of November; UCD -Ireland

[7] Componenta, *ADI Handbook*, ADI News, CD ROM by Componenta

[8]Miguel Angel Yescas-Gonzalez. *Modelling the microstructure and the mechanical properties of austempered ductile irons*. Darwing College, Cambridge. PHD Thesis. November 2001.

[9]D.Q. Sun, W.Q. Wang, Z.Z. Xuan, Z.A. Ren and D.X. Sun. *Transformation characteristics, microstructure and mechanical properties of austempered ductile iron welds.* Jilin University. Materials Science and Technology 2007 vol. 23. DOI: 10.1179/174328407X158479.

[10] ASTM Handbook, Volume 15 Casting, Section: *Testing and Inspection of Casting defects.*

[11] ASTM Handbook Volume 17, Nondestructive Evaluation and Quality Control, Article: *Nondestructive Inspection of Castings.*

[12] Vito J.Colangelo, Francis A. Heiser, *Analysis of metallurigical failures*, Wiley-Interscience

[13] G. Rivera, R. Boeri and J. Sikora, *Reveling and Characterizing Solidification Structure of Ductle Cast Iron*, National University of Mar de la Plata. Materials Science and Technology, June 2002, vol. 18, DOI: 10.1179/026708302225003668

[14] Doru M. Stefanescu, *Solidification and modelling of cast iron – A short history of defining moments*, The Ohio State University, Material Science and Engineering A 413-414 (2005) 322-323.

[15] Doru M. Stefanescu, *Modelling of cast iron solidification – The defining moments*, The Ohio State University, Metallurgical and Material Transactions A, vol. 38 A, July 2007, DOI: 10.1007/s11661-007-9173-y

[16] P. David, J. Massone, R. Boeri and J. Sikora. *Mechanical Properties of Thin Wall Ductile Iron-Influence of Carbon Equivalent and Graphite Distribution*. National University of Mar de la Plata. ISIJ International, vol. 44 (2004), No. 7,pp. 1180-1187.

[17] M. Nili Ahmadabadi. *A Transmission Electron Microscope Study of 1 PCT Mn Ductile Iron with Different Austempering Treatments.* Teheran University. Metallurgical and Materials Transactions A, volume 29A, September 1998.

[18] voigt r.c MT

[19] *Structure and properties of cast materials subjected to the heat treatment so called ADI-treatmen*

[20] R. Boeri, J. Sokora. *Advances in ductile iron research: New metallurgical understanding and its technological significance*. Archives of Foundry, Volume 5, 2005.
[21] A. Basso, R. Martínez and J. Sikora. *Development of Dual Phase ADI.* National University of Mar de la Plata. Science and Processing of Cast Iron VIII. Edited by L. Yanxiang, Shen Houfa, Xu Qingyan, Han Zhiqiang.
[22] M. Heydarzadeh Sohi, M.Nili Ahmadabadi, A. Bahrami Vhadat, *The role of austempering parameters on the structure and mechanical properties of heavy section ADI*. Department of Metallurgy and Materials, Journal of Materials Processing Technology 153-154 (2004) 203-208
[23] ASTM Handbooks, Volume 4 Heat treating, Section: *Quenching media for austempering*
[24] Jianghuai Yang, Susil K. Putatunda. *Effect of microstructure on abrasion wear behaviour of asutempered ductile cast iron (ADI) processed by a novel two-step austempering process*. Wayne State University, Detroit. Materials Science and Engineering A 406 (2005) 217-228.
[25] Chih-Kuang Lin, Chih-Wei Chang, "Influence of heat treatment on fatigue crack growth of austempered ductile iron", Department of Mechanical Engineering, National Central University, Taiwan, 2002
[26] Chih-Kuang Lin, Wen-Jeng Lee, "Effects of highly stressed volume on fatigue strength of austempered ductile irons", Department of Mechanical Engineering, National Central University,1997
[27] M. Tayanc, K. Aztekin, A.Bayram, "The effect of matrix structure on the fatigue behaviour of ADI", Materials and desing, 2005.
[28] M. Bahmani, R. Elliott, "The relationship between fatigue strength and microstructure in an austempered Cu-Ni-Mn-Mo alloyed ductile iron", Manchester Materials Science Centre, University of Manchester. Sharif University of Technology, Tehran, Iran,1997.
[29] K. Ibrahim and A. ElSawy. *Influence of Graphite Morphology and Matrix Structure on Fatigue Strength and Wear Resistance of Ductile and Austempered Ductile Iron*.
[30] R.A. Martínez, R.E. Boeri y J.A. Sikora. *Mecanismos de fractura en fundiciones de grafito esferoidal austemperizada –ADI*. Jornadas SAM 2000 - IV Coloquio Latinoamericano de Fractura y Fatiga, Agosto de 2000, 615-622.
[31] J.M. Barsom, S.T. Rolfe. *Fracture and fatigue control in structures, Aplication of fracturemechanics*, 2nd ed. Prentice-Hall, Englewood Cliffs, New Jersey 07632 USA, 1987.
[32] D. Broek, *Elementary engineering fracture mechanics, 4th ed.* Kluwer Academic Publishers, 101 Philip Dr., Norwell, MA 02061 USA, 1991.
[33] Z.K. Fan and R.E. Smallman. *Some observations on the fracture of austempered ductile irons*. Scripta Metallurgica et Materialia, vol. 31, No. 2, pp. 137-142, 1994.
[34] P. Prasad Rao, Susil K. Putatunda. Investigations on the fracture toughness of austempered ductile irons austenitized at different temperatures. Materials Science and Engineering A349 (2003) 136-149.
[35] A.S.H. Ali, K.I. Uzlov, N. Darwish, R. Elliot. Materials Science and Technology. 10 (1994) 35-45
[36] J.Sikora and R.Boeri. Solid State transformation in ductile irons- influence of prior austenite matrix microstructure. Int. J. Cast Metals Res., 1999, 11.
[37] A.J. Trowsdale and S.B. Pritchard. *Dual Phase Steel- High Strength Fasteners without heat treatment*.
[38] G.R. Speich. *Dual Phase Steels*. Metals Handbook vol. 2, 10th edition. Properties and selection, irons, steels, high performance alloys. ASM International. 1990.
[39] P. Shanmugan, K.R. Karthikeyan. *Dual Phase Steel Tubes for Automotive Applications*. AHHSSS Proceedings 2004.

[40] S. Nemecek, Z.Novy, H. Stanková. *Optimization of heat treatment of TRIP steels*. La Metallurgia Italiana 2/2006.
[41] J. Kliber, B. Masek, O. Zacek, H. Stankova. Transformation induced plasticity (TRIP) near forming technologies of carbon CMnSi Steel.
[42] J. P. Monchoux, C. Verdu, G. Thollet, R. Fougères and A. Reynaud. *Morphological Changes of Graphite Spheroids During Heat Treatment of Ductile Cast Irons*. Elsevier
[43] Toshiro Kobayashi and Shinya Yamada. *Effect of Holding Time in the (alfa+gamma) Temperature Range on Toughness of Specially Austempered Ductile Irons.* Toyohashi University of Technology. Metallurgical and Materials Transactions, vol. 27A, 1996.
[44] Bo Bergman, Bengt Klefsjö, *Quality from Customers Needs to Costumer Satisfaction*, Studentlitteratur (2007)
[45] Stéphane Forsik, *Neural Networks: A set of four case studies* http://www.msm.cam.ac.uk/phase-trans/2003/MP9/MP9-6.pdf